PERFORMANCE OF TPA LOADED SBA-15 CATALYST IN POLYPROPYLENE DEGRADATION REACTION

A THESIS SUBMITTED TO
THE GRADUATE SCHOOL OF NATURAL AND APPLIED SCIENCES
OF
MIDDLE EAST TECHNICAL UNIVERSITY

BY

ULVİYE ERSOY YALÇIN

IN PARTIAL FULFILLMENT OF THE REQUIREMENTS
FOR
THE DEGREE OF MASTER OF SCIENCE
IN
CHEMICAL ENGINEERING

DECEMBER 2019

Approval of the thesis:

PERFORMANCE OF TPA LOADED SBA-15 CATALYST IN POLYPROPYLENE DEGRADATION REACTION

submitted by **ULVİYE ERSOY YALÇIN** in partial fulfillment of the requirements for the degree of **Master of Science in Chemical Engineering Department, Middle East Technical University** by,

Prof. Dr. Halil Kalıpçılar
Dean, Graduate School of **Natural and Applied Sciences** _____

Prof. Dr. Pınar Çalık
Head of Department, **Chemical Engineering** _____

Prof. Dr. Naime Aslı Sezgi
Supervisor, **Chemical Engineering, METU** _____

Assist. Prof. Dr. Zeynep Tutumlu
Co-Supervisor, **Material Science and Nanotechnology Engineering, TOBB ETU** _____

Examining Committee Members:

Prof. Dr. Halil Kalıpçılar
Chemical Engineering, METU _____

Prof. Dr. Naime Aslı Sezgi
Chemical Engineering, METU _____

Prof. Dr. Nuray Oktar
Chemical Engineering, Gazi University _____

Assoc. Prof. Dr. Erhan Bat
Chemical Engineering, METU _____

Assoc. Prof. Dr. Dilek Varışlı
Chemical Engineering, Gazi University _____

Date: 12.12.2019

I hereby declare that all information in this document has been obtained and presented in accordance with academic rules and ethical conduct. I also declare that, as required by these rules and conduct, I have fully cited and referenced all material and results that are not original to this work.

Name, Surname: Ulviye Ersoy Yalçın

Signature:

ABSTRACT

PERFORMANCE OF TPA LOADED SBA-15 CATALYST IN POLYPROPYLENE DEGRADATION REACTION

Ersoy Yalçın, Ulviye
Master of Science, Chemical Engineering
Supervisor: Prof. Dr. Naime Aslı Sezgi
Co-Supervisor: Assist. Prof. Dr. Zeynep Tutumlu

December 2019, 136 pages

Plastic materials are widely used due to their low cost and easy processing properties. With an increase in plastic usage, the amount of plastic wastes has also increased, and this situation causes environmental problems. Landfilling, incineration, and recycling are the methods used for the disposal of plastic wastes. Landfilling is not a convenient method as it causes soil pollution. Incineration is also not preferred due to its harmful effects on the environment caused by toxic gases. Recycling seems to be the most convenient method to eliminate environmental problems.

In this study, tungstophosphoric acid (TPA) loaded SBA-15 catalysts with different TPA loadings were synthesized via one-pot hydrothermal method. To investigate the performance of these catalysts in the degradation of PP, pyrolysis experiments were carried out at 315 ^{o}C and 400 ^{o}C for 30 minutes, with a heating rate of 5°C/min, under nitrogen atmosphere at a flow rate of 60 cc/min and a catalyst to polymer weight ratio of 1/2. Characterization of the synthesized materials was done using various characterization methods.

Synthesized materials exhibited Type IV isotherms, and pore sizes changed between 6.7-9.7 nm, showing the mesoporosity of the materials. Surface areas of the

synthesized materials decreased with an increase in the amount of TPA loaded. All catalysts exhibited both Lewis and Brønsted acid sites.

TPA loaded SBA-15 catalysts decreased the activation energy of PP degradation reaction from 172 kJ/mol to 100.5 kJ/mol.

The liquid product amount increased with an increase in the reaction temperature and TPA loading while the gas product amount decreased. The solid residue was not observed when the catalysts were used. TPA loaded SBA-15 catalysts had high isobutane and ethylene selectivity among gas products. The majority of the liquid products consisted of C_8-C_{14} at both temperatures. SBA15-TPA 0.20 showed the best performance in the catalytic degradation of PP with the highest selectivity of C_{10} at 315°C and C_{14} at 400 °C. Products in the gasoline range can be obtained mostly at 315 °C, while products in the diesel range can be obtained mostly at 400 °C.

Keywords: Plastic Waste, Recycling, Catalytic Degradation, Polypropylene, SBA-15, Tungstophosphoric Acid

ÖZ

TPA YÜKLÜ SBA-15 KATALİZÖRÜNÜN POLİPROPİLENİN BOZUNMA REAKSİYONUNDAKİ PERFORMANSI

Ersoy Yalçın, Ulviye
Yüksek Lisans, Kimya Mühendisliği
Tez Danışmanı: Prof. Dr. Naime Aslı Sezgi
Ortak Tez Danışmanı: Dr. Öğr. Üyesi Zeynep Tutumlu

Aralık 2019, 136 sayfa

Plastik malzemeler, düşük maliyetleri ve kolay işlenebilirlik özelliklerinden dolayı yaygın olarak kullanılmaktadır. Plastik kullanımındaki artış, plastik atık miktarında da artışa neden olmakta ve bu durum çevresel problemlere yol açmaktadır. Gömme, yakma ve geri dönüşüm, plastik atıkların imha edilmesi için kullanılan yöntemlerdir. Gömme yöntemi toprak kirliliğine neden olduğu için uygun bir yöntem değildir. Yakma yöntemi ise, açığa çıkardığı zehirli gazların çevre üzerindeki olumsuz etkileri nedeniyle tercih edilmemektedir. Geri dönüşüm, bu problemleri ortadan kaldırmak için en uygun yöntem olarak görünmektedir.

Bu çalışmada, tungstofosforik asit (TPA) yüklü SBA-15 katalizörleri hidrotermal yöntemle, farklı TPA yüklemelerinde sentezlenmiştir. Bu katalizörlerin polipropilenin bozunmasındaki performansının araştırılması için 315 ºC ve 400 ºC'de 30 dakika sürede, 5°C/dk ısıtma hızıyla, 60 cc/dk akış hızında azot atmosferi altında ve katalizör polimer kütlece 1/2 oranında piroliz deneyleri gerçekleştirilmiştir. Sentezlenen malzemelerin karakterizasyonu farklı karakterizasyon yöntemleri kullanılarak yapılmıştır.

Sentezlenen malzemeler IV. Tip izoterm göstermiş ve gözenek büyüklükleri 6.7-6.9 nm arasında değişerek mezogözenekliliği göstermiştir. Sentezlenen malzemelerin

yüzey alanları yüklenen TPA miktarındaki artışla azalmıştır. Tüm katalizörler Lewis ve Brønsted asit bölgeleri göstermiştir.

TPA yüklü SBA-15 katalizörleri PP'in bozunma tepkimesinin aktivasyon enerjisini 172 kJ/mol den 100.5 kJ/mole indirmiştir.

Sıvı ürün miktarı tepkime sıcaklığı ve katalizörlerdeki TPA miktarının artmasıyla artarken gaz ürün miktarı azalmıştır. Katalizörler kullanıldığında katı kalıntı gözlemlenmemiştir. TPA yüklü SBA-15 katalizörleri gaz ürünler arasında yüksek izobütan ve etilen seçimliliğine sahiptir. Sıvı ürünlerin büyük çoğunluğu her iki sıcaklıkta C_8-C_{14}'den oluşmaktadır. SBA15-TPA 0.20, 315°C'de en yüksek C_{10} ve 400°C'de en yüksek C_{14} seçiciliği ile, polipropilenin bozunma tepkimesinde en iyi performansı göstermiştir. 315 °C'de çoğunlukla benzin aralığındaki hidrokarbonlar elde edilirken 400 °C'de çoğunlukla dizel aralığındaki hidrokarbonlar elde edilmiştir.

Anahtar Kelimeler: Plastik Atık, Geri Dönüşüm, Katalitik Bozunma, Polipropilen, SBA-15, Tungstofosforik Asit

To my dear husband Muammer, my family and Badem…

ACKNOWLEDGEMENTS

Firstly, I would like to express my greatest appreciation to my supervisor Prof. Dr. Naime Aslı Sezgi, for her patience, guidance, advice and encouragement through my thesis research.

I would also like to thank my co-supervisor, Asst. Prof. Zeynep Tutumlu for her helpful suggestions.

I want to thank METU Chemical Engineering Department for giving me the chance to conduct my thesis studies and making it possible to complete my thesis studies properly.

I want to thank Mihrican Açıkgöz for her help with TGA analysis. I would also like to thank Gülten Orakçı for her help and support in gas chromatography and BET analyses.

I want to thank METU Central Laboratories for TGA, XRD, and SEM analyses.

I would also like to thank BAP for their financial support for this study.

I want to thank Tülay Bursalı, Ceren Kasapoğlu, Arzu Arslan, Abdul Rahman Rajabali Habib, and Seda Sivri for helping me in my experiments. I would also like to thank İlker Şener for his help with my BET and FTIR analyses and gas chromatography system.

I want to thank my family, my mother Emine Ersoy, my father Abdulkadir Ersoy, and my brothers Samet Ersoy and Emre Ersoy for their endless love and support.

I would also like to thank my dear husband Muammer Yalçın for his support, patience, and encouragement through my study.

TABLE OF CONTENTS

APPENDICES

LIST OF TABLES

TABLES

LIST OF FIGURES

FIGURES

LIST OF ABBREVIATIONS

AMS	Anionic Surfactant Templated Mesoporous Silica
BJH	Barrett, Joyner, and Halenda
EDS	Energy-Dispersive X-Ray Spectroscopy
FID	Flame Ionization Detector
FSM-16	Folded Sheet Mesoporous Material
FTIR	Fourier Transform Infrared
GC	Gas Chromatograph
HDPE	High Density Polyethylene
HMS	Hexagonal Mesoporous Silica
IUPAC	International Union of Pure and Applied Chemistry
LDPE	Low Density Polyethylene
LLDPE	Linear Low Density Polyethylene
MCM-41	Mobil Composition of Matter No.41
PE	Polyethylene
PP	Polypropylene
PVC	Polyvinyl Chloride
SBA-15	Santa Barbara Amorphous-15
SEM	Scanning Electron Microscope
TCD	Thermal Conductivity Detector

TEOS	Tetraethyl Orthosilicate
TGA	Thermal Gravimetric Analyzer
TPA	Tungstophosphoric Acid
VLDPE	Very Low Density Polyethylene
XLPE	Crosslinked Polyethylene
XRD	X-ray Diffraction
ZSM – 15	Zeolite Socony Mobil–15

LIST OF SYMBOLS

A	Pre exponential factor
E	Activation energy of the reaction (kJ/mol)
MW_i	Molecular weight of species i, (g/mol)
M_i	Mass of the component of i (g)
n	Order of the reaction
n_i	Number of moles of component i, (mol)
q	Heating rate (°C/min)
R	Gas constant (J/kmol)
S_i	Selectivity of the component i
T	Temperature (°C)
t	Time (min.)
w_i	Weight fraction of the component i
y_i	Mole fraction of the component i
z_i	Volume fraction of component i
α	Fraction of polymer decomposed
β_i	Calibration factor of the compound i

CHAPTER 1

INTRODUCTION

Plastics have extensive usage area in various applications such as household products, food industry, packaging, electronics due to their many advantages, and they substituted other important materials such as wood, metal, and glass. According to the statistics, the global production of plastics was about 299 million tons in 2013 and has increased by 4 % over 2012 (Sharuddin et al., 2016). With an increasing consumption rate of polymers depending on the growing demand, waste generation has also increased considerably. According to the statistics, thirty-three million tons of plastic were generated in the US only in 2013 (Sharuddin, 2016). This considerable increase brought environmental pollution problems along, and plastic recycling has been a very popular research area to find solutions for the elimination of this problem. Since 1994, various studies have been carried out, and multiple regulations have been developed in the EU considering waste management such as Waste Framework Directive and the Packaging and Packaging Waste Directive.

The principal methods for plastic waste management are landfilling, incineration, and recycling. Due to the decrease in landfill areas, the cost of the process increases. Most of the plastics are also not biodegradable. Because of these facts, landfilling is not considered a convenient method nowadays. Another technique for the treatment of plastic wastes is incineration, and reduction of waste volume by 90-99% can be achieved with this method (Al-Salem et al., 2009). Owing to the emission of harmful and pollutant chemicals, incineration is also considered unfavorable. That is why most of the studies are focusing on environmentally friendly, cost-effective, and long-lasting alternative methods for plastic waste treatment.

Recycling is considered as one of those alternative methods. There are various types of recycling, such as mechanical recycling and chemical recycling (Goto, 2009). In mechanical recycling, plastic wastes are treated by mechanical means so that they can be used again in plastic product manufacturing. But this technique can only be applied to single-polymer plastics such as polyethylene, polypropylene, etc. It is also difficult to recycle mixed and contaminated plastic wastes via this method (Al-Salem et al., 2009). Another problem is that products obtained after mechanical recycling show lower mechanical properties than the original materials (Bursalı, 2014).

In chemical recycling, plastic materials are converted into liquid or gas products that can be used as fuels. One of the main advantages of chemical recycling is the broad application area. All kinds of plastic wastes can be treated via chemical recycling with a limited pre-treatment stage. High product yield is also obtained via this method. There are various techniques used for chemical recycling such as pyrolysis, hydrogenation, and gasification. Pyrolysis can be described as thermal degradation of polymers under an inert atmosphere. With this technique, many types of plastic wastes can be recycled, producing high calorific value fuels that can be used in the market. This can be an alternative technique to landfilling and incineration by decreasing toxic gas emissions.

Pyrolysis can be carried out catalytically and non-catalytically. In the catalytic pyrolysis, catalysts are added to increase the number of valuable products and selectivity, decrease the energy consumption of the pyrolysis reaction. There are various catalysts that can be used in catalytic pyrolysis and they can be classified in three different categories such as; fluid cracking catalysts containing zeolites, silica alumina and clays, reforming catalysts containing transition metals loaded in silica alumina and activated carbon loaded with or without transition metals (Kunwar et al., 2016). Properties of the catalysts such as pore size, particle size, surface area, and stability affect the amount and quality of the pyrolysis products. Catalysts with acidic behavior enhance conversion by protonating the defective sites of the polymers

forming on-chain carbonium ions (Buekens et al., 1998). The acidic strength of the catalyst is essential for selectivity and fuel quality of the products. When the pore size effect of the catalysts was examined, it was found that mesoporous and microporous acid catalysts provide the higher conversion. Zeolites are the most famous examples of microporous catalysts. They have attracted considerable attention in the last few years with the advantage of having strong Brønsted acid sites, but when large reactants are involved, they have diffusion problem to the catalytic sites as microporous structure hinders the access of polymeric molecules to the active sites of the catalyst (Aydemir, 2010). To overcome this problem, studies focused on increasing the pore size of the zeolites to the mesoporous range so that large molecules could enter the pores and processed there (Taguchi et al., 2005). With discovery of Mobil Composition of Matter No.41 (MCM-41) in 1992, mesostructured materials gained great importance and synthesis of other mesoporous materials such as MCM-48, MCM-50, Folded Sheet Mesoporous Material (FSM-16), Anionic Surfactant Templated Mesoporous Silica (AMS), Hexagonal Mesoporous Silica (HMS), and Santa Barbara Amorphous-15 (SBA-15) followed it. These materials possess high regular arrays of uniform pore channels ranging from 1.5 nm to 10 nm in size and large surface area (Obalı, 2012). However, mesoporous catalysts do not show high activity in cracking reactions due to low acid sites, so to improve their catalytic activity, acid sites need to be introduced to them. With their highly acidic character, heteropoly acids can be a good acid source. But as it is not convenient to use them alone due to their low thermal stability and surface area, SBA-15 as a mesoporous material can support heteropoly acids providing high thermal stability and high surface area (Aydemir, 2010).

In this study, tungstophosphoric acid (TPA) loaded SBA-15 catalyst was synthesized through the hydrothermal method at different TPA/SBA-15 ratios, and their properties were determined using various characterization techniques. The performance of synthesized catalysts in polypropylene pyrolysis reaction and product distribution obtained from this reaction was investigated.

CHAPTER 2

DEGRADATION OF POLYMERS

2.1. Polymers

Origin of the word “polymer” comes from the Greek, where *poly* means many and *mere* means unit. Conventionally a polymer can be defined as a long-chain molecule built up by the repetition of small identical units. The starting material of the polymer is called as the monomer. Identical units can be connected to each other via primary bonds such as ionic, covalent, coordinate, and metallic bonds or secondary bond forces such as dipole forces, induction forces, dispersion forces, and hydrogen bonds.

Polymeric materials are generally used due to their excellent mechanical properties, and these properties are obtained as a result of their high molecular weight. The length of the polymer chain can be specified by the number of the repeating units in the chain, and this is called as degree of polymerization (DP). Polymers which have high molecular weight consisting of at least 100 DP so that desired mechanical and physical properties can be obtained (Sharma, 2005).

According to the origin, polymers can be classified as natural and synthetic polymers. Natural polymers such as proteins, starch, cellulose, wool have been known for many years. But due to the limitation of natural polymer supplies, synthetic polymers were developed. Some examples for the natural and synthetic polymers are given in Table 2.1.

Table 2.1. Natural and synthetic polymer examples (John et al., 2012)

Natural Polymer Examples	***Synthetic Polymer Examples***
Starch	Polypropylene
Cellulose	Poly (ethylene terephthalate)
Chitin	Polyethylene
Collagen/gelatin	Poly (vinyl chloride)
Casein, albumin, fibrogen, silks	Polystyrene
Poly(hydroxyalkanoates)	Poly (tetrafluoroethylene)
Lignin	Polyurethane
Lipids	Polyamide
Natural rubber	Polyacrylamide

When structural forms of the chains are considered, polymeric materials can be divided into three groups as linear, branched, and network polymers. Linear polymers are formed from two functional monomers or from single double-bonded monomers where branches are formed from three functional or double-double bonded monomers. Branched polymers have long chains and shorter side chains. When branched chains are connected to each other by multifunctional units, a three-dimensional crosslinked polymer is formed called network polymers. The structure of linear, branched, and network polymers are shown in Figure 2.1.

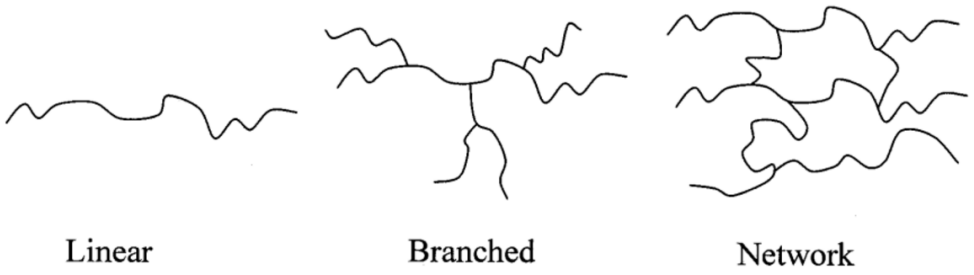

Figure 2.1. Linear, branched and network polymers (Brodhacker, 2006)

2.1.1. Classification of Polymers

2.1.1.1. Thermoplastics

Thermoplastic polymers are formed from linear or slightly branched chains. Their molecular structure may be amorphous or semicrystalline (Tuttle, 2012). The molecular structure of a semicrystalline thermoplastic polymer is shown in Figure 2.2. When heat is increased, intermolecular forces are weakening rapidly, so polymer soften and flow and softening of the polymer results in reshaping of these polymers. When the polymer is cooled, it solidifies again. Due to its reversible heat characteristics, thermoplastics can be recycled and reprocessed.

Many thermoplastics are good electrical and thermal insulators. Their lightweight, high strength, and relatively low cost make thermoplastics very usable for many applications. Polyethylene, polypropylene, polyvinyl chloride, and polycarbonate can be given as examples to thermoplastic polymers. Application areas of thermoplastics can be listed as electrical products, glass frames, toys, phones, windows, cables, sheets, rope, and so on.

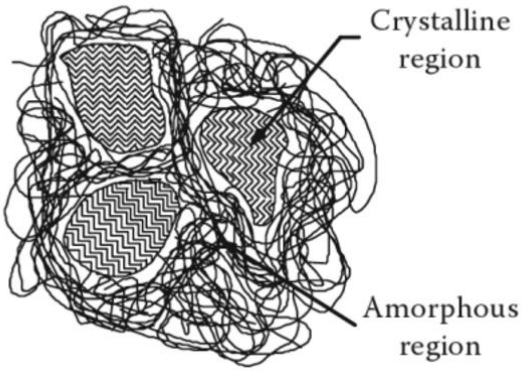

Figure 2.2. Molecular structure of a semicrystalline thermoplastic polymer (Tuttle, 2012)

2.1.1.2. Thermosets

Thermoset polymers exhibit irreversible heat characteristics, which means once they are shaped by applying heat, their shape is set, and they can not be reprocessed or recycled. Crosslinking reactions occur during shaping, so they decompose rather than melting with heat. When compared to thermoplastics, thermoset polymers have higher modulus and improved creep resistance due to the cross-linked network structure, but as their chains are below the glass transition temperature, they are more brittle. Polyurethane, epoxy, polyester, and polyimide can be given as examples to thermoset polymers.

Thermoset polymers are formed from cross-linked thermoplastic polymer chains (Figure 2.3). The thermoplastic polymer precursor is shaped, and then it is cross-linked to obtain the thermoset. Conversion of the raw material to the glassy thermoset polymer upon solidification is called curing. Curing can be done by heat, radiation, or catalyst. Crosslinks are formed during curing reaction, and they immobilize the molecules providing strength to the polymer.

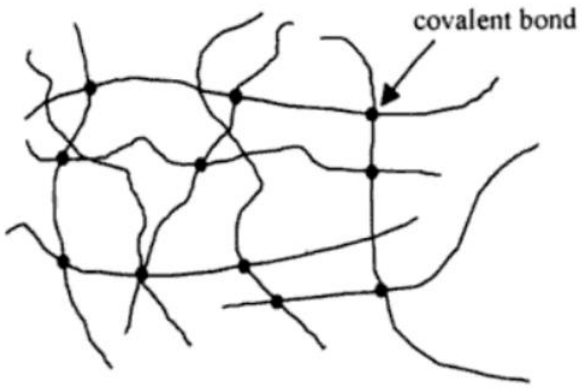

Figure 2.3. Thermoset polymer *(*Aguado et al., 1999)

2.1.1.3. Elastomers

Elastomeric polymers or rubbers are viscoelastic polymers that have polymer chains above their glass transition temperature, providing them segmental motion capability. Vulcanization is carried out to make the polymer chains cross-linked, and this results in a "spaghetti and meatball" structure where polymer chains signify spaghetti and cross-link points signify meatballs (Figure 2.4). Vulcanization is the process of usually adding sulfur or other chemicals to improve the properties of elastomers by creating cross-links. These cross-links are covalent and provide elastomers excellent flexibility. Elastomers are widely used in tires, shoes, household supplies, balls, toys, etc.

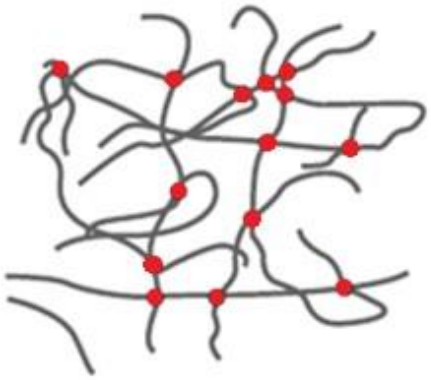

Figure 2.4. Spaghetti and meatball structure of elastomers *(*Rubber, 2015)

2.1.2. Some Important Polymers

2.1.2.1. Polypropylene (PP)

Polypropylene is one of the most essential commodity thermoplastic polymers which can be used in various applications such as packaging, automotive industry, furniture, etc. due to its many favorable properties. For example, one of the most common usage areas of polypropylene is food packaging for biscuits, snack foods, and dried foods because it has a moderate barrier to moisture, gases, odors and a higher barrier to water vapor which is not affected by changes in humidity (Mazrouaa, 2012). Polypropylene resin was first developed by Giulio Natta in 1954, but its commercial production began in 1957, and the production amount increased from that time on (Andrady et al., 2009).

According to the statistics, polypropylene is the third most commonly produced polymer by volume after polyethylene and polyvinylchloride (Maier et al., 1998). Most widely available commercial polypropylene types are homopolymer (HP), random copolymer (RACO), and impact copolymer (Malpass et al., 2010).

Polypropylene is produced via polymerization reaction of propylene monomers joining together to form one large molecule of polypropylene (Figure 2.5). There may be three possible sequences for polypropylene polymerization (Figure 2.6). Monomer addition can be head-to-tail resulting in a polypropylene chain with pendant methyl groups attached to alternating carbons. Tail-to-tail or head-to-head addition is not very commonly used as these mechanisms disrupt the crystalline structure and lower the melting point of polypropylene.

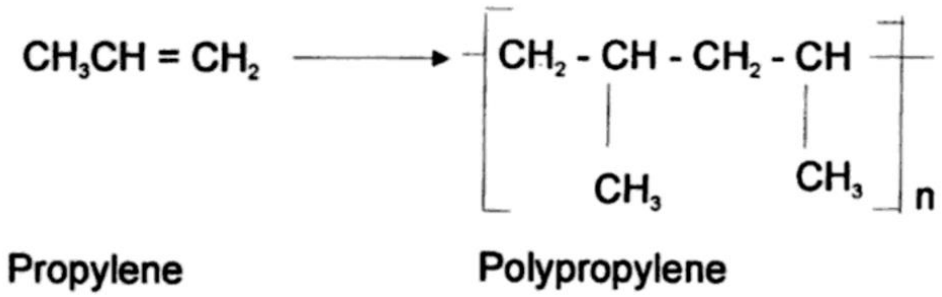

Figure 2.5. Polypropylene structure (Goswami et al., 2004)

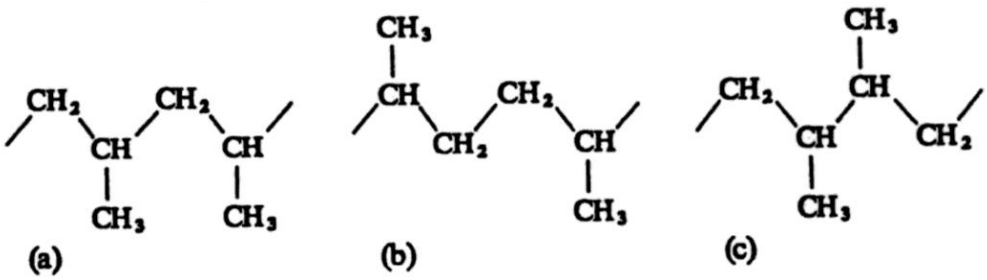

Figure 2.6. Isomerism for positions in polypropylene (a) head-to-tail (b) head-to head (c) tail-to-tail (Karger-Kocsis, 1995)

According to the stereo chemical configuration (orientation of the pendant methyl groups attached to alternate carbon atoms), polypropylene can be isotactic, syndiotactic, or atactic (Figure 2.7). Due to the high crystallinity and good mechanical properties, the most common commercial structure is isotactic polypropylene, in which substituents are all on the same side of the polymer chain. Syndiotactic polypropylene contains alternating substituents on opposite sides of the polymer backbone. In atactic polypropylene, substituents do not have a regular orientation and are present randomly with respect to the polymer backbone resulting in low crystallinity.

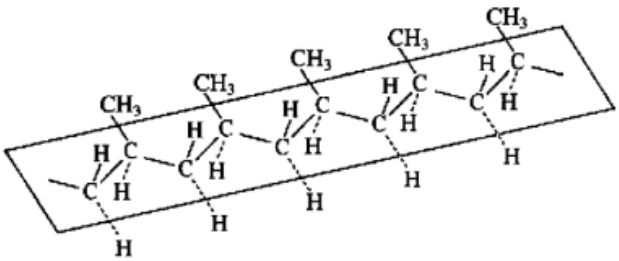

Isotactic (all methyl groups on same side of chain)

(a)

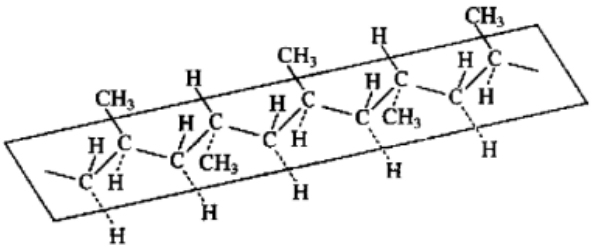

Syndiotactic (methyl groups on alternating sides)

(b)

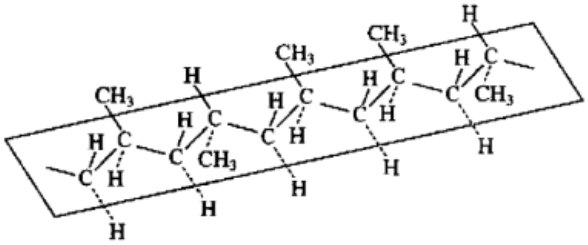

Atactic (methyl groups situated at random)

(c)

Figure 2.7. Tacticity of polypropylene (a) Isotactic (b) Syndiotactic (c) Atactic (Mantia, 2002)

2.1.2.2. Polyethylene (PE)

Polyethylene is the most commonly produced thermoplastic polymer in the world, with approximately 80 million tons of annual global production (Piringier et al., 2008). It is a semi-crystalline polymer with excellent chemical resistance, good fatigue, and wear resistance, and a wide range of properties (Vasile et al., 2005). Due to these different properties, it is widely used in our daily lives in various applications such as plastic bags, containers, bottles, textiles, toys, etc. Mechanical and thermal properties of polyethylene vary depending on the structure, molecular weight and molecular weight distribution, crystallinity, temperature, and stress. There are various types of polyethylene structures (Peacock, 2000).

- High density polyethylene (HDPE)
- Low Density Polyethylene (LDPE)
- Linear Low Density Polyethylene (LLDPE)
- Very Low Density Polyethylene (VLDPE)
- Ethylene-Vinyl Ester Copolymers
- Ionomers
- Cross-linked Polyethylene (XLPE)

Modern polyethylene was first produced by chemists of Imperial Chemical Industries, Eric Fawcett and Reginald Gibson while trying to condense ethylene with benzaldehyde at very high pressure and temperature (Malpass, 2010). After that, various chemists worked on the production of larger amounts of polyethylene, leading to commercial applications.

Polyethylene is produced via polymerization reaction of ethylene monomers. It consists of a long chain of carbon atoms with two hydrogen atoms attached to each carbon atom (Figure 2.8).

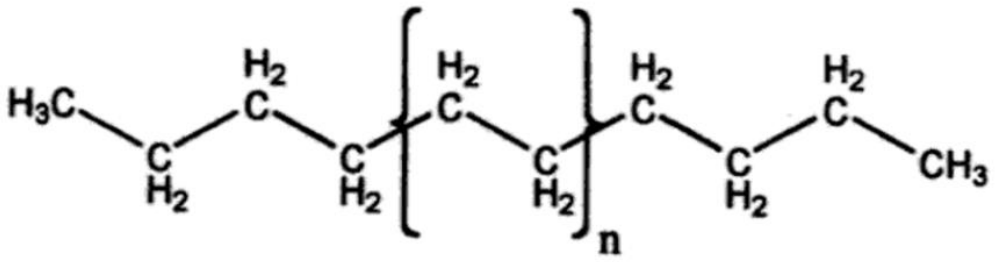

Figure 2.8. Molecular structure of polyethylene (Peacock, 2000)

2.1.2.3. Polyvinyl Chloride (PVC)

PVC is one of the most popular polymers which has widespread use in our daily lives. It is compatible with different kinds of additives, so many properties of PVC can be altered for useful applications. For example, plasticizers can be added to make PVC more flexible so that it can be used in different fields. One of the most advantageous properties of PVC is its excellent electrical insulation, and this makes PVC an ideal material for cable manufacturing. According to the statistics, PVC is the third most widely produced synthetic polymer after polyethylene and polypropylene (Geyer et al., 2017).

PVC is prepared by the polymerization reaction of the vinyl chloride monomer (Figure 2.9). Its production can be via suspension, emulsion, and bulk polymerization. Among other polymers, PVC is unique because the bulky chlorine atom provides a strongly polar nature to the PVC polymer chain, and syndiotactic structure leads to a limited level of crystallinity resulting in good mechanical properties (Owen, 1984). Some applications of PVC is given in Table 2.2.

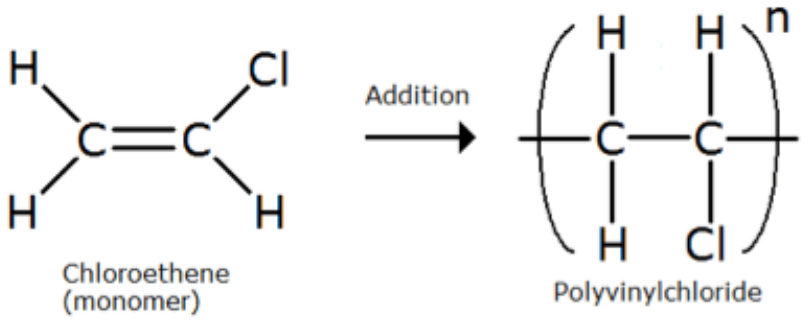

Figure 2.9. Polymerization reaction of PVC

Table 2.2. Typical Applications of PVC (Patrick, 2005)

Construction	Window frames, doors, roller shutters, potable pressure pipe, sewage and drainage pipe, guttering, cladding, roofing membrane, cable duct and conduit, flooring, wall covering, reservoir lining, fencing, corrugated and insulation sheets, slats and blinds
Electrical	Keyboards, computers, power tools, electrical and, telecommunication cables, duct, fuse boxes, wall plugs
Automotive	Interior trim, dashboard skin, coated fabric for seat coating and door panels, wire harness systems, window seals and gaskets, windscreen sandwich film, sealant for underbody and joints, sound insulation, decorative and protective profiles, tarpaulins
Medical	Pharmaceutical blister packs, blood and plasma bags, tubing for dialysis, endotracheal, infusion kits, surgical and examination gloves, inhalation masks, pouches for waste products
Packaging	Food packaging: PVC-U: thermoformed blister packs/display trays/egg boxes, tamper-evident packaging, bottles for mineral water/fruit squash/cooking oils PVC-P: cling and stretch film for wrapping food products, cap seals/closures and food can linings/hose and tubing for drinks transportation
	Non-food packaging: Trays, containers, and bottles for cosmetics, medicines, and detergents, bottle cap sealing closures, adhesive tapes, shrink film
Leisure and Sports	Toys, footballs, buoyancy aids, life vests, leisure boats, garden hose, temporary structures, coated garden tool handles, gloves (garden), luggage; credit and debit cards, smart cards, identity cards
Clothing	Raincoats, shoe soles, boots, imitation leather, fashion items
Office	Office supplies, folders, ring binders, covers
Miscellaneous	Conveyor belting, polyurethane sealants (PVC component gives non-sag consistency), waterproof membranes (for road foundations and tunnels), wire fencing, furniture coatings, inks, lacquers and adhesives, valves and fittings (chemical industry), gauntlet gloves, upholstery

2.2. Disposal of Plastic Wastes

Polymers have a non-negligible amount of application fields in our daily lives, from greenhouses, coating and wiring, building and construction, agriculture to packaging, and transportation. We use plastic materials more and more every day, and of course, this brings some drawbacks such as environmental pollution due to an increase in plastic waste generation rate. In the European Union countries, over 250 x 10^6 tons of municipal solid waste are produced each year with an annual growth of 3%, and in general, approximately 10.6 wt% of municipal waste consists of plastics (Bloom, 1995). Hence, the disposal of plastic wastes has become one of the more substantial issues for governments. There are some methods such as landfilling, incineration, and recycling to overcome plastic waste problems arising from the high amount of plastic usage. These methods will be discussed below in detail.

2.2.1. Landfilling

Cossu gave one description for landfills as "reactors in which liquid, solid and gaseous materials interact giving rise to liquid (leachate) and gas (biogas) emissions, together with a solid phase (the landfilled waste) representing a source of potential residual emissions" (Cossu, 2010). In landfills, the biodegradable organic matter contained in solid wastes is degraded to landfill gases containing mainly methane and carbon dioxide via anaerobic biological processes (Velinni, 2007). Ammonia, carbon monoxide, hydrogen, and oxygen can also be present in landfill gases. Emissions of the landfills depend on the waste inputs. Some inputs that can be treated in the landfills are:

- Residual wastes which are collected from household and commercial sources
- Sorting residues that are obtained from waste sorting processes
- Biologically treated materials
- Ash that is obtained from thermal treatment processes

There are different solid waste landfilling technologies such as dumps, conventional landfills, and engineered landfills, including bioreactors, flushing-bioreactors and, semi-aerobic landfills (Manfredi et al., 2009). Landfills are generally used for wastes that cannot be recycled, composted, or used to generate energy. Landfilling has incontrovertible problems such as environmental pollution with uncontrolled gas leakages and the release of large amounts of methane, which accelerate global warming. This method has not been preferred due to its high cost, environmental problems, and decreasing landfilling spaces.

2.2.2. Incineration

Incineration is another waste treatment process that involves the combustion of organic substances contained in waste materials. With this thermal treatment method, wastes are converted into ash, flue gas, and heat. In a typical incineration facility, there are various process sections, and they are given below: (Sloot et al., 1997).

- Waste receiving and storage area: waste is stored in this section until it is treated
- Waste feed system: waste is fed to the incinerator for thermal treatment
- Combustion system: waste can be burned after it is fed to the furnace directly without any pre-treatment, or waste can be pre-treated, and certain materials can be separated from the waste to improve the combustion. The bulk residue is produced in this section.
- Boiler: the heat energy generated during incineration is converted to usable energy
- Residue handling: solid residues (ash, slag or fly ash) which are generated during the incineration process are handled and disposed

Use of incineration and landfilling facilities for waste management was compared in terms of financial and environmental issues and according to the research, incineration was found to be better environmentally while landfilling was found to be more economic (Assamoi et al., 2012). Despite some of its benefits such as reduction in the volume and weight of waste especially of bulky solids with a high combustible content and recovery of energy from organic wastes with sufficient calorific value, incineration is not considered a convenient method due to the formation of some highly toxic pollutants such as polyaromatic hydrocarbons, dioxins, and furans (Hester et al., 1994; Obalı, 2009).

2.2.3. Recycling

Recycling comes as a perfect solution in terms of waste disposal eliminating environmental problems. Mechanical recycling and chemical recycling are the most investigated recycling methods with different applications, various advantages, and disadvantages.

In mechanical recycling, physical and mechanical techniques such as grinding, heating, and extruding are used to convert plastics into new products (Azapagic et al., 2003). Plastics are separated by resins, washed to remove contaminants, grinded, and crushed to reduce particle size, extruded by heat, and reprocessed to obtain new plastic goods (Aguado et al., 1999). Extrusion moulding, injection moulding, blow moulding, vacuum moulding, and inflation moulding are some of the methods that can be used to reprocess the recycled materials (Al-Salem et al., 2009). Mechanical recycling permits easy reuse of the same material by using conventional apparatuses (Mantia, 2002). However, waste that is used in this method should be clean and homogeneous, which means that it is not convenient to use mixed plastics in this method. Also, for mechanical recycling, only thermoplastic materials are of interest, thermoset polymers cannot be recycled in this way as the effect of heat cannot reshape them. A schematic process for mechanical recycling is given in Figure 2.10.

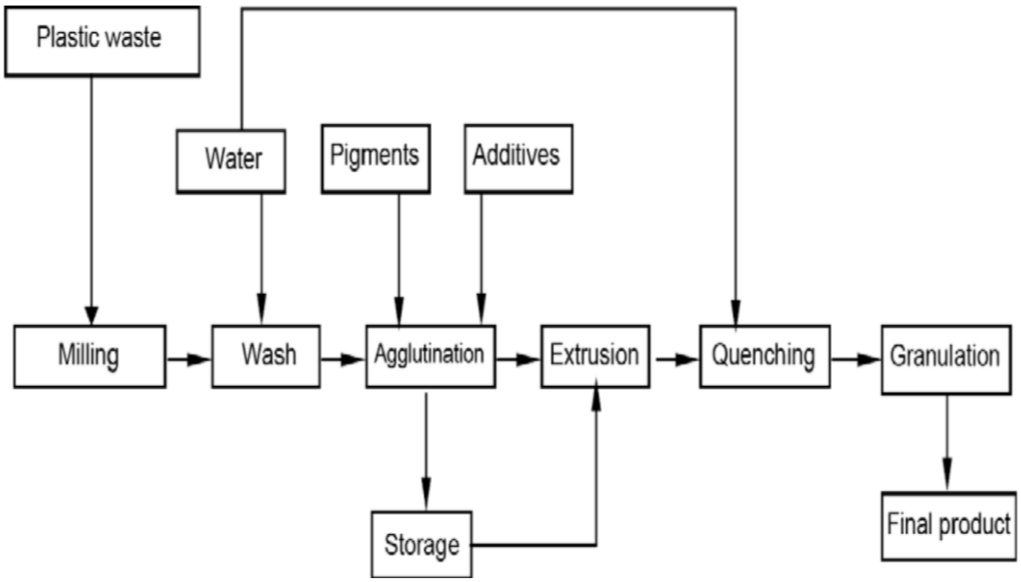

Figure 2.10. Mechanical recycling of plastics (Aznar et al., 2006)

In chemical recycling (also known as feedstock recycling), chemical processes are used for the breakdown of the polymers leading back to their chemical constituents to convert them into useful products (Azapagic et al., 2003). Chemical recycling is mainly based on the decomposition of polymers using heat and sometimes with the addition of catalysts to yield outputs that can be used for the production of new polymers and chemicals or as a source of fuels. Compared to mechanical recycling, chemical recycling enables the use of thermosets and elastomers. It is also possible to use heterogeneous and contaminated polymers with limited pre-treatment. There are different types of chemical recycling processes, and some of them are explained below:

Gasification: Gasification can be considered to be a partial oxidation process of carbonaceous materials leading predominantly to a mixture of carbon monoxide, carbon dioxide and hydrogen. Oxygen, air, or steam can be used as gasification agents.

The most important advantages of using air instead of oxygen alone are to simplify the process and to reduce cost (Al-Salem et al., 2009). However, nitrogen contained in the air reduces the calorific value of obtained fuels. Hence steam can be used. In a common gasification process (Texaco gasification process), plastic waste is first depolymerized into synthetic heavy oil and gas fractions (condensable and non-condensable). Oil and condensed gas are gasified with oxygen and steam at a temperature of 1200-1500^{o}C, and dry synthesis gas (also known as syngas) is obtained after some cleaning processes. Syngas contains majorly carbon monoxide and hydrogen with small amounts of methane, carbon dioxide, water and some inert gases. Moreover, generally high amount of char which needs further treatment is produced in the gasification process. By this method, it is not necessary to separate different polymers in the plastic wastes. However, the economics of this method depends on the value and possible applications of the synthesis gas (Alonso et al., 2007).

Hydrogenation (Hydrocracking): In this method, plastic wastes are broken down into smaller molecules in the presence of hydrogen under high pressure. Plastic waste is first depolymerized where the agglomerated waste is kept between 350 to 400^{o}C in order to allow the waste to be mixed to higher proportions (Azapagic, 2003; Letcher et al., 2011). Most hydrogenation processes are carried out in the presence of a catalyst to promote hydrogen addition reactions. Oxide or zeolite supported transition metals can be used as catalysts (Andrady, 2015). The main disadvantages of this method are high cost and high-pressure operation need (Alonso et al., 2007).

Depolymerization: This method can be described as a breakdown of the polymers by reaction with certain chemicals, converting the polymeric molecules back to their starting monomers (Aguado et al., 1999; Pielichowski et al., 2005). Organic materials decompose on a molecular level with an increase in their internal energy. Unfortunately, this method is generally restricted to the recycling of condensation polymers, and it is not suitable for recycling of most addition polymers (Aguado et al., 1999).

Chemical depolymerization: Chemical depolymerization consists of the breakdown of the polymer leading back to the starting monomers via various routes such as glycolysis, methanolysis, hydrolysis, ammonolysis etc. One of the major disadvantages of chemical depolymerization is that it is restricted to the recycling of condensation polymers such as polyurethane, PET, nylon, etc. and this method cannot be used for most of the addition polymers which are the main components of the plastic waste stream (Alonso et al., 2007). This method also requires high energy, and it is not economical unless huge amounts of waste are used (Islam et al., 2010).

Thermal depolymerization (Pyrolysis): Pyrolysis is the thermal decomposition of materials at very high temperatures ending up with smaller molecules. By this method, the high molecular weight can be converted into useful end-products. Products are generally gases, liquids, and coke varying according to the reaction conditions. Temperature and the heating rate is the most critical reaction parameters influencing pyrolysis products. A schematic representation of a pyrolysis process for plastics is given in Figure 2.11.

Pyrolysis has operational, environmental, and financial advantages. For example, the residual output can be used as a fuel or feedstock for other petrochemical processes. Compared to other disposal methods, this is also an environmentally friendly way for disposal of plastic wastes. As a financial advantage, this method produces high calorific value fuel. However, it also has some disadvantages, such as the requirement of treatment for the final product to obtain specific products and the need for handling of produced char (Al-Salem et al., 2009).

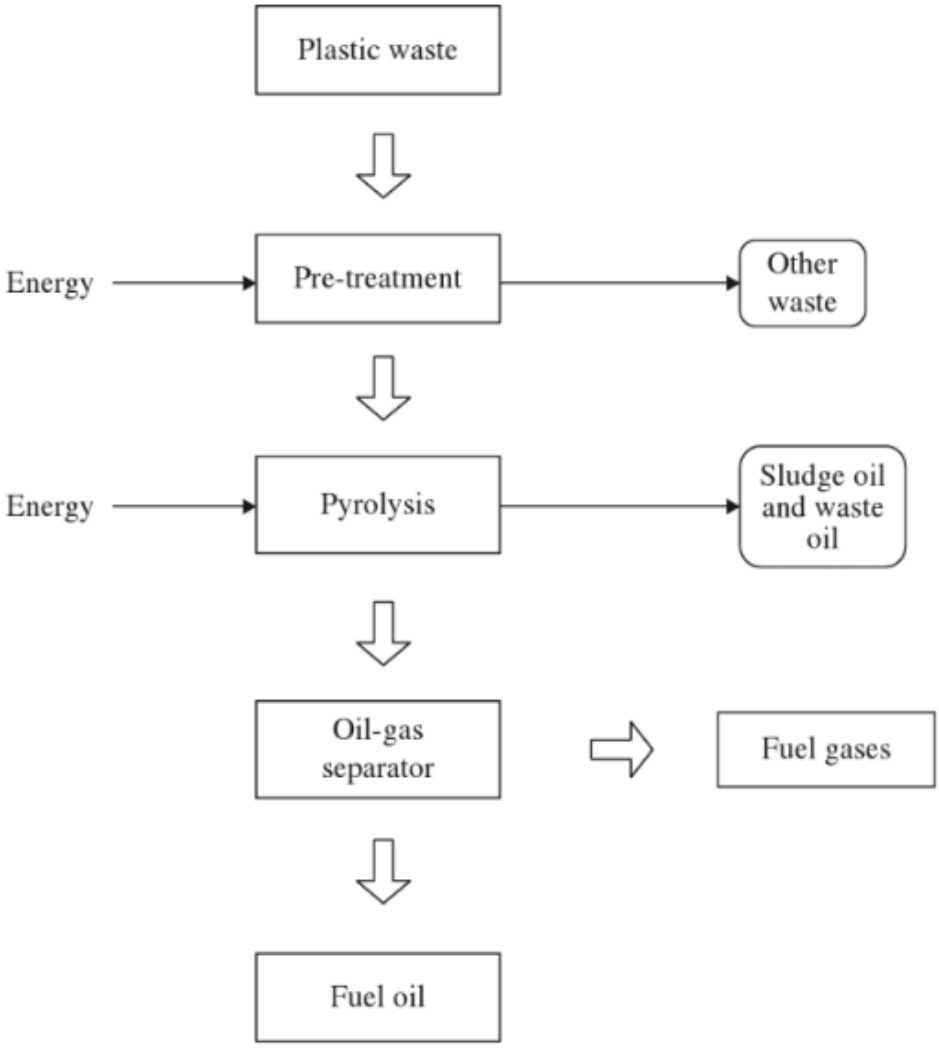

Figure 2.11. Schematic representation of a pyrolysis process for plastics (Andrady, 2015)

2.3. Degradation of Polymers

2.3.1. Non-catalytic Thermal Degradation

Non-catalytic thermal degradation is a method for upgrading waste plastic into liquid products at high temperatures (400-600 °C) in the absence of oxygen (Lee et al., 2006). Due to the low thermal conductivity of plastic wastes, this process requires high energy consumption and, generally it takes relatively long reaction times. When the non-catalytic thermal degradation of polymers is considered, there are three major pathways that can be followed: side-group elimination, random scission, and depolymerization (Pielichowski et al., 2005).

Side-Group Elimination: Side group elimination takes place generally in two stages in which the polymer chain is first stripped of atoms or molecules attached to the backbone of the polymer (Figure 2.12). This leaves an unstable polyene macromolecule that undergoes further reaction, including the formation of aromatic molecules, scission into smaller fragments, or the formation of char (Pielichowski et al., 2005).

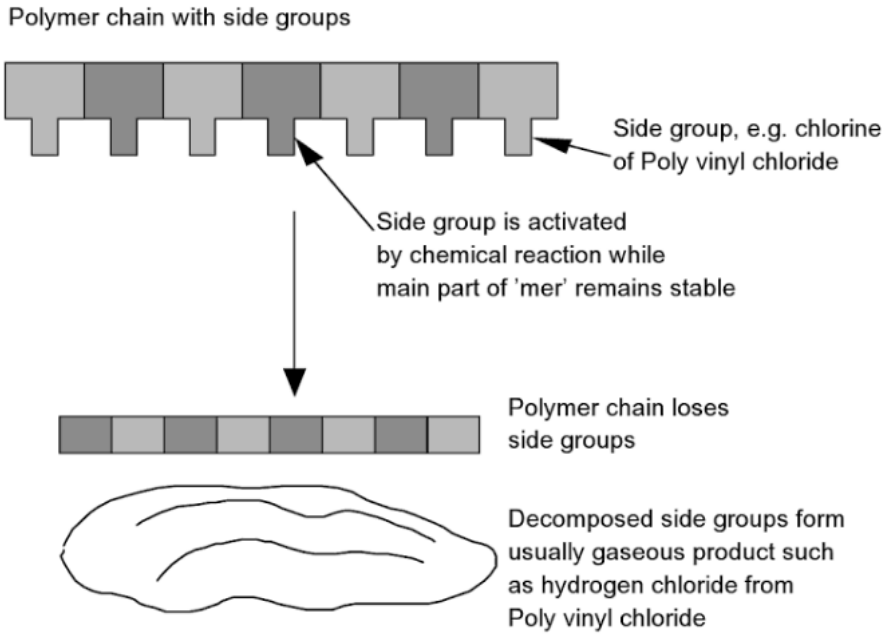

Figure 2.12. Side group elimination mechanism for PVC (Batchelor et al., 2011)

Random Scission: Random scission involves the formation of a free radical at some point on the polymer backbone, producing small repeating series of oligomers usually differing in chain length by the number of carbons (Figure 2.13). Polymers that do not depolymerize generally decompose by thermal stress into fragments that break again into smaller fragments and so on. The degree of polymerization decreases without the formation of free monomeric units. Statistical fragmentation can be initiated by chemical, thermal or mechanical activation, or by radiation (Pielichowski et al., 2005).

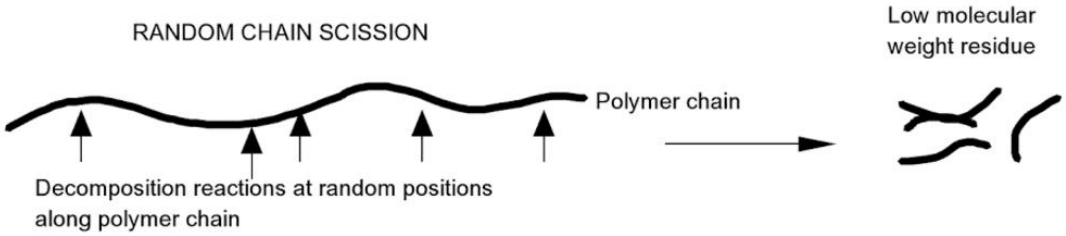

Figure 2.13. Random scission mechanism (Batchelor et al., 2011)

Depolymerization: Depolymerization is a free-radical mechanism in which the polymer is reverted to the monomer or comonomers that make up the polymer (Figure 2.14). Unlike random scission, which produces fragments of a variety of chain lengths, in depolymerization, the formation of a free radical on the backbone of the polymer causes the polymer to undergo scission to form small unsaturated molecules and propagate to the free radical on the polymer backbone. The mechanism of depolymerization can occur under the same conditions as statistical fragmentation. The mechanism, according to which monomeric unit split off from the end of the polymeric chain, is the reverse mechanism to polymerization. Several polymers can be depolymerized until the equilibrium between monomer and polymer at a given temperature is reached in a closed reaction system (Pielichowski et al., 2005).

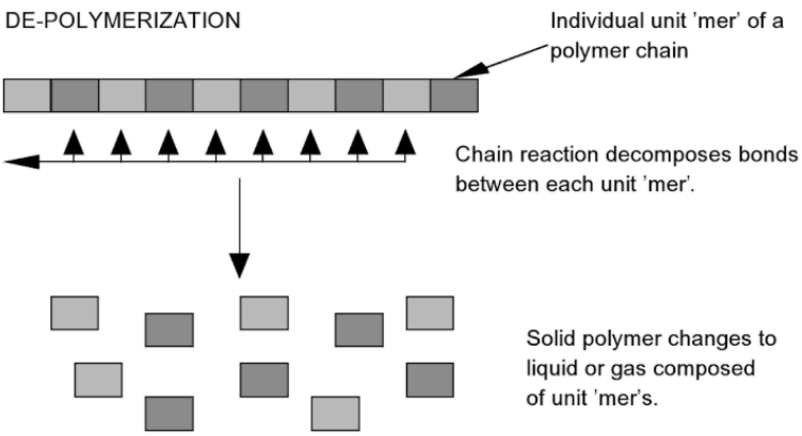

Figure 2.14. Depolymerization mechanism (Batchelor et al., 2011)

2.3.2. Catalytic Thermal Degradation

There have been many studies conducted for catalytic thermal degradation of plastics over different types of catalysts. Various types of catalysts have been tested in catalytic pyrolysis, such as homogeneous catalysts, mesoporous acid catalysts, non-acid mesoporous catalysts, fluid cracking catalysts (FCC), zeolites, metallic oxides etc. (Lopez et al., 2011). Differences in the catalytic activity of the catalysts may vary according to the properties such as surface area, particle size, or pore size distribution, and these may affect the degradation process. Besides, the presence of contaminants and chemical alterations that take place in the polymeric structure during its use may be the other parameters to affect thermal degradation (Aguado et al., 2007). Mesoporous and microporous acid catalysts are widely preferred for catalytic pyrolysis of plastic wastes. Primary cracking takes place in the macroporous surface, and once the polymer is cracked, further cracking is enhanced by micropores (Kunwar et al., 2016).

Pyrolysis of plastics in the presence of a catalyst provides many advantages when compared to the non-catalytic pyrolysis such as; (Aydemir, 2010; Marcilla et al., 2006).

- Obtaining value-added products with a broader number of applications
- Lower reaction temperatures leading to efficient use of energy
- Higher reaction rates leading to time efficiency

CHAPTER 3

POROUS MATERIALS IN CATALYSIS

Porous materials can be defined as materials containing relatively small spaces, so-called pores or voids, where porosity is the fraction of the bulk volume of the porous material which is occupied by pores (Dullien, 1992). Porous materials can be encountered almost everywhere in our lives. Textiles, leathers, paper towels, bricks, filters, etc. can be given as examples to porous materials from our daily lives.

Porous materials have highly developed internal surface area that can be used to perform specific functions. Almost all solids are porous except for ceramics fired at extremely high temperatures, some dense rocks, and some plastics (Dullien, 1992; Rouquerol et al., 1999). There are three parameters used as a measure of porosity (Figure 3.1):

- Specific surface area,
- Specific pore volume or porosity,
- Pore size and its distribution.

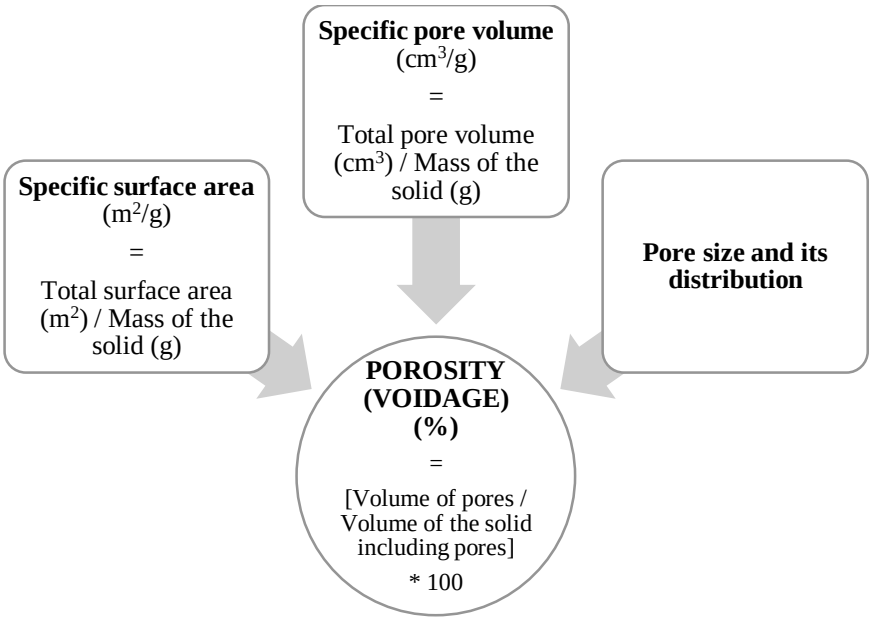

Figure 3.1. Measure of porosity (Adapted from Dullien, 1992)

According to IUPAC standards, there are three types of porous materials. These materials and their sizes are given in Figure 3.2. Materials with a pore size less than 2 nm are called microporous materials, materials with pore size between 2 and 50 nm are called mesoporous materials and materials with pore size greater than 50 nm are called macroporous materials (Sing, 1985).

The discovery of porous materials and the use of them in catalysis has brought many significant benefits such as an increase in the yield and quality of products (Perego et al., 2013). There are many parameters such as pore shape, surface area, specific pore volume, and pore size distribution, which determine the efficiency of porous catalysts. Microporous and mesoporous inorganic solids are used as heterogeneous catalysts extensively (Beck et al., 1992). These materials allow molecules access to large internal surfaces and cavities, enhancing catalytic activity and adsorptive capacity. Zeolites are the most widely synthesized and used microporous materials. However,

the size of the pores remains a strong limitation for their application when large reactant molecules are involved, especially in liquid-phase reactions as is frequently the case in the synthesis of fine chemicals due to the fact that mass transfer limitations are very severe for microporous materials (Obalı, 2010). To overcome this problem, materials with void dimensions in the range of mesopores can be a good alternative (Perego et al., 2013).

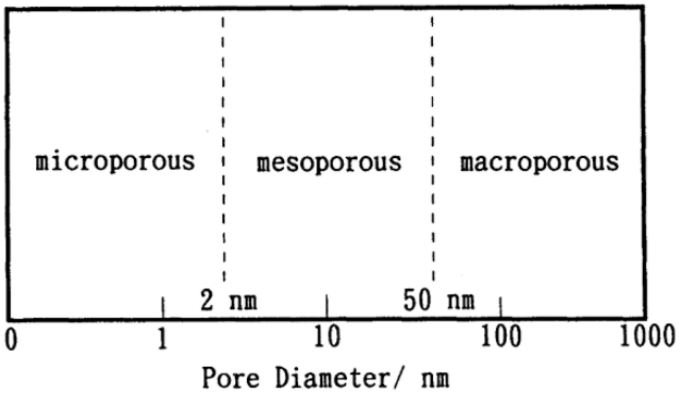

Figure 3.2. Classification of porous materials according to IUPAC standard (Ishizaki et al., 1998)

3.1. M41S Family Members

M41S family materials were discovered by Mobil Technology Company researchers while trying to identify new zeolites that could selectively convert high molecular weight petroleum-based molecules. First, they developed pillared layered materials that offered the ability to tune pore size, active site density, and composition; variables that the traditional aluminosilicate zeolites did not possess. Variation of pillar size and pillar density made available to tune the pore systems for desired applications. However, these pillared layered materials did not have sufficient thermal and

hydrothermal stability or catalytic activity. Also, varying pillar composition was not achieved as conceived. So, researchers worked to develop large pore frameworks by attempting to combine both the concepts of the pillared layer materials and the formation of zeolites, considering that some zeolites were formed via layered intermediates. Thus, if this intermediate could be isolated and used as a layered composition to form pillared porous materials, the resultant product would be composed of crystalline walls that would be thermally stable and catalytically active. With this approach, MCM-22 was developed, and with further studies, MCM-36, MCM-41, MCM-48, and MCM-50 materials were developed (Schwarz et al., 2004).

M41S family members have different methods of synthesis and applications based on stability and limitation of mesoporous structure. They are highly ordered materials with large specific surface area, hexagonal array, and uniform mesoporous channel. Therefore, these materials are generally used as adsorbents, catalysts, and supports. Among them, MCM-41 and MCM-48 are the most commonly used ones (Rahmat et al., 2010). Different structures of most widely used M41S family members are shown in Figure 3.3.

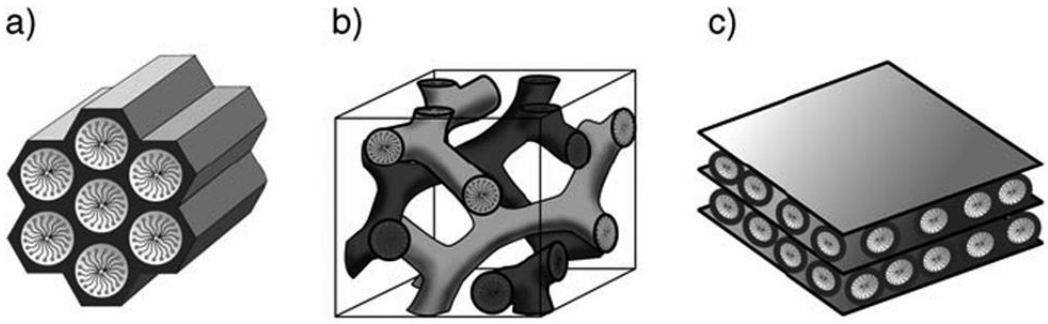

Figure 3.3. Different structures of M41S Family Members (a) MCM-41 (b) MCM-48 (c) MCM-50 (Gibson, 2014)

3.2. SBA-15

Since the introduction of mesoporous materials in 1992, significant progress has been made in their morphology control, pore size adjustment, composition variation, and application developments. The Stucky Group first introduced Santa Barbara Amorphous (SBA) type catalysts in 1998, and SBA-15 is the most famous member of that family (Ambili, 2011).

SBA-15 is a mesoporous silica sieve based on uniform hexagonally ordered mesopores interconnected by micropores (Figure 3.4) and these interconnections facilitate diffusion inside the entire porous structure (Obalı, 2010). SBA-15 exhibits favorable properties, which make it preferable for various applications such as adsorption and separation analytics, optics, catalysis, etc. (Thielemann et al., 2011). For example, the thickness of the framework walls is about 3.1 to 6.4 nm, which gives the material higher hydrothermal and mechanical stability than M41S family materials (Thielemann et al., 2011). Moreover, a high internal surface area of typically 400–900 m^2/g makes SBA-15 a well-suited material for various applications (Thielemann et al., 2011). Uniform pore size (4-30 nm), the small crystallite size of primary particles, and complementary textural porosity are other advantages of SBA-15 (Huirache-Acuna et al., 2013).

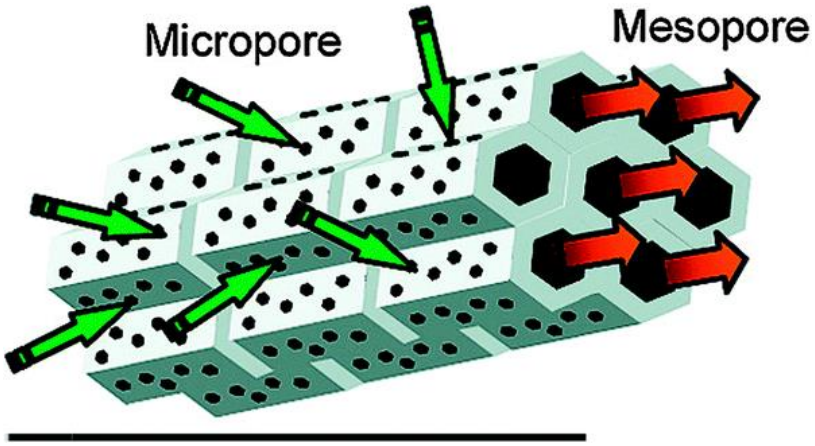

Figure 3.4. Structure of SBA-15 (Gibson, 2014)

SBA-15 is typically synthesized using triblock copolymer poly(ethylene oxide)-poly(propylene oxide)-poly(ethylene oxide) as a surfactant and tetramethyl orthosilicate (TMOS), tetraethyl orthosilicate (TEOS) or tetrapropyl orthosilicate (TPOS) as a silica source in a highly acidic media (Rahmat, 2010). Zhao et al. synthesized the ordered hexagonal SBA-15 with uniform pore size up to 30 nm using amphiphilic triblock copolymer in strongly acidic media, i.e., pH ~ 1. According to Zhao *et al.*, the use of non-ionic triblock copolymers provided remarkable advantages like easy separation, nontoxicity, biodegradability, and low cost as a surfactant in the synthesis of SBA family materials (Huirache-Acuna et al., 2013). Surfactants contain hydrophilic head groups and hydrophobic tail within the same molecule so it will self-organize itself to minimize the contact with incompatible ends. Removal of surfactant is a critical aspect in synthesis since this step affects the final properties of the desired porous structure. Calcination is the most widely used method for the removal of surfactant where washing with pure water or ethanol and extraction can be the other alternatives. Zhao *et al.* reported that the calcination of SBA-15 at 500 °C would result in the achievement of final porous material with pore volume fraction up to 0.85 and silica wall thickness of 31-64 angstroms (Zhao, 1998).

Despite favorable properties of SBA-15 in different applications, it is not possible to use them alone for catalytic activities due to the low acidity strength resulting in low catalytic activity. Modification or functionalization of SBA-15 can be done to overcome this problem. Modified and functionalized SBA-15 can be classified into three main classes given below (Rahmat, 2010).

- Functionalization SBA-15 with sulfonic, aminopropyl, imidazole, triazole group (Grieken et al., 2005, Li et al., 2008)
- Enzyme immobilization onto SBA-15, i.e., *Porcine pancreatic* Lipase, Cyctochrome-c (Li et al., 2009, Washmon-Kriel et al., 2000)
- Different types of metal support and incorporation into SBA-15 framework, i.e., Al, Ce, La, Ti, Mg, Ca, Pd-Zn, Co (Calles et al., 2009, Eswaramoorthie et al., 2009 Kim et al., 2004, Prieto et al., 2009 Vizcaino et al., 2009, Yue et al., 2000)

3.3. Heteropoly Acids (HPAs)

A heteropoly acid (HPA) is "a class of acids made up of a particular combination of hydrogen and oxygen with certain metals and non-metals" (Gupta et al., 2014)). HPAs are usually formed of a central ion which is bonded to various numbers of oxygen and surrounded by a cluster of octahedral metallic species bonded via shared oxygen atoms (Augustine, 1996). This structure is illustrated in Figure 3.5 for 12-tungstophosphoric acid.

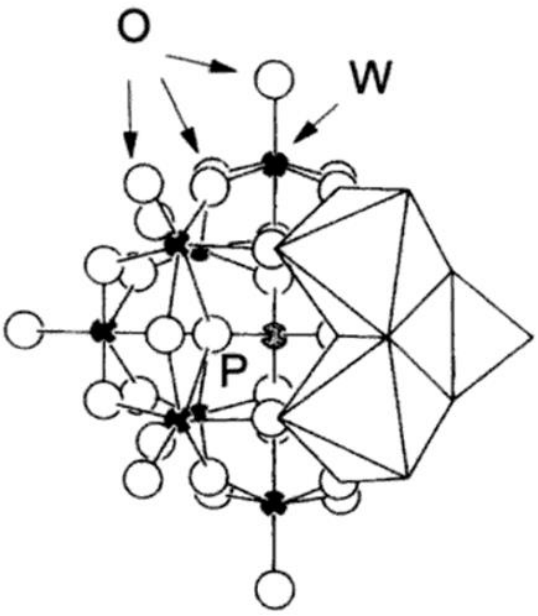

Figure 3.5. Keggin structure of $PW_{12}O_{40-3}$ (Augustine, 1996)

The main compounds that HPAs contain are listed below (Gupta et al., 2014; Augustine, 1996).

- An “addenda” atom-metallic species associated with the octahedral structure such as tungsten, molybdenum, or vanadium;
- Oxygen;
- A central atom or “heteroatom” commonly from the p-block of the periodic table such as silicon, phosphorus or arsenic termed as hetero-atom;
- Acidic hydrogen atoms

There are various types of HPAs with different structures each. Examples of these structures are given as (Patel, 2013);

- Keggin structure
- Wells-Dawson structure
- Silverton structure
- Waugh structure
- Anderson structure

Keggin and Dawson are the most commonly known structures of HPAs (Figure 3.6). Keggin heteropoly acids have the general formula of $X^{n+}M_{12}O_{40}^{n-8}$, where X is the heteroatom, n is the oxidation degree, and M is the addenda atom. Wells-Dawson heteropoly acids have the general formula of $[X_2M_{18}O_{62}]$, where X is the heteroatom (P^{5+}, S^{6+}, As^{5+}), and M is the addenda atom (W^{6+} or Mo^{6+}).

HPAs have very strong acidity compared to conventional solid acids. Patel attributed this strong acidity to the "delocalization of surface charge density throughout the large-sized polyanion, leading to a weak interaction between the protons and the anion." The acidity of HPAs can be modified by changing heteroatom and metallic species.

HPAs are widely used as catalysts in a variety of applications in virtue of its many beneficial properties such as excellent water-tolerant ability, strong Brønsted acidity, high catalytic activity, and stability (Gupta et al., 2014). However, there are some disadvantages of HPAs, including thermal stability and low surface area, which disable them to be used alone effectively for catalytic activities. These problems can be overcome by adding support materials.

(a) **(b)**

Figure 3.6. Keggin and Wells-Dawson structures (a) Keggin structure (b) Wells-Dawson structure (Patel, 2013)

CHAPTER 4

LITERATURE SURVEY

Disposal of plastic wastes has been a significant environmental problem due to the considerable increase in the consumption of plastics everywhere. That is why plastic recycling has been a trendy research area to find promising solutions for this environmental problem. Among the plastic recycling methods, chemical recycling in which plastic materials are converted into liquid or gaseous products is a favorable way to treat plastic wastes. In this method, pyrolysis is one of the most common techniques used in which polymers are thermally degraded under inert atmospheres at high temperatures. Pyrolysis can be carried out both catalytically and non-catalytically. Many types of catalysts can be used for catalytic thermal degradation of polymers. Below, some studies for the synthesis of the catalysts and degradation of polymers in the literature are reviewed.

4.1. Catalyst Properties

Fulvio *et al.* (2005) reported a short-time synthesis of SBA-15 by using two different silica sources; sodium metasilicate ($Na_2SiO_3 \cdot 9H_2O$) and tetraethyl orthosilicate (TEOS). They synthesized SBA-15 from sodium metasilicate, in which the self-assembly step is limited to 2 hours instead of 24 hours, usually used. An SBA-15 sample was also prepared from TEOS by using the same recipe for comparison. Samples were treated hydrothermally at 100 ^{o}C for 48 h. Calcined samples were characterized, and both samples were highly ordered according to the results of small-angle X-ray scattering (SAXS). When the surface areas and pore volumes were compared, it was observed that surface areas were similar while the pore volume of the sample prepared from TEOS was slightly larger than the sample synthesized from

sodium metasilicate. However, the latter exhibited higher microporosity and thicker walls. It was concluded that the self-assembly step of the synthesis could be reduced from 24 h to 2 h.

Kozhevnikov (2007) focused on several approaches that can be useful in overcoming the deactivation of HPA catalysts in his study. One of these approaches was the development of novel HPA catalysts such as solid catalysts comprising W (VI) polyoxometalates on ZrO_2 and Nb_2O_5, which exhibit good regeneration and reuse. Still, they have weaker acid sites and lower catalytic activity than standard HPA catalysts. The second approach was the modification of HPA catalysts by Pt and Pd in order to enhance coke combustion. By this method, effective catalyst regeneration by coke combustion at 350^oC without destroying the structure of HPA could be obtained. The third approach was preventing the coke formation on HPA catalysts by the addition of nucleophilic molecules such as water, methanol, and acetic acid. These molecules, mainly water, was very useful in removing coke from the catalyst surface. Another approach in this study was using supercritical fluids in the heterogeneous catalysts. The lifetime of HPA catalysts was found to be considerably longer in supercritical systems compared to gas and liquid systems.

Obalı *et al.* (2009) studied the effect of MCM-like aluminosilicate catalysts in the polypropylene pyrolysis reaction. MCM-41-like catalysts using different aluminum sources and different Al/Si ratios were synthesized via hydrothermal method. Lower Al/Si ratios provided more effective aluminum incorporation into the structure. When aluminum nitrate was used as the aluminum source, incorporation to the structure was higher, and this type of catalysts reduced the degradation temperature and activation energy of the reaction more than aluminum isopropoxide containing catalysts.

Brahmkhatri *et al.* (2011) synthesized 12-tungstophosphoric acid anchored SBA-15 material for biodiesel production. SBA-15 was synthesized without hydrothermal conditions. Then TPA in the ratio of 10-40% was impregnated to SBA-15. According

to the surface area, pore size and, pore volume results, it was observed that as the TPA loading increases, surface area, pore diameter, and pore volume sharply decrease compared to the SBA-15 support. Due to the location of the TPA species in the mesopores of SBA-15. All synthesized materials showed Type IV isotherms and exhibited H1 hysteresis loop, which is a characteristic of mesoporous solids. XRD results of TPA impregnated SBA-15 catalysts showed that TPA was dispersed well in the hexagonal channels of SBA-15. Morphology of the synthesized catalysts was analyzed by SEM, and according to the results, the surface morphology of the catalysts was very similar to the pure SBA-15, showing good dispersion of TPA in the SBA-15 support.

Obalı *et al.* (2011) synthesized aluminum loaded SBA type catalysts using different aluminum sources and Al/Si ratios and investigated their effect in the polypropylene degradation reaction. Aluminum loaded SBA-15 catalysts were synthesized via impregnation, and aluminum isopropoxide and aluminum sulphate were used as the aluminum sources. According to the characterization results, aluminum incorporated into the structure very effectively for all synthesized catalysts, and they had mesoporous structure, high surface area, and it exhibited type IV nitrogen adsorption/desorption isotherm with H1 hysteresis loop. When TGA analysis results were compared, catalysts synthesized using aluminum sulphate decreased the activation energy value of the degradation reaction more than catalysts synthesized with aluminum isopropoxide. It was deduced that catalysts synthesized using aluminum sulphate were more effective than the other one in the polypropylene degradation reaction.

Aydemir *et al.* (2012) synthesized TPA impregnated SBA-15 catalysts and studied their effect on polyethylene degradation reaction. SBA-15 was synthesized via the hydrothermal method, and TPA was incorporated into the structure with different W/Si ratios. All synthesized materials exhibited Type IV isotherm with H1 type hysteresis loop. TPA was effectively incorporated into the structure of the catalysts,

and they all had Lewis and Brønsted acid sites. With an increase in the TPA amount of the catalysts, degradation temperature, and activation energy of the degradation reaction decreased. TPA impregnated SBA-15 catalysts helped to reduce the activation energy to nearly half-value of the value obtained from the non-catalytic reactions.

Chen *et al.* (2013) synthesized mesoporous molecular sieves MCM-41 and bulk 12-tungstophosphoric acid (TPA) to prepare 5-45 wt% TPA/MCM-41 mesoporous materials for catalytic oxidation of benzaldehyde to benzoic acid. The wet impregnation method was used for the synthesis of the mesoporous materials. According to the characterization results, TPA units were highly dispersed on the MCM-41 supports, and the materials retained their mesopore structure when the TPA loading was less than 35 wt%. However, when loading was more than 40 wt%, poor dispersion and agglomeration of the TPA were observed. With increasing TPA loading, surface area, and pore volume of the catalysts decreased.

Aydemir *et al.* (2016) synthesized aluminum incorporated MCM-41 catalysts with different Al/Si ratios and studied their performance in polyethylene pyrolysis reaction using thermogravimetric analysis. All the synthesized catalysts showed mesoporous structure and exhibited Type IV isotherm with H2 type hysteresis loop. Aluminum incorporation created Brønsted acid sites in the catalyst structure. The degradation temperature of the polyethylene decreased effectively in the presence of the synthesized catalysts. However, activation energy increased with an increase in the aluminum amount in the catalyst, and this result is not expected. This was attributed to the non-uniform distribution of aluminum in the MCM-41 structure.

Che *et al.* (2019) studied the preparation of ZSM-5 catalysts and modification of it using green templates such as sucrose, cellulose, and starch to create additional mesopores. When ZSM-5 was modified with sucrose and cellulose, an increase in the

micropores was observed. When starch was used for modification, mesopore volume increased, and this favored the production of more aromatics.

4.2. Degradation of the Polymer

Puente *et al.* (1998) tested the performance of various acidic catalysts in the conversion of polystyrene into benzene at 550 °C in a fluidized-bed batch reactor. They used; mordenite, zeolite ZSM-5, sulfur-promoted zirconia (S-ZR), and an equilibrium conventional fluid catalytic cracking catalyst (E-CAT) as catalysts. Experiments were performed with very short contact times of up to 12 s. Depending on the catalyst properties and the contact time, main products were in the gasoline range, including benzene, toluene, ethylbenzene, styrene, and minor amounts of C_{9-12} aromatics and light C_5 compounds. The high amount of coke was formed. According to the comparison of performances of the different catalysts used in this study, E-CAT (conventional FCC catalyst) showed the best product distribution in terms of gasoline composition when yields were compared.

Walendziewski (2002) carried out two series of experiments for the cracking of waste polymers (Walendziewski, 2002). Polyethylene, polystyrene, and polypropylene were chosen as polymers. The first series of polymer cracking experiments were carried out in a glass reactor at atmospheric pressure and in a temperature range of 350-420 °C, the second one in an autoclave under hydrogen pressure (3-5 MPa) in the temperature range of 380-440 °C. The effect of reaction temperature, catalyst, the composition of the polymer feed on product yield and distribution was investigated. According to the results of the experiments, catalysts lowered the reaction temperature as well as boiling temperature range and density of the liquid products. In addition, catalyst increased gas product yield, but no apparent effect of the catalyst on gas composition was observed. Gas composition was found to be dependent on feed composition and process conditions. Cracking of polymers under atmospheric pressure and hydrogen pressure (3-5 MPa) was compared. Cracking of waste plastics in autoclaves under

hydrogen pressure at a long contact time and high temperature resulted in higher conversion (the difference between the weight of the feed and the residue), higher gas and gasoline fraction yields and relatively lower boiling and lower freezing point products.

Durmuş *et al.* (2005) studied the thermal degradation of additive-free polypropylene powder over different types of zeolite catalysts. As catalysts, Zeolite Beta (BEA), Zeolite Socony Mobil-5 (ZSM-5), and Mordenite (MOR) were used. Surface areas, Si/Al molar ratios, and pore structures of these catalysts were different from each other. Degradation rates of polypropylene in the presence of zeolite catalysts were determined by thermogravimetric analysis. Results showed that, catalytic activity of zeolites decreased as BEA>ZSM-5a (Si/Al = 12.5)>ZSM-5b (Si/Al = 25)> MOR. It was concluded that acidity, pore structure, and pore size are critical factors to determine the activity of catalyst in polymer degradation reaction.

Aguado *et al.* (2007) investigated the catalytic activity of zeolitic and mesostructured catalysts in the cracking of pure and waste polyolefins. Pure low-density polyethylene, pure high-density polyethylene, and recycled polyethylene were used. As zeolitic catalysts, standard ZSM-5, nanocrystalline n-ZSM-5 and Zeolite Beta were used. As mesostructured catalysts; Al-MCM-41 synthesized with different methods such as hydrothermal, sol-gel, and aluminum loaded SBA-15 were used. Mesostructured catalysts showed weaker acidic properties than the zeolitic catalysts. However, their pore size was larger than the zeolitic catalysts. According to the cracking analysis, standard ZSM-5 showed the lowest activity on the polyolefins except for high-density polyethylene. This was attributed to its microporous structure hindering the access of large polymer molecules to the acid sites. Besides, nanocrystalline n-ZSM-5 showed the highest activity, and this was attributed to its strong acidity combined with the small crystal sizes which allow the access of the polymer molecules into the acid sites. When polymer types were compared, a significant reduction was observed in the catalytic activity of polyethylene waste. This was attributed to two things; 1) cross-

linking reactions which occur in the polymer through its use and this makes the polymer more resilient to the catalytic degradation, 2) extraneous matters such as additives, dust, etc. which reduce the catalytic activity of the acid sites or favor the coke formation. In conclusion, nanocrystalline n-ZSM-5 and hydrothermal Al-MCM-41 showed the strongest catalytic activities for the degradation of pure and polyethylene waste.

Kaminsky *et al.* (2007) studied the Lewis acids and mixtures of Ziegler-Natta catalysts in the pyrolysis of polypropylene. Pyrolysis experiments were carried out in a batch reactor and a fluidized bed reactor under different conditions. $AlCl_3$ and mixture of $TiCl_4$ and $AlCl_3$ in the weight ratio of 1:1 were used as the catalyst. In the absence of catalyst, longer chain hydrocarbons were obtained compared to the use of catalysts. The use of $AlCl_3$ or mixture of $TiCl_4$ and $AlCl_3$ catalysts in the pyrolysis process reduced the process temperature dramatically. In the use of 0.1% $AlCl_3$ catalyst, products obtained at 400 °C were found to be very similar to the products obtained at 500 °C in the absence of a catalyst. Pyrolysis of polypropylene was also possible at 300 °C when higher amounts of the catalyst were used. According to the analysis, the increase in the amount of catalyst led to a rise in the light oil fraction (< C13) and gas fraction amounts.

Chaianansutcharit *et al.* (2007) studied the degradation of polypropylene and polyethylene over pure hexagonal mesoporous silica (HMS) and aluminum-containing hexagonal mesoporous silica (Al-HMS) catalysts in liquid-phase-contact (LPC) and vapor-phase-contact (VPC) modes at 380 °C and 430 °C. Pure HMS and Al-HMS with different Si/Al mole ratios were used as catalysts. Effects of aluminum content, cracking temperature, and catalyst contact mode (LPC and VPC) on the product yield, product distribution, degradation rate were investigated. In LPC mode, catalyst and polymer were heated together, and melted polymer was in contact with the catalyst. In VPC mode, polymers were heated to obtain volatile compounds first, and then these compounds contacted with the catalyst. Results showed that pure silica

HMS catalyst did not have any catalytic activity in the degradation of polypropylene and polyethylene. Mainly hydrocarbons with boiling point temperature range of 36-405 °C were obtained as liquid products where propene, butane, and ethane were the mainly observed gaseous products. For the Al-HMS catalysts, it was observed that degradation rates of PP into liquids in LPC and liquid yields increased with an increase in aluminum content. An increase in the degradation temperature also increased the degradation rate without any change in product distribution. In VPC, increasing the amount of aluminum content and the cracking reaction temperature reduced the liquid product yield while increasing the gaseous product yield.

Obalı *et al.* (2012) investigated the catalytic activity of aluminum-containing MCM-41 and SBA-15 catalysts in the thermal degradation of polypropylene. For catalytic degradation reactions, the weight ratio of polymer to the catalyst in the mixture was adjusted as two. Degradation temperature of pure polypropylene shifted to a lower temperature range in the presence of both types of catalysts. Increasing the reaction time and temperature led to an increase in the amount of liquid product and a decrease in the amount of residue. Methane, ethane, acetylene, ethylene, propylene, and butane were obtained as gaseous products in the non-catalytic degradation of polypropylene. With an increase in temperature, the selectivity of methane, butane, propylene, and acetylene increased where selectivity of ethylene decreased. In the catalytic thermal degradation reaction, ethylene, propylene, n-butane, and i-butane gases were obtained as products where methane, ethane and acetylene gases did not form. MCM-41 and SBA-15 type catalysts showed similar liquid product distribution. Both types of catalysts improved the yield of gaseous products and provided better selectivity in the product distribution. They were both effective in converting polypropylene into lighter hydrocarbons, which were in the carbon range of C_5-C_{12}.

Aydemir *et al*. (2013) studied the catalytic performance of alumina impregnated MCM-41, and tungstophosphoric acid loaded SBA-15 in the pyrolysis of polyethylene. Both MCM-41 and SBA-15 were synthesized via hydrothermal method.

According to the thermogravimetric analysis, aluminum impregnated MCM-41 type catalysts did not cause a significant change in the activation energy of the PE degradation, where TPA loaded SBA-15 catalysts reduced the activation energy considerably. However, MCM-41 materials reduced the degradation temperature of PE more effectively than TPA loaded SBA-15 materials. Polyethylene pyrolysis reactions were carried out catalytically and non-catalytically under the nitrogen atmosphere at 390 °C and 430 °C for 15 minutes. According to the degradation reaction gas product results, MCM-41 materials were selective to propylene, n-butane, and iso-butane where TPA loaded SBA-15 materials were highly selective to ethylene and n-butane. For TPA loaded SBA-15 materials, liquid pyrolysis products were distributed in a range of C_8 to C_{14}, and for aluminum loaded MCM-41 materials, liquid pyrolysis products were distributed in a range of C_5-C_{14}. An increase in TPA and aluminum loading for SBA-15 and MCM-41 increased the liquid product yield. Results showed that both catalysts improved gaseous product yield and selectivity.

Bursalı (2013) investigated the catalytic activity of SAPO-34 catalyst in the degradation of polypropylene and polystyrene. Microporous SAPO-34 was synthesized using the hydrothermal method. Pyrolysis experiments were carried out at different temperatures; 315 °C, 400 °C, 425 °C, 440 °C for 15 and 30-minute reaction times. SAPO-34 catalyst reduced the activation energy of polypropylene from 172 kJ/mol to 131±11 kJ/mol. It also decreased the activation energy of polystyrene degradation reaction from 357±4 kJ/mol to 262±4 kJ/mol. In the non-catalytic thermal degradation reactions of PP, mainly gas products were obtained where the yield of liquid products increased with increasing reaction temperature. In catalytic thermal degradation reactions, a high amount of gas products was obtained, and the yield of liquid products increased with increasing reaction temperature.

Aydemir *et al.* (2016) studied the performance of aluminum incorporated MCM-41 catalyst in the polyethylene pyrolysis reactions. Pyrolysis reactions were carried out catalytically and non-catalytically. Acetylene, ethane, ethylene, propylene, propane,

and n-butane were obtained as gaseous products from non-catalytic reactions. In the catalytic reactions, propane was not formed where i-butane was observed. When the aluminum amount was increased in the catalysts, liquid hydrocarbons in the range of C_{13}-C_{18} degraded to the lower hydrocarbons in the range of C_5-C_{12}.

Jiraroj *et al*. (2016) studied the catalytic cracking of polypropylene using SBA-15 and MCM-22 catalysts. SBA-15 catalyst was synthesized using the hydrothermal method. Alumina was integrated into SBA-15 using sodium aluminate in different ratios, and Na-Al-SBA-15 catalysts were derived. MCM-22 catalyst was also synthesized via the hydrothermal method, and sodium aluminate was used to obtain Na-MCM-22 catalysts in different SiO_2/Al_2O_3 ratios. Besides, Na^+ ion exchange for H^+ was carried out for the synthesized SBA-15 and MCM-22 catalysts and derived catalysts were named H-Al SBA-15 and H-MCM-22. According to the catalyst characterization, BET specific surface areas of the catalysts decreased with an increase in the aluminum content. Besides, aluminum addition to the catalysts increased the acid strength of SBA-15, where acid strength of MCM-22 catalysts remained similar at different SiO_2/Al_2O_3 ratios. For the cracking process, PP waste was used as 5 g where the catalyst was used at 10 wt% of the PP. The reaction temperatures were chosen as 350, 380, and 400 ^oC and reaction time was 30 min. Reaction was carried out under nitrogen flow. Effect of Na^+ ions, aluminum content, and reaction temperature were investigated. PP conversion levels for the H-Al-SBA-15 and H-MCM-22 catalysts were 92-98% and 49-95%, respectively. H^+-form of the catalysts provided higher product value compared to the Na^+-form. When H-Al-SBA-15 was used, the main product was the liquid fraction, and when H-MCM-22 was used, the main product was gas fraction. For H-MCM-22, conversion of PP to gas and liquid products, and gas fraction yield increased with a decrease in the Al content where high Al content led to the high amount of C_7-C_8 hydrocarbon products in the liquid fraction for H-Al-SBA-15. Increasing the reaction temperature from 350 to 400 ^oC led to a higher PP conversion to gas and liquid products for H-MCM-22 while this did not make a considerable effect when the H-Al-SBA-15 catalyst was used.

Li *et al*. (2016) studied the catalytic performance of microporous and mesoporous catalysts in the pyrolysis of plastic waste. As microporous catalysts; 1) Highly uniform nanocrystalline Zeolite Socony Mobil-5 (HUN-ZSM-5), 2) Conventional ZSM-5 (C-ZSM-5) and 3) β-zeolite, as mesoporous catalysts; 1) Highly hydrothermally stable Al-MCM-41 with accessible void defects (Al-MCM-41 (hhs)), 2) Kanemite-derived folded silica (KFS-16B) and 3) Well-ordered Al-SBA-15 (Al-SBA-15(wo)) were used. As plastic waste, polyethylene/polypropylene mixture with a 6/5 ratio was used. HUN-ZSM-5, Al-MCM-41(hhs), and Al-SBA-15(wo) were modified and remaining catalysts were used for comparison. PE/PP mixture showed different thermal behavior in comparison with single PE and PP. Negligible amounts of solid residue were produced, indicating high conversion. According to the pyrolysis results, microporous catalysts showed higher gas yields in comparison with the mesoporous catalysts. This was attributed to the high acidity of the zeolitic catalysts. Among the microporous catalysts, C-ZSM-5 exhibited the highest cracking activity where Al-SBA-15(wo) showed the weakest cracking activity among all of them.

Chi *et al*. (2018) investigated the pyrolysis of polypropylene and cellulose using MCM-41 and Al-MCM-4. Co-pyrolysis of cellulose and polypropylene was also studied in this research. In the presence of both catalysts, the pyrolysis temperature of PP decreased from 458^{o}C to 340^{o}C. Also, the activation energy value of PP decreased remarkably when both catalysts were used. When PP was added to cellulose in the pyrolysis reactions, the yield of olefins and aromatic hydrocarbons increased significantly. Al-MCM-41 was found to have a better cracking effect providing a higher yield of olefins and aromatics.

Qi *et al.* (2018) studied the pyrolysis of Nannochloropsis sp. (NS), PP, and their mixture in the presence and absence of HZSM-5 catalyst. Researchers investigated the effects of reaction temperature (500^{o}C-900^{o}C) and the mass ratios of NS/PP and feedstock/catalyst on the product distribution. Compared to the pyrolysis of NS and PP separately, their co-pyrolysis with 1:1 NS/PP mass ratio favored the formation of

aromatic hydrocarbons. When the reaction temperature increased, liquid product and solid residue yield decreased while gas product yield increased.

Rajabali Habib (2019) investigated the performance of aluminum and TPA loaded silica aerogel support in the pyrolysis of polyethylene and polypropylene. Pyrolysis temperatures were 400^{o}C and 430^{o}C. Metal loading decreased the activation energy of both PP and PE degradation reactions. Aluminum and double metal (Al&TPA) loaded catalysts were propylene selective, while TPA loaded catalysts were isobutene selective in the PP degradation reactions at 400^{o}C. All metal loaded catalysts were methane selective in the PE degradation reactions at 430^{o}C. The use of catalysts in the pyrolysis of PP and PE resulted in an increase in the C_5-C_{12} hydrocarbon product range.

4.3. Aim of the Study

This brief review of the literature survey shows that there are various studies for catalytic degradation of polypropylene using different catalysts. However, there is few studies for thermal degradation of polypropylene over tungstophosphoric acid loaded catalysts. Therefore, the objective of this study is;

- To synthesize tungstophosphoric acid (TPA) loaded SBA-15 with different amount of TPA loading using one-pot hydrothermal method,
- To characterize synthesized catalysts using various methods,
- To determine kinetic parameters of polypropylene degradation reaction using a thermogravimetric analyzer (TGA),
- To investigate the activity of these catalysts and the product distribution for polypropylene pyrolysis reaction.

CHAPTER 5

EXPERIMENTAL METHOD

For the experimental part of this study, the catalytic activity of TPA loaded SBA-15 catalyst was investigated in polypropylene degradation reaction. This catalyst was synthesized at different W/Si ratios. For the first part of the experimental study, TPA loaded SBA-15 catalyst was synthesized and characterized using various characterization techniques such as X-Ray Diffraction, Physical adsorption, Scanning Electron Microscopy, Fourier Transform Infrared Spectroscopy. Then, the performance of the synthesized catalysts was tested in polypropylene degradation reaction using the thermogravimetric analyzer, and activation energies were determined. Finally, degradation reactions of polypropylene in the presence of synthesized catalysts were carried out, and products were identified using gas chromatography.

5.1. Synthesis of TPA Loaded SBA-15

Reagents used for the synthesis of TPA loaded SBA-15 is given below:

- **Surfactant:** Triblock copolymer poly (ethylene glycol)-poly(propylene glycol)-poly(ethylene glycol), (Sigma-Aldrich Co)
- **Silica Source:** Tetraethyl orthosilicate (TEOS), (Merck)
- **Acid Source:** Tungstophosphoric acid (TPA), (Acros Organics)
- HCl, fuming, (Merck)
- Deionized water

TPA loaded SBA-15 catalyst was synthesized hydrothermally at different W/Si ratios. Amount of TPA which will be added to the solution was calculated according to the method given in Appendix A. For the synthesis of the catalysts, 4 g of surfactant was dissolved in 120 ml, 2 M HCl solution and continuously stirred at a rate of 350 rpm at 40 °C for 4 hours. After 4 h, 8 g of TEOS was added to the mixture dropwise and continued stirring for another 30 min. The predetermined amount of TPA was dissolved in 2 ml deionized water. After 30 min, dissolved TPA was added to the mixture under stirring and kept stirring for 24 h. After 24 h, the final mixture was transferred into a teflon-lined stainless steel autoclave for the hydrothermal synthesis at 100 °C for 48 h. After 48 h, the final mixture was washed with deionized water, filtered, and dried in the oven at 80 °C for 24 h and at 60 °C for another 24 h. The solid product was calcined at 500 °C for 8 h in a tubular furnace with a flow of dry air to remove organic materials within the pores of the catalyst. The synthesis procedure of TPA loaded SBA-15 is given schematically in Figure 5.1. The naming of the synthesized materials is given in Table 5.1.

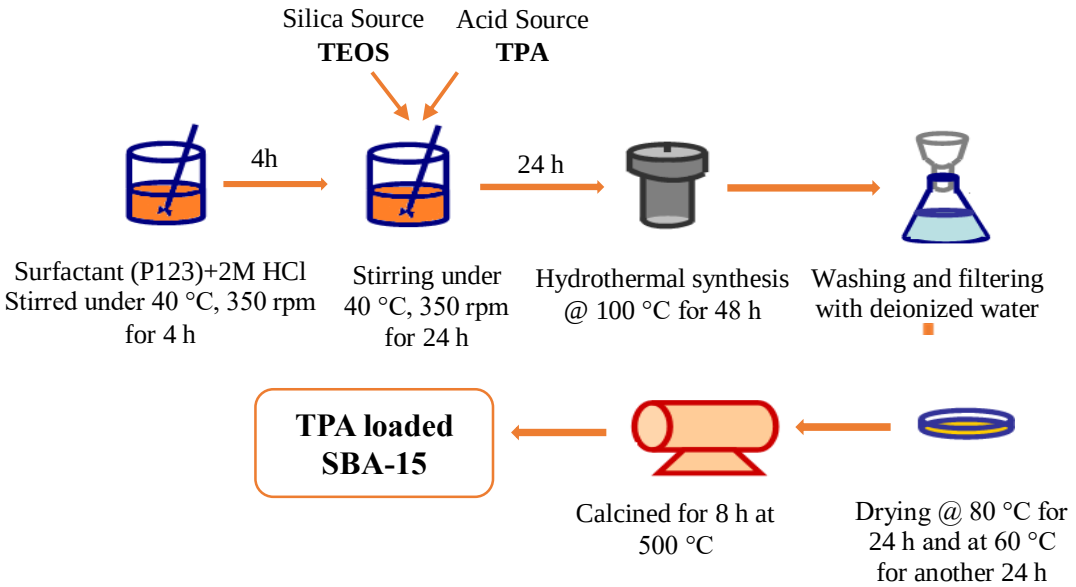

Figure 5.1. Synthesis procedure of TPA loaded SBA-15

Table 5.1. Naming of the synthesized materials

W/Si Molar Ratio	Material Name
0.05	SBA15-TPA0.05
0.10	SBA15-TPA0.10
0.15	SBA15-TPA0.15
0.20	SBA15-TPA0.20

5.2. Characterization of Catalysts

Synthesized materials were analyzed using various characterization techniques such as X-Ray Diffraction, Physical Adsorption, Scanning Electron Microscopy, and Diffuse Reflectance Infrared Fourier Transform Spectroscopy for the determination of their structural and physical properties. Detailed information about these characterization techniques is given below.

5.2.1. X-Ray Diffraction (XRD)

X-ray diffraction is an advantageous method for visualization of the crystal structure of the materials. Rigaku Ultima-IV Diffractometer was used for small and wide angle X-ray diffraction analysis of the samples in Central Laboratory at METU. The Bragg angle range for small angle analyses was 0.8^0 to 8^0, and for wide angle analyses was 5^0 to 80^0. The scanning rate for small angle analyses was 0.1^0/min, where scanning rate for wide angle analyses was 2^0/min. Analyses were performed at 40 kV and 40 mA with Ni-filtered CuK α_1 radiation.

5.2.2. Physical Sorption

The adsorption of gases onto porous solids is a primary method by which the physical properties of solids are characterized (Fraissard, 1997). Specifically, the surface area, pore volume, and pore size distribution can be inferred and calculated from the analyses of the relationship between the volume adsorbed and the pressure of a physically adsorbing gas.

In this study, nitrogen adsorption was done to determine the physical properties of samples using Micromeritics Tristar II 3020 equipment at the METU Department of Chemical Engineering. The analyses were performed at a relative pressure range of 0.0000065 to 0.99 at a liquid nitrogen temperature of 77.3 K. The samples were degassed at 200°C for 3 hours before the analysis.

5.2.3. Scanning Electron Microscopy (SEM) & Energy Dispersive X-ray Spectroscopy (EDS)

The scanning electron microscope is used to get information about the morphology of the materials. In this method, the area to be examined is irradiated with an electron beam, and the signals obtained from specific emission volumes within the sample are used to determine morphologic properties of the sample such as surface topography (Goldstein, 1981).

In this study, analyses were carried out using QUANTA 400F Field Emission Scanning Electron Microscope at METU Central Laboratory. Special sample preparation was done before the analysis. First, small pieces of double-sided sticky carbon tapes were attached onto the metal apparatus, which is used in the equipment. Then, small amounts of samples were put onto the carbon tapes one by one. Finally, samples were coated with gold and palladium prior to the analyses to prevent the accumulation of static electric charge.

Energy dispersive X-Ray spectroscopy analysis was carried out to get information about the elements in the synthesized samples. JSM 6400 Electron Microscope equipped with NORAN system 6X-Ray Microanalysis System & Semafore Digitizer was used for this analysis.

5.2.4. Diffuse Reflectance Infrared Fourier Transform Spectroscopy (DRIFTS)

DRIFTS analyses of the synthesized materials were performed at the wavelength between 400-4000 cm^{-1}. First, fresh samples were analyzed without any treatment. Then, to examine acid sites of the samples, pyridine was added, and samples were dried at 40 ^{o}C for 2 h. Then, these samples were analyzed. After that, the difference of the spectra of pyridine adsorbed samples and the spectra of pyridine free samples were taken to get information about the acid sites of the materials.

5.3. Thermogravimetric Analysis (TGA)

In this study, isotactic polypropylene (Aldrich Co.) with average M_w 250,000, average M_n 67,000, density 0.9 g/ml, melt index 12 g/10 min, and a melting point range of 160-165 ^{o}C was used.

Thermogravimetric analysis was carried out to test the performance of the synthesized catalysts in the degradation reaction of polypropylene and to determine the activation energy of polypropylene degradation reaction. Catalyst/polymer ratio was determined from the literature study. In the literature (Kasapoğlu., 2013), TGA analysis for the polymer-catalyst mixtures at different weight ratios was carried out, and it was found out that the catalyst to polymer ratio of ½ decreased the degradation temperature most. Therefore, this ratio was chosen for the experiments in this study. The Shimadzu DTG-60H equipment at the METU Department of Chemical Engineering was used. TGA experiments were performed for samples prepared with a catalyst/polymer ratio of ½,

and analysis was carried out under a nitrogen atmosphere with a flow rate of 60 cc/min. The temperature range and heating rates were 300-600 ^{o}C and 5^{o}C/min, respectively.

The amount of coke formation in the used catalysts was also found using the thermogravimetric analyzer. Used catalysts were analyzed under air at 60cc/min with a heating rate of 5^{o}C/min at a temperature range between room temperature and 900 ^{o}C.

5.4. Polymer Degradation System

5.4.1. Experimental Setup

The performance of the synthesized catalysts in the polypropylene degradation reaction was tested in a degradation reaction system. A schematic diagram for the degradation reaction system is given in Figure 5.2. Nitrogen was selected as the carrier gas, and it was fed to the system from a nitrogen tank entering the reactor from the lower part of the reactor. The flow rate of the carrier gas was adjusted using a rotameter. A soap bubble meter was used to check the gas flow rate of nitrogen. Degradation reaction took place in a glass reactor. The bottom of the reactor was designed spirally and filled with glass particles so as to increase the contact surface area to provide the carrier gas to reach the reaction temperature before entering the reaction part. There was a porous part above the spiral part of the reactor, where the polymer and catalyst were put together. This porous glass provided good dispersion of gas while preventing the backflow of the polymer melt into the spiral part.

Glass reactor was placed in a tubular furnace, and it was heated up to the desired reaction temperature. The tubular furnace was covered with an isolating material to prevent heat loss during the reaction. The reactor temperature was measured using a thermocouple inserted into the reactor, and thermocouple was connected to a digital thermometer readout. The connection line between the reactor and the condenser was

heated by heating tape. The temperature of the heating tape was controlled and heated up to the reaction temperature in order to prevent the early condensation of the products.

Vapors coming from the reactor was sent to the spiral condenser. Cold water coming from the water bath was used to cool down the non-volatile vapors. Condensed liquid products were collected in the glass collectors surrounded by water cooling jackets. Non-condensable gas products were collected in a gas balloon.

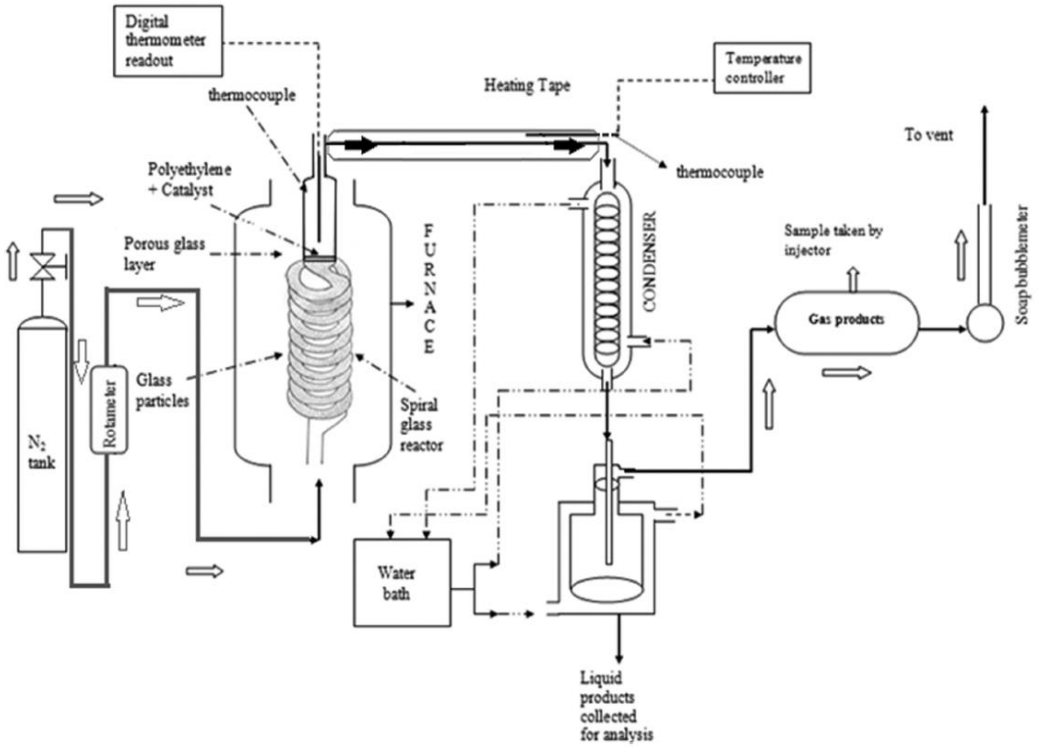

Figure 5.2. Schematic diagram for degradation reaction system (Aydemir et al., 2013)

5.4.2. Experimental Procedure

The catalytic thermal degradation of polypropylene was carried out under nitrogen with a flow rate of 60 cc/min under atmospheric pressure. Catalyst and polymer were used in a catalyst/polymer weight ratio of ½. 1 gr of polypropylene and 0.5 gr of catalyst were weighed and put into the reactor from the upper part. The thermocouple was inserted into the reactor, and fittings were tightened. After starting the nitrogen flow to the system, potential gas leakages were checked. The furnace temperature was adjusted to the desired reaction temperature with a constant heating rate of 5°C/min using an electric furnace. The heating tape which was used to heat the connection between the reactor and the condenser was also adjusted to the same temperature and kept constant. The temperature of the water bath was set to approximately -9°C using spirit, for the condensation of the products. The flow rate of the nitrogen was adjusted using a rotameter. During the experiment, furnace temperature, reactor temperature, gas flow rate, and water bath temperature were recorded at intervals of 15 minutes. During the reaction, gas products were collected within the gas sampling bulb and taken from there by using a gas-tight injector for gas chromatography analysis. Then, the system was cooled down to the room temperature, solid residue/catalysts, and liquid products were collected, weighed, and recorded. The amount of solid residue was found taking the difference between the remaining solid amount at the end of the reaction and initial catalyst amount. The amount of gas products was also calculated taking the difference between the initial polymer amount and the total amount of solid residue and liquid products. The experimental conditions of the reactions are given in Table 5.2. Experiments with SBA15-TPA 0.05 at 315 °C and 400 °C were carried out two times in order to ensure the reproducibility of the results.

Table 5.2. Experimental conditions for catalytic thermal degradation reactions of polypropylene

Sample	Reaction Temperature (°C)	Reaction Time (min)
PP + SBA15-TPA0.05	315	30
PP + SBA15-TPA0.10	315	30
PP + SBA15-TPA0.15	315	30
PP + SBA15-TPA0.20	315	30
PP + SBA15-TPA0.05	400	30
PP + SBA15-TPA0.10	400	30
PP + SBA15-TPA0.15	400	30
PP + SBA15-TPA0.20	400	30

5.4.3. Product Analysis Procedure

Gas products obtained from the experiments were analyzed using gas chromatography equipment. Gas samples were collected from the gas balloon using a gas-tight syringe to avoid gas loss. Gas products were collected as soon as the reaction ends and injected into the gas chromatograph.

5.4.3.1. Gas Product Analysis

Gas products were analyzed using Varian Star Chromatography Workstation version 6.2 program, and analysis conditions are given in Table 5.3. A packed column (Porapak Q) with the sizes of 6' and 1/8" was used for the analysis.

Table 5.3. Gas chromatography analysis conditions for gas products

Oven Temperature (ºC)	80 (isothermal)
Injection Temperature (ºC)	110
Injection Amount (µL)	0.3
Detector Type	TCD
Detector Temperature (ºC)	120
Column Pressure (psi)	30
Analysis Time (min)	35
Carrier Gas	He
Carrier Gas Flow Rate (ml/min)	30

5.4.3.2. Liquid Product Analysis

Liquid products were collected in the system, kept in the suitable collecting bottles with tightened lids to avoid evaporation. These products were taken from the collecting bottles using suitable a syringe and analyzed using GC equipped with HP-5 capillary column (28.5 m x 0.320 mm x 0.25 µm). GC analysis conditions for liquid products are given in Table 5.4.

Table 5.4. Gas chromatography analysis conditions for liquid products

Oven Temperature	40 ºC (10 min hold) to 150 ºC at 5 ºC/min (15 min hold) and then to 200 ºC at 1 ºC/min (70 min hold)
Injection Temperature (ºC)	210
Injection Amount (µL)	0.5
Detector Type	FID
Detector Temperature (ºC)	225
Column Pressure (psi)	5
Analysis Time (min)	167
Carrier Gas	He
Carrier Gas Flow Rate (ml/min)	1.5
Split Ratio	100:1

CHAPTER 6

RESULTS AND DISCUSSION

In this study, TPA loaded SBA-15 catalysts were synthesized with different W/Si ratios using the one-pot hydrothermal method. The synthesized catalysts were characterized using various methods such as X-Ray Diffractometer, Physical Sorption, Scanning Electron Microscopy (SEM), Energy Dispersive X-Ray Spectroscopy, and Diffuse Reflectance Infrared Fourier Transform Spectroscopy (DRIFTS). The performance of the synthesized catalysts in the degradation reaction of polypropylene was also tested using a thermogravimetric analyzer with a catalyst/polymer weight ratio of 1/2. The synthesized catalysts were used in the degradation of polypropylene. Reaction temperatures were chosen as 315ºC and 400 ºC. The effect of TPA loading amount and reaction temperature in the degradation reaction was examined.

6.1. Characterization Results of TPA Loaded SBA-15 Catalysts

6.1.1. X-Ray Diffraction Results

The X-ray Diffraction patterns of TPA loaded SBA-15 samples at low and wide Bragg angle are shown in Figures 6.1 and 6.2. For low angle pattern (Figure 6.1), it was seen that the main peak was observed at a 2Θ value of 0.8°, the second and third peaks were at 1.42° and 2.12°, respectively. These results are consistent with the XRD pattern of SBA-15 (Obalı et al., 2011). Except for SBA15-TPA 0.15 sample, intensities of the peaks decreased with an increase in the TPA loading amount, which indicates a distortion in the ordered structure of the material.

In Figure 6.2, the wide angle X-ray diffraction patterns of TPA loaded SBA-15 materials are given. A broad peak at 2Θ value of 24° was observed in all materials. This peak corresponds to silica (Aydemir, 2012) and shows that all synthesized materials are in the amorphous structure. Characteristic peaks of TPA were not observed in the synthesized catalysts, and this shows good dispersion of TPA in the structure of catalysts.

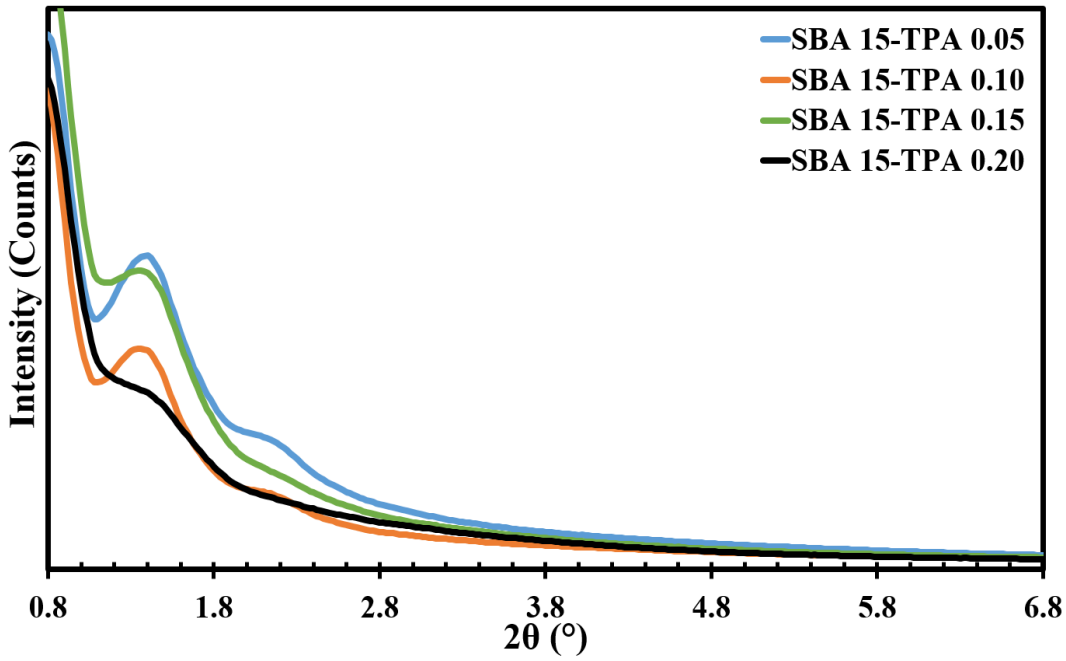

Figure 6.1. Low angle X-ray diffraction patterns of TPA loaded SBA-15 materials

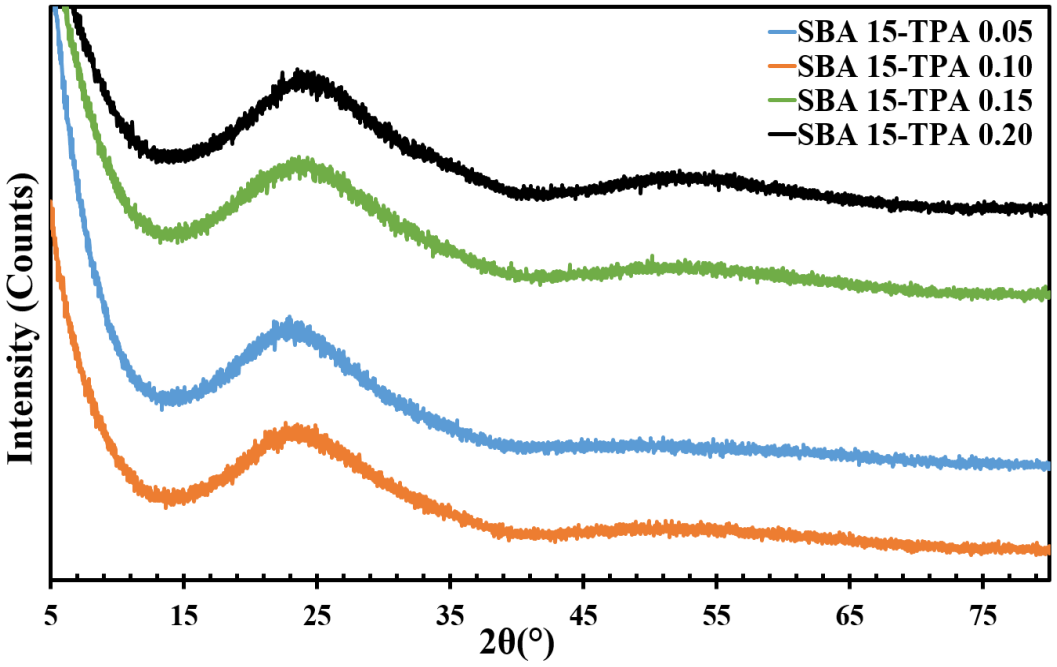

Figure 6.2. Wide angle X-ray diffraction patterns of TPA loaded SBA-15 materials

6.1.2. Physical Sorption Results

Nitrogen adsorption/desorption isotherms of the synthesized catalysts are given in Figure 6.3. The synthesized materials exhibited Type IV isotherm, which is the indication of mesoporous material according to IUPAC classification. All materials showed H1 type hysteresis at a relative pressure range of 0.65-0.82, associated with the capillary condensation taking place in mesopores and limiting uptake over a range of high relative pressure, which is an indication for the materials exhibiting a narrow pore size range. It can be clearly seen that adsorbed nitrogen volume decreased with an increase in the TPA amount in the catalysts.

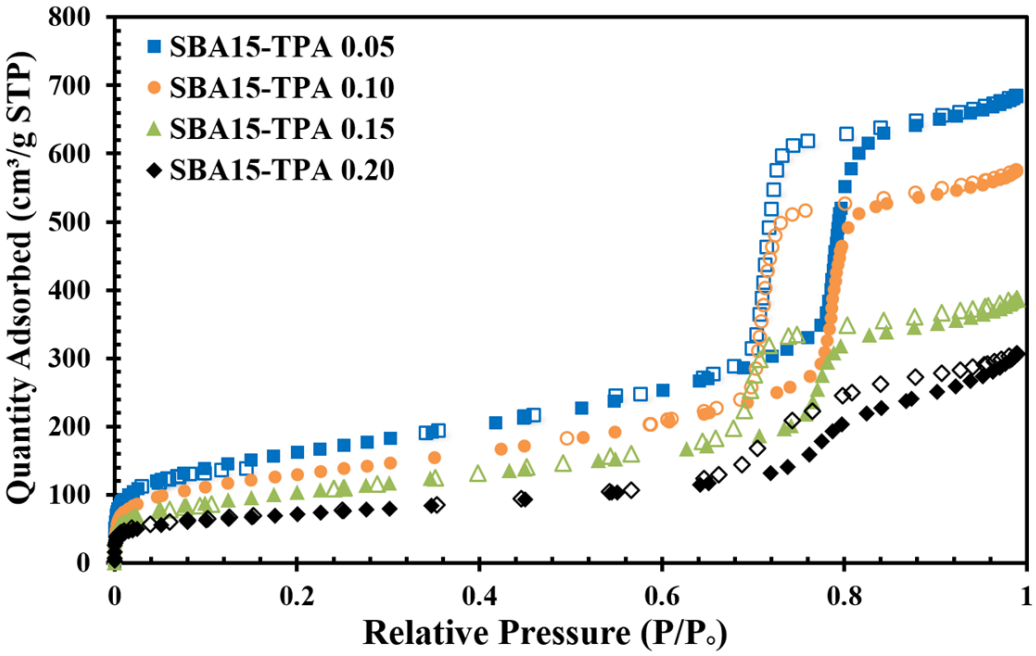

Figure 6.3. Nitrogen adsorption / desorption isotherms of the synthesized materials (filled boxes: adsorption branch, blank boxes: desorption branch)

BET surface area, pore volume, and pore diameter values of the synthesized materials are given in Table 6.1. The surface area values of the materials significantly decreased with an increase in the TPA loading. Pore volume also decreased with the addition of TPA to the structure of the materials. An increase in the amount of TPA may have affected the formation of cylindrical structure negatively. The pore diameter of the materials obtained using the BJH model changed between 6.69-9.70 nm, and this narrow pore size distribution indicates mesoporous structure as expected (Figure 6.4).

Table 6.1. Physical properties of the synthesized materials

Sample	Surface Area Multi Point BET, (m^2/g)	Pore Volume BJH Des., (cc/g)	BJH Des. Av. Pore Diameter (nm)	Microporosity (%)
SBA15-TPA0.05	568.2	1.07	9.70	13.6
SBA15-TPA0.10	457.2	0.90	9.32	13.2
SBA15-TPA0.15	367.6	0.61	6.70	15.6
SBA15-TPA0.20	254.9	0.50	6.75	14.4

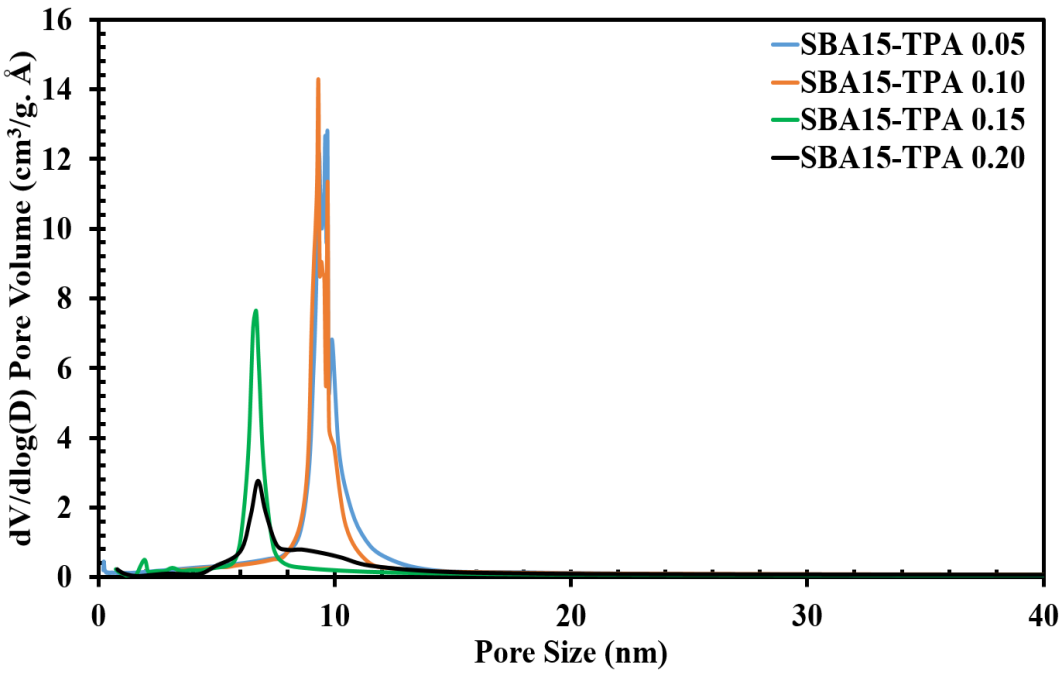

Figure 6.4. Pore size distribution of the synthesized materials

6.1.3. Scanning Electron Microscopy (SEM) & Energy Dispersive X-ray Spectroscopy (EDS) Results

Scanning electron microscopy was used to observe the morphology of the synthesized materials. SEM images of the synthesized materials are given in Figures 6.5-6.8. For SBA15-TPA 0.05 and SBA15-TPA 0.10 catalysts, hexagonal particles in the catalyst structure were observed (Figures 6.5 and 6.6). It can be deduced that TPA entered the structure of the SBA-15 effectively during the formation of silica structure, and hexagonal form was preserved for these catalysts. Some little changes in the morphology were observed in the SBA15-TPA 0.10 structure and these changes were shown with yellow circles (Figure 6.6). Agglomerations were observed in the structure of SBA15-TPA 0.05 and SBA15-TPA 0.10 (Figures 6.5 and 6.6). When the TPA loading amount was increased to 15% and 20%, the morphology of the catalysts became different, and hexagonal structure was not observed (Figure 6.7 and 6.8). SEM images of SBA15-TPA 0.15 and SBA15-TPA 0.20 did not show the typical SBA-15 structure. An increase in the TPA amount may have hindered the formation of the cylindrical structure. Some spherical particles with different sizes were observed in the structure of SBA15-TPA 0.20, which were highlighted with yellow circles (Figure 6.8). These particles may be indicating the presence of silica source (TEOS) which is one of the raw materials used for the synthesis. The average size of these spherical particles was 1.67 μm.

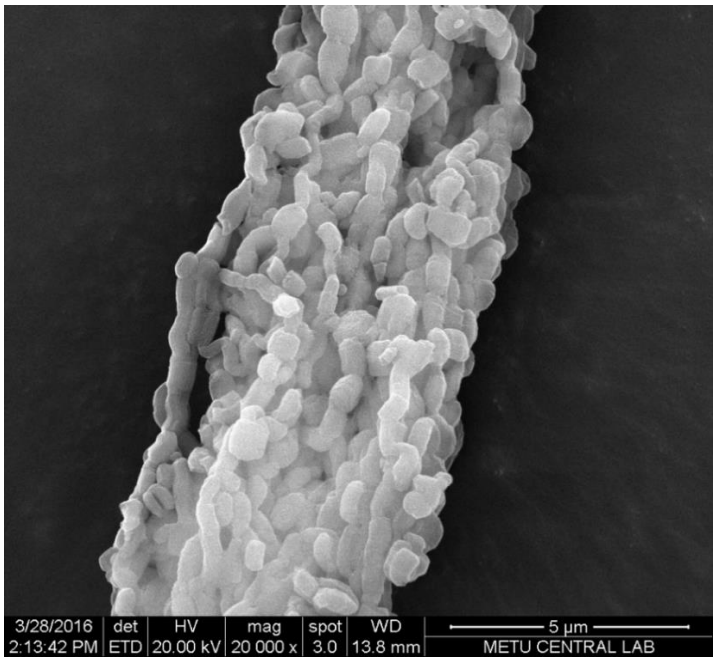

(a)

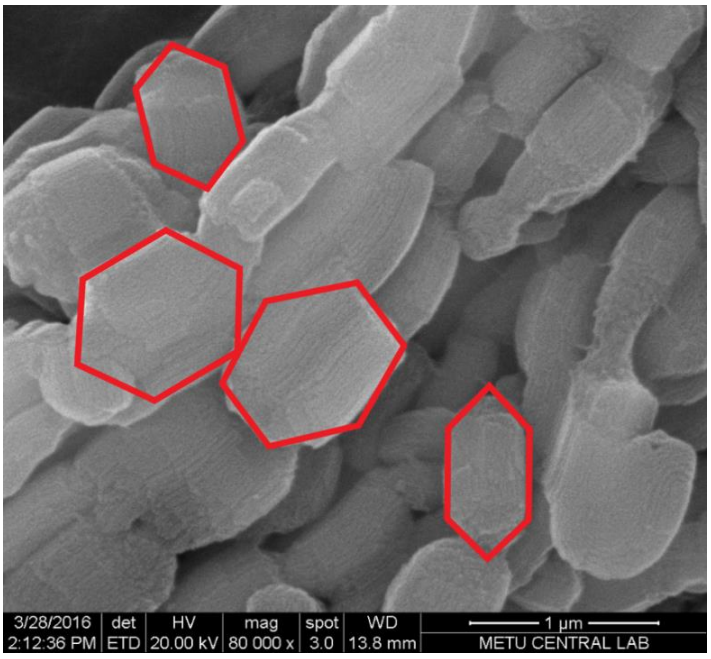

(b)

Figure 6.5. SEM images of SBA15-TPA0.05 at (a) 20000x magnification, (b) 80000x magnification

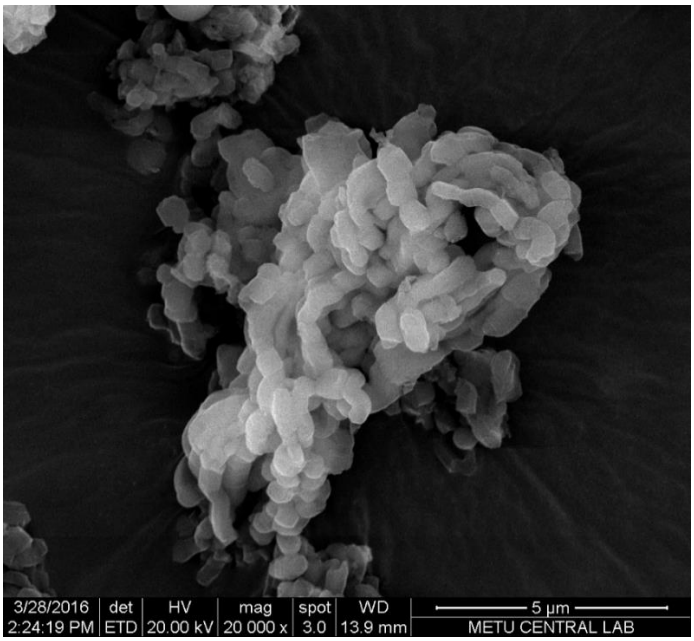

(a)

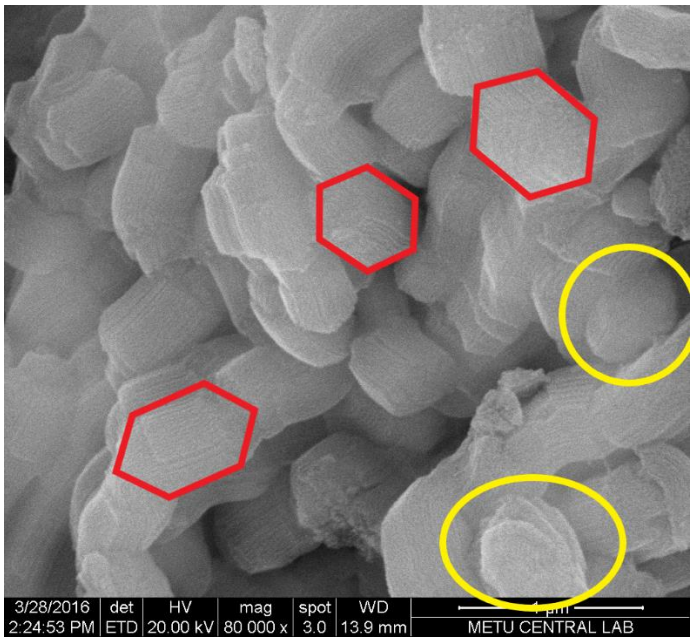

(b)

Figure 6.6. SEM images of SBA15-TPA0.10 at (a) 20000x magnification, (b) 80000x magnification

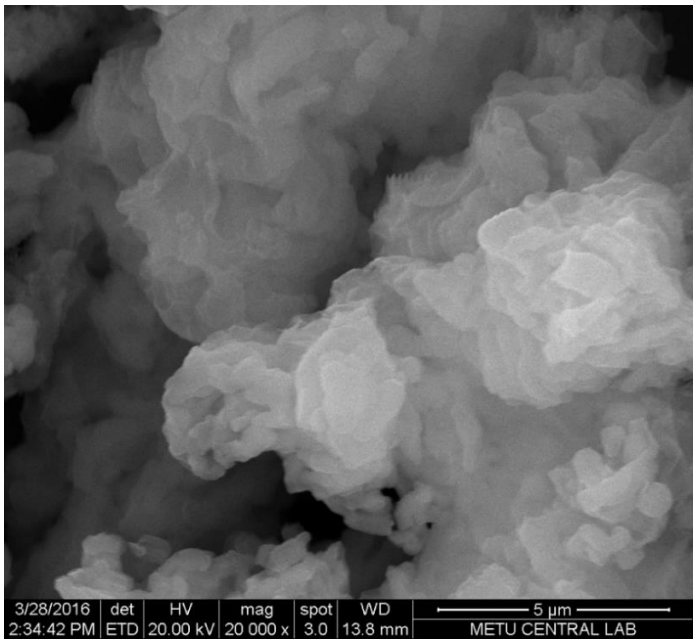

(a)

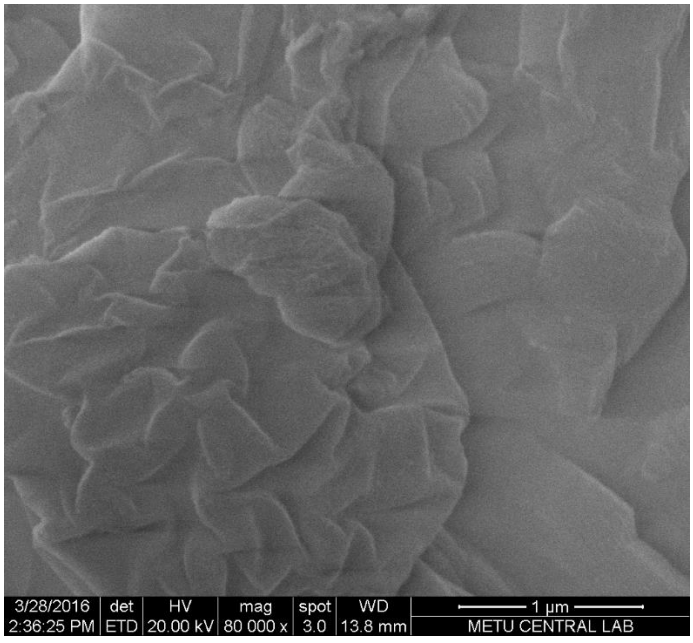

(b)

Figure 6.7. SEM images of SBA15-TPA0.15 at (a) 20000x magnification, (b) 80000x magnification

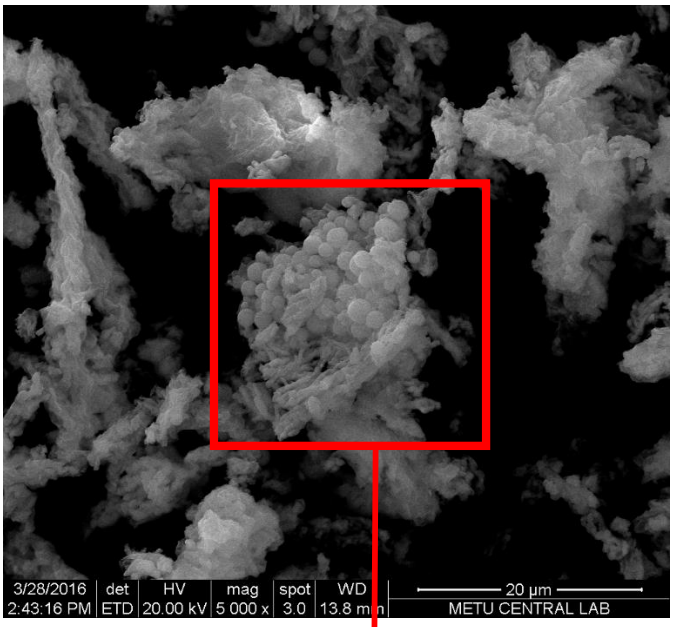

(a)

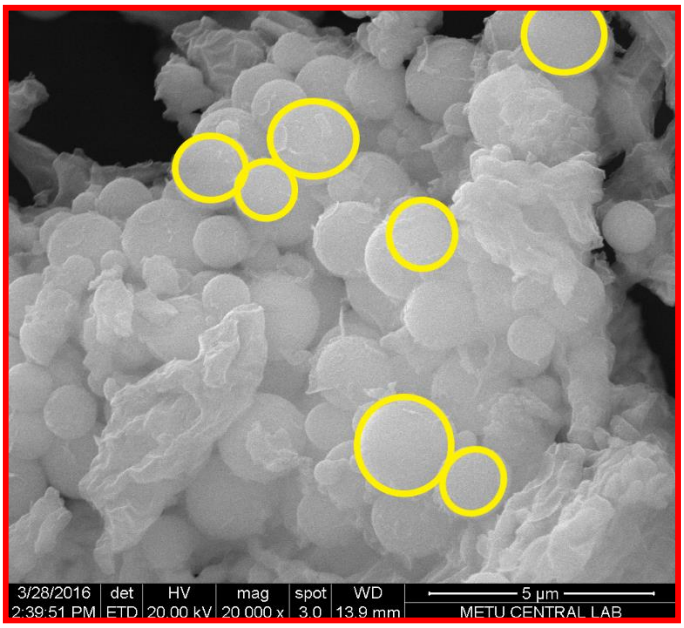

(b)

Figure 6.8. SEM images of SBA15-TPA0.20 at (a) 5000x magnification, (b) 20000x magnification

A typical EDX spectra is given in Figure 6.9, and spectra of all synthesized materials are also given in Appendix B. Carbon, oxygen, silicon, gold, palladium, phosphorous, and tungsten peaks were observed. Gold and palladium peaks came from the coating of the samples. Carbon came from the tape, which was used in the preparation of the sample. Oxygen came from the formation of SiO_2. Phosphorous and tungsten belong to TPA.

Energy Dispersive X-Ray Spectroscopy analysis results of synthesized catalysts are given in Table 6.2. For the SBA15-TPA 0.05 and SBA15-TPA 0.10 catalysts, TPA amounts in the initial synthesized solution were nearly the same as the amount of TPA that was introduced to the structure of the samples. For the SBA15-TPA 0.15 and SBA15-TPA0.20, the amount of TPA that was introduced to the structure of the materials decreased with the increasing amount of TPA in the initial synthesized solution. This shows that in TPA loadings less than %15, TPA entered the structure of the catalyst as expected. But when the amount of TPA is more than 10%, TPA may have entered the structure less than desired. TPA distribution in the SBA15-TPA 0.15 and SBA15-TPA 0.20 is not uniform, which is not consistent with the XRD results. In conclusion, TPA loading was more successful at low loading ratios.

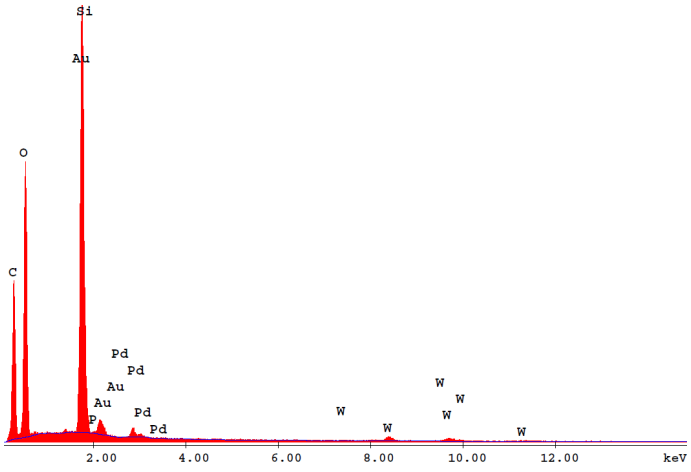

Figure 6.9. Typical EDX spectrum of TPA loaded SBA-15 catalyst

Table 6.2. EDX results of TPA loaded SBA-15 materials

Sample	W/Si Ratio (EDX)	W/Si Ratio (Synthesized Solution)
SBA15-TPA0.05	0.047	0.05
SBA15-TPA0.10	0.10	0.10
SBA15-TPA0.15	0.11	0.15
SBA15-TPA0.20	0.10	0.20

6.1.4. Diffuse Reflectance Infrared Fourier Transform Spectroscopy (DRIFTS) Results

FTIR spectra of the fresh catalysts are given in Figure 6.10. The band at 808 cm^{-1} is because of the W-O_c-W stretching vibrations. Subscript c stands for the oxygen binding to tungsten by edge-sharing. The band at around 960 cm^{-1} is due to W=O_t vibrations (Aydemir, 2010). These peaks showed the successful incorporation of the TPA to the structure. Bands at around 1050 cm^{-1} and 1200 cm^{-1} is due to the asymmetric Si-O-Si stretching vibrations.

The broad peak at a maximum of 3400 cm^{-1} is due to the hydrogen-bonded silanol groups and adsorbed water. The peak at 1639 cm^{-1} is assigned to the bending of H-O-H from adsorbed water (Obalı et al., 2011). The band at 3737 cm^{-1} is associated with the free silanol groups.

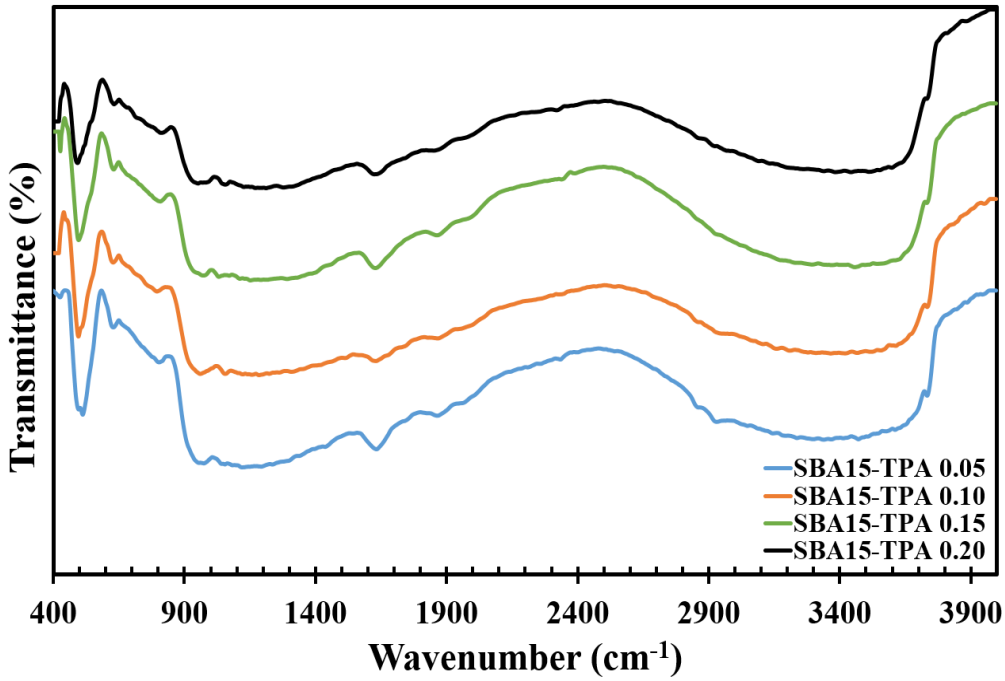

Figure 6.10. FTIR spectra of the fresh catalysts

DRIFTS analyses were performed to evaluate the relative strength of Brønsted and Lewis acid sites of the synthesized materials. Pyridine was adsorbed on the synthesized catalysts in order to observe the acid sites. In Figure 6.11, the DRIFTS spectra of the difference between pyridine adsorbed and fresh catalysts are shown.

All catalysts had peaks at a wavelength of 1447 cm^{-1} and 1598 cm^{-1} corresponding to Lewis acid sites, 1489 cm^{-1} corresponding to the combination of Lewis and Brønsted acid sites, and 1540 cm^{-1} corresponding to the Brønsted acid sites. Only SBA15-TPA 0.20 had peak at a wavelength of 1640 cm^{-1} corresponding to Brønsted acid sites.

For SBA15-TPA 0.05, SBA15-TPA 0.10, SBA15-TPA 0.15 and SBA15-TPA 0.20, the ratio of Brønsted acid sites at 1540 cm^{-1} to Lewis acid sites at 1447 cm^{-1} was 0.73,

1.00, 1.13 and 0.90, respectively. The ratio of Brønsted acid sites at 1640 cm^{-1} to Lewis acid sites at 1447 cm^{-1} for SBA15-TPA 0.20 was 0.95.

In the literature, pure SBA-15 was found to have only Lewis acid sites (Aydemir, 2010), and it can be concluded that TPA loading favored the formation of Brønsted acid sites in the structure. Increasing the TPA amount in the catalysts enhanced the Brønsted acid sites at 1540 cm^{-1} except SBA15-TPA 0.20.

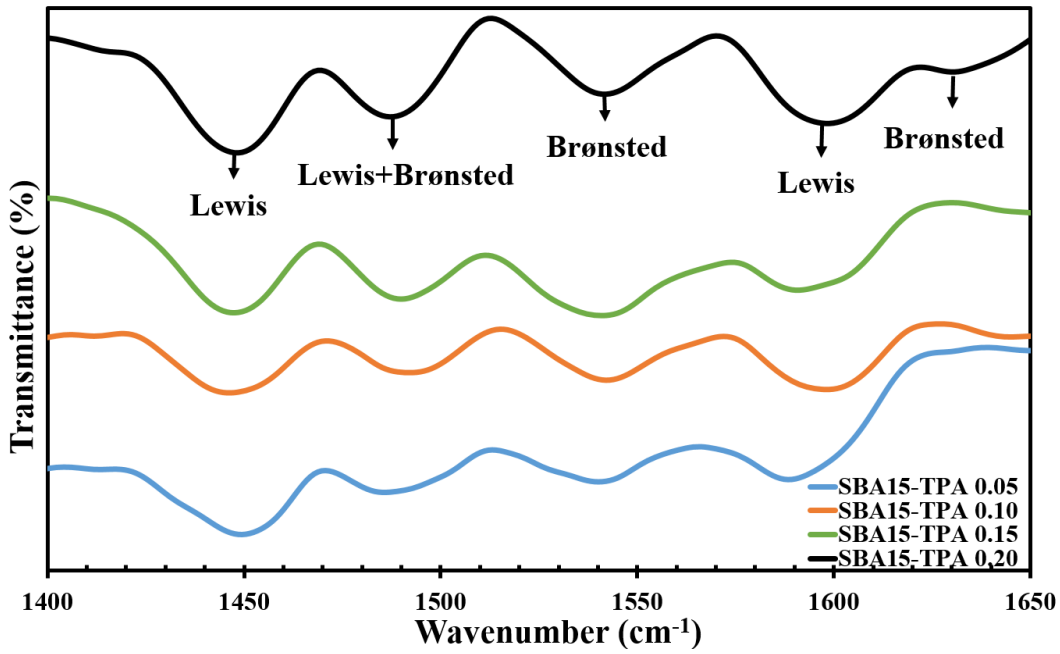

Figure 6.11. DRIFTS spectra of the synthesized catalysts

6.2. Thermogravimetric Analysis (TGA) Results

In this study, thermogravimetric analyses were carried out to determine the activation energy of the polypropylene thermal degradation reaction. The catalyst/polymer ratio was 1/2 in these experiments. TGA plots of pure PP and PP-catalyst mixtures are given in Figure 6.12.

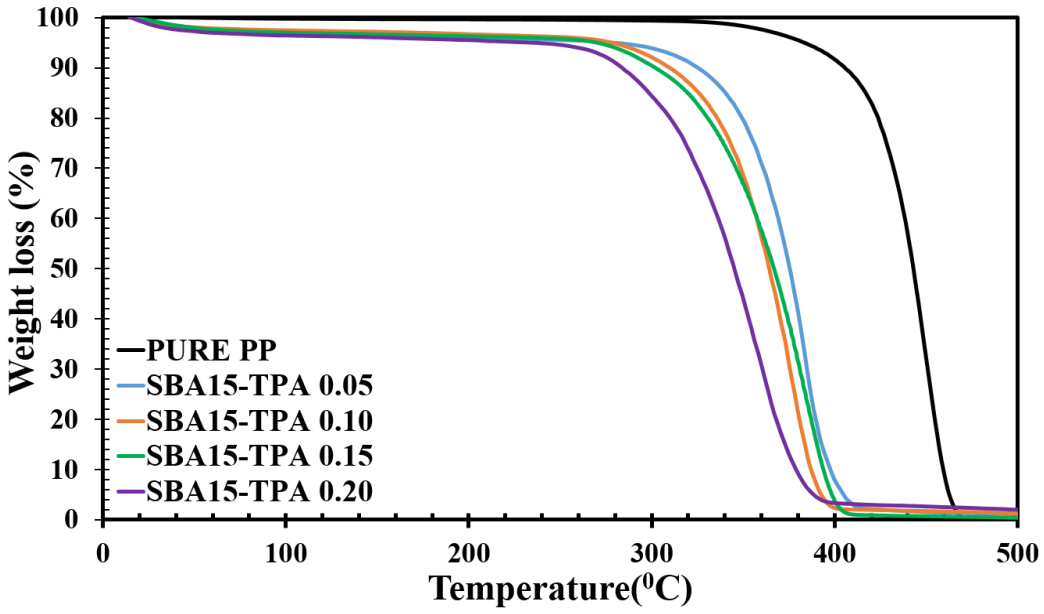

Figure 6.12. TGA plots of the synthesized materials

Pure PP started to degrade at around 350 ºC and showed a steep weight loss from this temperature to 480 ºC (Obalı et al., 2011). In the presence of TPA loaded SBA-15 catalysts, polypropylene showed a steep weight loss at a lower temperature range than the temperature range in the absence of the catalysts. In other words, decomposition temperature shifted to left as the degradation reaction occurred in lower temperatures in the presence of the catalyst. This shift is due to the Brønsted and Lewis acid sites

introduced by TPA loading to the structure, and they made the catalysts more acidic, providing a positive effect on the activity of the catalyst in the degradation reaction.

When the effect of the TPA amount in the catalyst on the polymer degradation reaction is investigated, it was observed that degradation temperature shifted left with an increase in the TPA amount. This is due to the increase in acidity, and this led to a decrease in the degradation temperature. To sum up, loading a higher amount of TPA in the structure of the catalyst had a positive effect on the thermal degradation of PP.

6.2.1. Determination of Activation Energy for Polypropylene Degradation Reaction

The activation energy value of the polypropylene catalytic thermal degradation reaction was determined using the TGA data, and this calculation method is given in Appendix C. Polypropylene degradation reaction order was found to be one. Activation energy values of the degradation reaction in the presence of the synthesized catalysts are given in Table 6.3.

Table 6.3. Activation energy values of the degradation reactions

Sample	Activation Energy (kJ/mol)
Pure PP	172.0
SBA15-TPA 0.05	141.1
SBA15-TPA 0.10	133.8
SBA15-TPA 0.15	106.5
SBA15-TPA 0.20	100.5

The activation energy value of the non-catalytic degradation reaction had been determined as 172 kJ/mole (Obalı et al., 2011). This value decreased to the range of 141.4-100.5 kJ/mol in the presence of the synthesized catalysts by means of the Brønsted and Lewis acid sites created by the loading of TPA. This is equal to nearly the 18-41% decrease in the activation energy of pure PP. The lowest activation energy was obtained in the presence of the SBA15-TPA 0.20 catalyst. According to the DRIFTS results, SBA15-TPA 0.15 seemed to be the most acidic catalyst compared to others due to the ratio of Brønsted acid sites at 1540 cm^{-1} to Lewis acid sites at 1447 cm^{-1}. But, Brønsted acid sites of SBA15-TPA 0.20 at 1640 cm^{-1} may have enhanced the acidity of this catalyst, and as a result, it provided the lowest activation energy.

6.3. Polymer Degradation Reaction Results

Non-catalytic and catalytic thermal degradation experiments of polypropylene were carried out isothermally in polymer degradation reaction system with 1 g of PP and 0.5 g of the catalyst at 315°C and 400 °C for 30 minutes under nitrogen atmosphere with a flow rate of 60 cc/min and a constant heating rate of 5 °C/min. Some of the pyrolysis experiments were carried out twice, and pyrolysis reaction results were found to be reproducible. Error margins of the repeated experiments were shown in the related figures. Gas and liquid products obtained from the pyrolysis reactions were analyzed using GC. Calibration factors that were used in these calculations for gas and liquid products are given in Appendix D and Appendix E, respectively. Mole and weight fractions and selectivity of these products were calculated using the sample calculation given in Appendix F, and related data for gaseous and liquid products are given in Appendix G and Appendix H, respectively.

For the non-catalytic degradation reaction, only gaseous products and solid residue were observed. For the catalytic reaction, only gaseous and liquid products were observed. Product yield for gas, liquid, and solid residue was calculated using the following equation:

$$\text{Yield (wt \%)} = \frac{\text{Weight of liquid or gas product (g)} * 100}{\text{Weight of initial polymer feed (g)}}$$

The effect of reaction temperature and TPA on the product yield is given in Figure 6.13. Pyrolysis reactions for pure PP were carried out at 315°C and 400 °C. The liquid product was not observed for both temperatures where solid residue yield decreased from %58.4 to % 37.6, and gaseous product yield increased from %41.6 to %62.4 as the reaction temperature increased. This is due to the cracking of higher hydrocarbons to the smaller hydrocarbons with an increase in the reaction temperature.

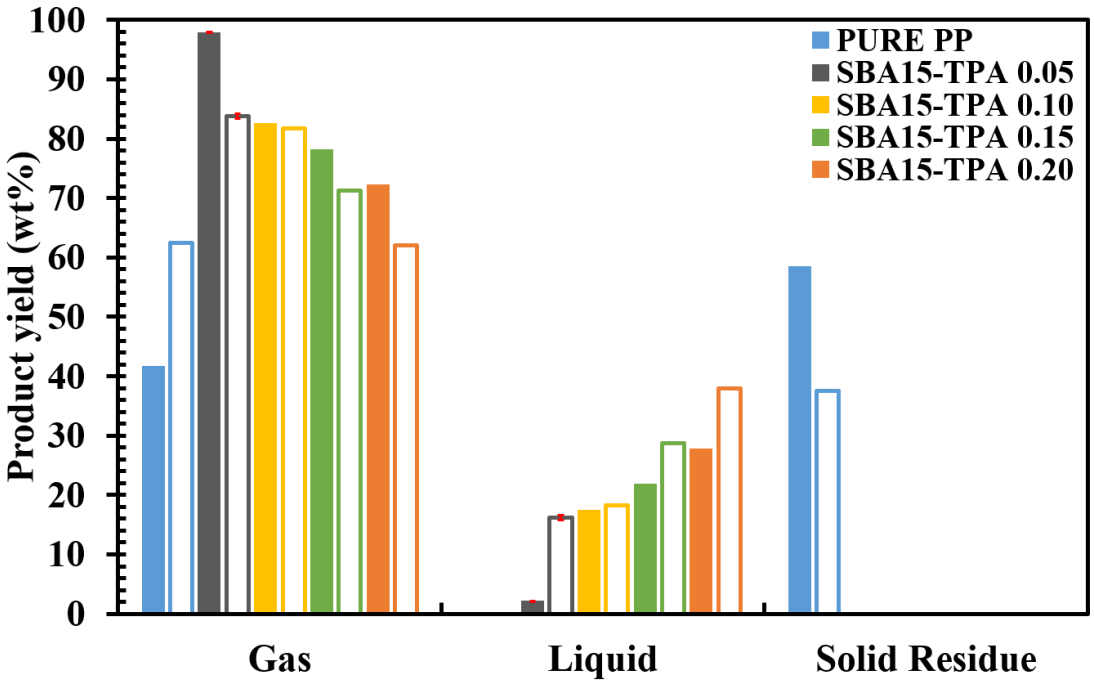

Figure 6.13. Effect of reaction temperature and TPA amount on the product yield (Filled boxes at 315 °C, empty boxes at 400 °C)

Catalytic pyrolysis experiments were performed at 315°C and 400 °C. Gaseous and liquid products were observed where there was no solid residue for both temperatures. In the presence of the catalyst, the yield of gaseous and liquid products increased compared to pure PP yields. In the catalytic degradation reaction at 315 °C, the yield of gaseous products decreased from % 97.9 to %72.2, where the yield of liquid products increased from %2.1 to %27.8 when the TPA amount in the catalyst increased. In the catalytic degradation reaction at 400 °C, the yield of gaseous products decreased from %83.8 to %62, where the yield of liquid products increased from %16.2 to %38 with an increase in the TPA amount in the catalyst.

It can be concluded that the use of catalysts favored the formation of liquid products and prevented the formation of solid residue. This absence of solid residue was due to an increase in the reaction rate with the catalyst. With an increase in the TPA amount in the catalyst, the amount of gas products decreased, and the amount of liquid products increased at both temperatures. The amount of liquid products also increased with an increase in the reaction temperature while the amount of gas products decreased.

6.3.1. Gas Product Distribution of Catalytic Thermal Degradation Experiments

The catalytic pyrolysis reactions of polypropylene were performed at 315 °C and 400 °C for 30 minutes using the synthesized catalysts with different TPA amounts. Gas products were analyzed using the GC. Each gas product was injected to the GC at least two times, and the average values of the injections were used for calculations. The effect of reaction temperature and TPA amount in the catalysts on mole fraction and selectivity of gas products are shown in Figures 6.14 and 6.15.

In the non-catalytic degradation reaction, only ethylene was obtained as a gas product at 315 °C. When reaction temperature was increased from 315 °C to 400 °C, ethane,

propylene, and i-butane formed in addition to ethylene, where propylene had the highest mole fraction and selectivity.

In the catalytic degradation reaction at 315 °C and 400 °C, ethylene, propylene, isobutane, and n-butane formed where ethane was not observed. An increase in the reaction temperature increased the mole fraction and selectivity of ethylene and decreased the mole fraction and selectivity of propylene and i-butane for all the catalyst types except SBA15-TPA 0.05. Mole fraction and selectivity of n-butane decreased with an increase in the reaction temperature when SBA15-TPA 0.05 and SBA15-TPA 0.20 were used. In the use of SBA15-TPA 0.10, when reaction temperature increased, mole fraction of n-butane did not change where its selectivity increased slightly.

For the catalytic degradation reaction at 315°C, ethylene, propylene, isobutane, and n-butane formed in the presence of all catalysts except SBA15-TPA 0.15. When SBA15-TPA 0.15 was used, n-butane was not observed. Mole fraction and selectivity of ethylene increased with increasing TPA amounts in the catalysts where mole fraction and selectivity of propylene decreased. Isobutane had the highest mole fraction and selectivity for all catalysts. The mole fraction of n-butane didn't show a significant change with different TPA loadings.

For the degradation reaction at 400°C, ethylene, propylene, isobutane, and n-butane were obtained in the presence of all catalysts except SBA15-TPA 0.15. When SBA15-TPA 0.15 was used, n-butane did not form. When SBA15-TPA 0.20 was used as the catalyst, propylene and n-butane were not observed. Mole fraction and selectivity of ethylene increased with increasing TPA loading of the catalyst where mole fraction and selectivity of propylene decreased. Isobutane had the highest selectivity for all the catalysts. Mole fraction and selectivity of n-butane remained nearly the same when SBA15-TPA 0.05 and SBA15-TPA 0.10 were used as catalysts.

It can be concluded that, with an increase in the TPA amount of the catalysts and reaction temperature, heavier hydrocarbons degraded into smaller hydrocarbon molecules.

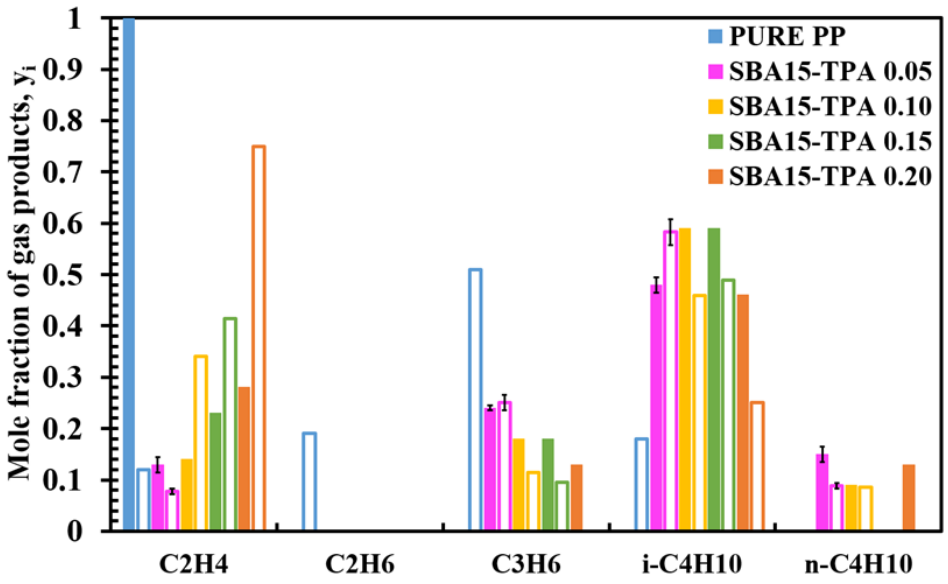

Figure 6.14. Variation of mole fraction of gas products with respect to reaction temperature (Filled box: 315 °C, empty box: 400 °C)

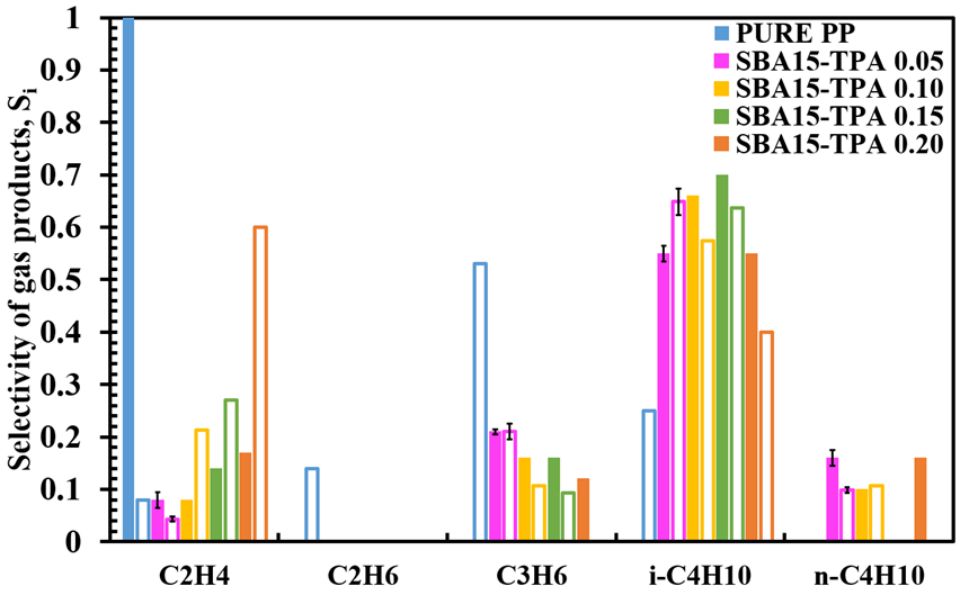

Figure 6.15. Variation of selectivity of gas products with respect to reaction temperature (Filled box: 315 °C, empty box: 400 °C)

6.3.2. Liquid Product Distribution of Catalytic Thermal Degradation Experiments

Liquid products obtained from the catalytic experiments at 315 °C and 400 °C were collected after each experiment and analyzed using the GC. Each product was injected into the GC two times, and average area values of injections were used for calculations. The effect of catalyst type and reaction temperature on the mole fraction and selectivity of liquid products are shown in Figures 6.16-6.17.

At 315 °C, hydrocarbons in the range of C_5-C_{18} formed in the presence of catalysts. C_5 was not observed when SBA15-TPA 0.10 and SBA15-TPA 0.15 were used, and its mole fraction and selectivity in the presence of other catalysts were very small. Similarly, C_{18} was not observed when SBA15-TPA 0.20 was used, and its mole

fraction and selectivity were very small in the presence of other catalysts. Mole fraction and selectivity of C_6, C_7, C_8, and C_{10} increased with an increase in the TPA amount of the catalyst, except SBA15-TPA 0.15. Mole fraction and selectivity of C_9 increased when the TPA amount increased from 5% to 10%, and this value stayed nearly the same in the presence of SBA15-TPA 0.20 while it decreased when 15% TPA loaded catalyst was used. Selectivity of C_{11} was nearly same for all catalysts except SBA15-TPA 0.10. Mole fraction and selectivity of C_{13} decreased with changing TPA amount in the catalyst from 5% to 10%, and this value stayed nearly the same in use of SBA15-TPA 0.20 while it increased slightly when 15% TPA loaded catalyst was used. Mole fraction and selectivity of C_{12}, C_{14}, and C_{16} decreased when the TPA amount in the catalyst increased except SBA15-TPA 0.15, indicating the degradation of heavy hydrocarbons to smaller hydrocarbons.

At 400 °C, hydrocarbons in the range of C_6-C_{18} formed in the presence of catalysts where C_5 was not observed. C_{18} was not observed in the presence of SBA15-TPA 0.05, and its mole fraction was between 0.004-0.014 for other catalysts, which is very small. Mole fraction and selectivity of C_6 stayed nearly the same for 5%, 15%, and 20% TPA loaded SBA-15 catalysts and increased twofold in the presence of 10% TPA loaded catalyst. Mole fraction and selectivity of C_7 was nearly the same for 5% and 10% TPA loaded catalysts and reduced by half when 15% and 20% TPA loaded catalysts were used. When the TPA amount was increased from 5% to 10%, mole fraction and selectivity of C_8 increased but for more acidic catalysts, these values decreased. Mole fraction and selectivity of C_9 increased when the TPA amount of the catalyst was raised from 5% to 10%, and it stayed nearly the same for other catalysts. An increase in the acidity of the catalysts led to an increase in the mole fraction and selectivity of C_{10} and C_{14} except SBA15-TPA 0.10 and a decrease in the mole fraction and selectivity of C_{13}.

The effect of the reaction temperature on the product distribution was examined. When SBA15-TPA 0.05 was used, the mole fraction, and selectivities of C_6-C_{10} liquid

products increased with an increase in the reaction temperature while the mole fraction and selectivities of C_{11}-C_{18} hydrocarbons decreased. This may be due to the effect of the large surface area and pore diameter of SBA15-TPA 0.05, allowing the heavier hydrocarbons to stay in the catalyst's pore and further degrade to lighter hydrocarbons. In the presence of SBA15-TPA 0.10, mole fraction and selectivity of C_6, C_{10}, C_{11}, C_{12}, and C_{14} decreased when the reaction temperature was increased, where mole fraction and selectivity of C_7, C_8, C_9, C_{13}, C_{16}, and C_{18} increased. In the use of SBA15-TPA 0.15, it was observed that mole fraction and selectivity of C_6, C_{10}, C_{11}, C_{12}, and C_{13} increased when the reaction temperature was raised from 315°C to 400°C and decreased for C_7-C_9 and C_{14}-C_{18}. Although SBA15-TPA 0.20 has the highest acid sites in its structure, selectivities of C_5-C_{11} hydrocarbons decreased with an increase in the reaction temperature while an increase in selectivity was observed for C_{11}-C_{18} hydrocarbons. This may be due to the significant decrease in the surface area and pore diameter of SBA15-TPA 0.20, hindering the stay of heavy hydrocarbons in the pore of the catalyst and not allowing their degradation to lighter hydrocarbons.

The majority of the liquid compounds consisted of C_8-C_{14} for both reaction temperatures indicating the degradation to lighter hydrocarbons. It can be said that the product distribution profile obtained from the synthesized catalysts are similar to each other. In the presence of SBA15-TPA 0.05, C_{12} had the highest selectivity at 315°C, and C_{11} had the highest selectivity at 400 °C. For %10 TPA loaded catalysts, C_{10} had the highest selectivity at both temperatures, while C_{11} had the highest selectivity for %15 TPA loaded catalysts at both temperatures. When %20 TPA loaded catalyst was used, the most selective liquid product changed from C_{10} to C_{14} when the reaction temperature increased from 315 °C to 400 °C. It is concluded that products in the gasoline range (C_5-C_{12}) can be obtained mostly at 315 °C, while products in the diesel range (C_{12}-C_{18}) can be obtained mostly at 400 °C.

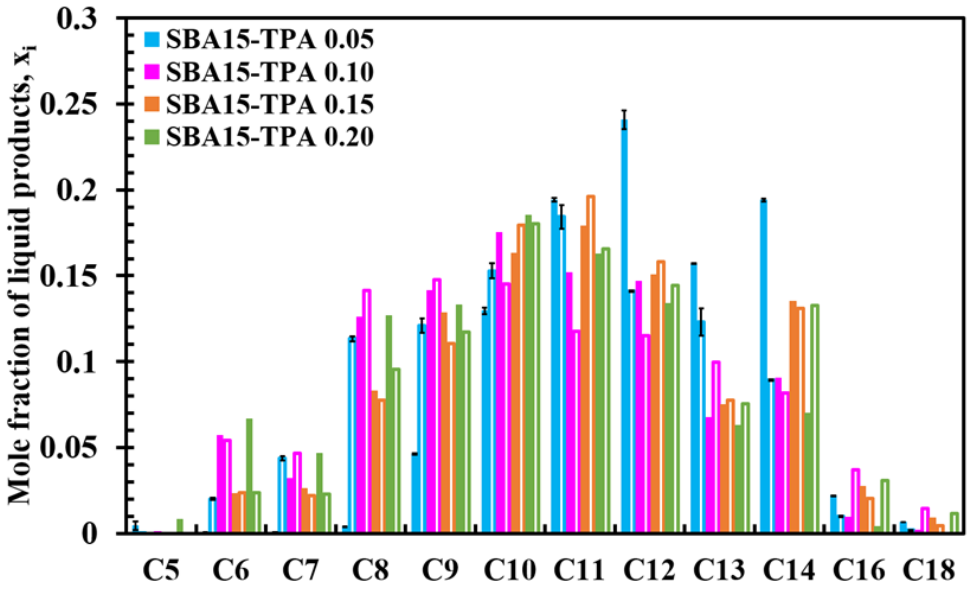

Figure 6.16. Variation of mole fraction of liquid products with respect to temperature (Filled boxes at 315 °C, empty boxes at 400 °C)

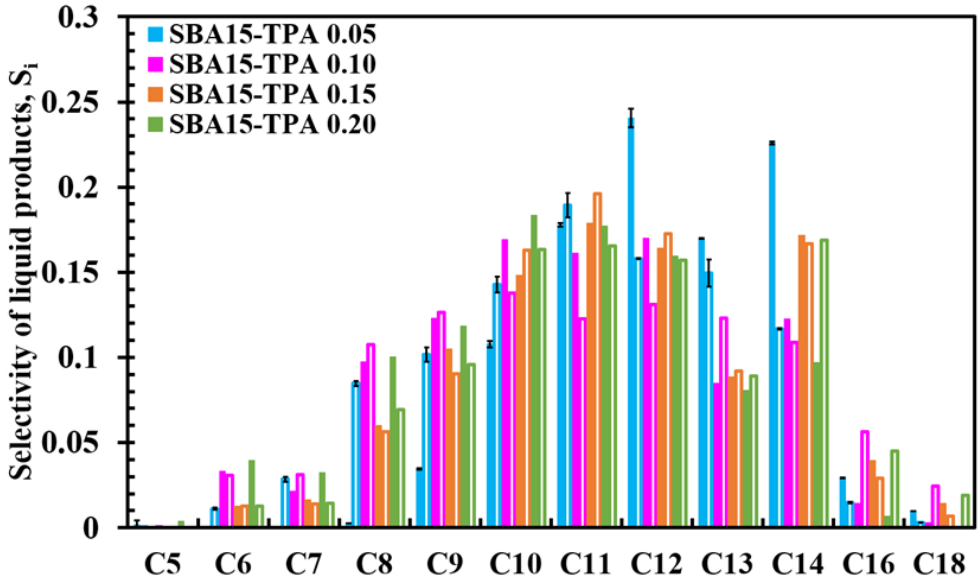

Figure 6.17. Variation of selectivity of liquid products with respect to temperature (Filled boxes at 315 °C, empty boxes at 400 °C)

6.3.3. Coke Formation Results for Thermal Degradation Experiments

TGA analyses were carried out in order to determine the coke formation in the used catalysts. Coke deposition percent of the catalysts which were used at different temperatures are given in Table 6.4. Coke formation was observed for all synthesized catalysts, but their amount is not very high. Coke formation values of the catalysts are close to each other. SBA15-TPA 0.05 had the highest value among all synthesized catalysts, and this value is nearly same for both temperatures. For 10%, 15%, and 20% TPA loaded SBA-15 catalysts, coke formation is almost the same and decreased by almost 41% compared to 5% TPA loaded SBA-15. The decrease in the coke amount of SBA15-TPA 0.05 with an increase in the TPA amount can be attributed to the reduction in the activation energies of the catalysts.

Table 6.4. Coke formation amount of the synthesized catalysts during pyrolysis reactions at different temperatures

Experimental Temperature	Catalyst	Coke Formation (wt%)
315 °C	SBA15-TPA 0.05	5.40
	SBA15-TPA 0.10	4.11
	SBA15-TPA 0.15	4.92
	SBA15-TPA 0.20	3.93
400 °C	SBA15-TPA 0.05	5.72
	SBA15-TPA 0.10	3.39
	SBA15-TPA 0.15	3.81
	SBA15-TPA 0.20	3.97

SBA15-TPA 0.20 catalyst showed the best performance in the catalytic degradation reaction of PP at 315 °C. It provided the highest selectivity of liquids in the range of C_5-C_7. It also decreased the selectivity of liquids in the range of C_{13}-C_{18}. These results showed that this catalyst favored the production of gasoline range hydrocarbons more compared to other catalysts. In addition, this catalyst provided the best results for the gas product analysis. Also, it had the lowest activation energy among all the synthesized catalysts. Lastly, it had the lowest coke formation.

The best catalyst results obtained from this study were compared with the literature. Obalı et al., used aluminum incorporated SBA-15 catalyst in the polypropylene degradation reaction at 315 °C for 30 minutes. When TGA results were compared, the most effective catalyst in the literature study decreased the activation energy value of the polypropylene degradation reaction to 50.7 kJ/mol, while the best catalyst in this study reduced the activation energy value of the polypropylene degradation reaction to 100.5 kJ/mol. When the product yields of the catalytic degradation reactions were compared, it was seen that gas and liquid products formed in both studies and the liquid product yield in this study was 3.5% lower than the yield in the literature. The solid residue was not obtained from the catalytic degradation reactions in both studies. According to the gas product results in the literature, all catalysts were ethylene selective, while in this study, all catalysts were i-butane selective. According to the liquid product results, the selectivity of C_{13} was found to be the highest for the most acidic catalyst in the literature, while C_{10} has the highest selectivity in this study for SBA15-TPA 0.20. It can be concluded that polypropylene degraded into lighter hydrocarbons. Nisar et al. studied the pyrolysis of polypropylene over zeolite mordenite ammonium at different reaction temperatures. According to the TGA results, the catalyst decreased the activation energy value of polypropylene degradation reaction up to 58.49 kJ/mol. Gas and liquid products and the solid residue were observed at 350-390°C in the presence of catalysts while no solid residue was observed in our study in the presence of all catalysts. Liquid product yield obtained with the catalyst was found to be 10% at 350°C and 9% at 390°C while the liquid yield

value was 38% at 400 °C in our study. Ethane, propylene, 2-butene, 1-propene-2-methyl, butane-2-methyl, pentane-2-methyl, 2-pentene, cyclopropane-1,2-dimethyl, butane-2,3-dimethyl, cyclopentane-methyl, and 1-pentene-2-methyl were obtained as gas products in this literature study. Propylene was the only common gas obtained from the catalytic pyrolysis reactions in both literature and our study. Liquid products in the range of C_4-C_{18} were obtained in the literature study consisting of mostly alkenes, while liquid products in our study consisted of primarily alkanes in the range of C_5-C_{18}.

CHAPTER 7

CONCLUSIONS

In this study, TPA loaded SBA-15 materials were synthesized via one-pot hydrothermal method with different TPA loadings to be used in the catalytic thermal degradation of polypropylene. Kinetic parameters of the polypropylene thermal degradation reaction in the presence of the synthesized catalysts were determined using a thermogravimetric analyzer. After TGA analyses, thermal degradation reactions of PP were carried out in the presence and absence of the synthesized catalysts. Obtained gas and liquid products were analyzed using the GC.

The following results were obtained from this study:

- TPA loaded SBA-15 catalysts were synthesized successfully. XRD results showed that synthesized catalysts had an amorphous structure, and the addition of TPA did not cause a significant change in the mesoporous structure of SBA-15.

- Physical sorption results showed that the synthesized materials exhibited Type IV isotherms, which indicates the mesoporous structure. All materials showed H1 type hysteresis. Surface areas of the materials decreased with an increase in the amount of TPA. The pore diameter of all materials changed between 6.70-9.70 nm. All synthesized catalysts were mesoporous, including microporosity, up to 15.6%.

- SEM results showed the hexagonal structure of SBA15 for 5% and 10% TPA loaded catalysts. When TPA loading was increased to 15% and 20%,

morphology changed. Agglomerations were observed for SBA15-TPA 0.05 and SBA15-TPA 0.10.

- According to the DRIFTS results, addition of TPA to the structure led to the formation of Brønsted acid sites in all catalysts. An increase in the TPA amount enhanced the Brønsted acid sites at 1540 cm^{-1} except SBA15-TPA 0.20. Only SBA15-TPA 0.20 had Brønsted acid sites at 1640 cm^{-1}.

- Activation energy of the degradation reactions decreased from 172 kJ/mole to a range of 141.1 and 100.5 kJ/mole with an increase in the TPA amount of the catalysts. SBA15-TPA 0.20 provided the lowest activation energy.

- Gaseous products and the solid residue were observed for pure PP at 315 °C and 400 °C. For all catalytic reactions, gaseous and liquid products were obtained where solid residue was not obtained. Liquid product yield increased with an increase in the reaction temperature and TPA amount in the catalyst while gas product yield decreased.

- The analysis of gaseous products in the presence of catalyst at 315 °C showed that isobutane had the highest mole fraction and selectivity. Mole fraction and selectivity of ethylene increased with the increasing amount of TPA in the catalysts, while propylene showed a decreasing mole fraction and selectivity trend. At 400 °C, it was observed that mole fraction and selectivity of ethylene increased when higher amounts of TPA was used in the catalysts while mole fraction and selectivity of propylene and isobutane decreased oppositely. N-butane was observed for 5%, 10%, and 20% TPA loadings at 315 °C and 5% and 10% TPA loadings at 400 °C. Mole fraction and selectivity of n-butane didn’t show a significant change for different catalysts. Heavy hydrocarbons cracked to lighter hydrocarbons in the presence of the catalyst at both

temperatures. SBA15-TPA 0.20 showed the best catalytic activity for the gas products in degradation to lighter hydrocarbons with an increase in the reaction temperature.

- For all types of catalysts, C_8-C_{16} hydrocarbons formed at both reaction temperatures as liquid products. Mole fraction and selectivity of C_5 and C_{18} were very small compared to other liquid products. C_{10}, C_{11}, and C_{12} were the most selective compounds at 315 °C where C_{10}, C_{11}, and C_{14} had the highest selectivity at 400 °C. With an increase in the TPA amount of the catalysts at 315 °C, the selectivity of C_5-C_{10} increased while the selectivity of C_{12}-$_{18}$ decreased except in the presence of SBA15-TPA 0.15. This is the indication of cracking to lighter hydrocarbons. The selectivity of C_{12} remained nearly the same for all types of catalysts at the mentioned temperature. When the TPA amount was increased from 5% to 10% at 400 °C, selectivity of C_6-C_9 increased where the selectivity of C_{10}-C_{14} decreased. For 15% and 20% TPA loadings, selectivity of C_7-C_9 and C_{13} decreased while the selectivity of C_{12} and C_{14}-$_{18}$ increased. This showed that when the temperature was raised from 315 °C to 400 °C, catalysts with TPA loadings more than 10% were less effective for liquid products in the degradation of heavier molecules to lighter hydrocarbons.

- The highest coke formation was observed in the use of SBA15-TPA 0.05 at both temperatures. This value decreased with an increase in the TPA amount of the catalysts.

- When TGA results, liquid product yield, and analysis of gas and liquid products were considered as a whole, SBA15-TPA 0.20 showed the best performance in the catalytic degradation of PP with the highest selectivity of C_{10} at 315°C and C_{14} at 400 °C.

- In the presence of all catalysts, products in the gasoline range can be obtained at 315 °C while products in the diesel range can be obtained at 400 °C.

REFERENCES

Aguado, J., Serrano, D., Miguel, G. S., Escola, J., & Rodríguez, J., (2007). *"Catalytic Activity of Zeolitic and Mesostructured Catalysts in the Cracking of Pure and Waste Polyolefins"*, Journal of Analytical and Applied Pyrolysis, 78(1), p.153-161.

Allsopp, M. W., & Vianello, G., (2000). *"Poly (Vinyl Chloride)"*, Ullmann's Encyclopedia of Industrial Chemistry, Weinheim: Wiley-VCH, p.441-467.

Alonso, J. A., & Serrano, D. P., (2007). *"Feedstock Recycling of Plastic Wastes"*, Cambridge: Royal Society of Chemistry, p.31-176.

Al-Salem, S., Lettieri, P., & Baeyens, J., (2009). *"Recycling and Recovery Routes of Plastic Solid Waste (PSW): A Review."*, Waste Management, 29(10), p.2625-2643.

Ambili, V. K., (2011). *"Studies on Catalysis by Ordered Mesoporous SBA-15 Materials Modified with Transition Metals"*, Doctoral Thesis, Cochin University of Science and Technology, Kochi, India.

Andrady, A. L., & M. A. Neal., (2009). *"Applications and Societal Benefits of Plastics"*, Philosophical Transactions of the Royal Society B: Biological Sciences 364 (1526), p.1977-984.

Andrady, A. L., (2015). *"Plastics and Environmental Sustainability"*, New Jersey: John Wiley & Sons, p.255-295.

Assamoi, B., & Lawryshyn, Y., (2012). *"The Environmental Comparison of Landfilling vs. Incineration of MSW Accounting for Waste Diversion"*, Waste Management, 32 (5), p.1019-1030.

Augustine, R. L., (1996). *"Heterogeneous Catalysis for the Synthetic Chemist",* New York: M. Dekker, p.179-193.

Aydemir, B., (2010). *"Synthesis of Mesoporous Catalysts and Their Performance in Pyrolysis of Polyethylene",* MSc Thesis, Middle East Technical University, Ankara, Turkey.

Aydemir, B., & Sezgi, N. A. (2013). "*Alumina and Tungstophosphoric Acid Loaded Mesoporous Catalysts for the Polyethylene Degradation Reaction*", Industrial & Engineering Chemistry Research, 52(44), p.15366-15371.

Azapagic, A., Emsley, A., & Hamerton, I, (2003). *"Polymers: The Environment and Sustainable Development"*, Chichester: John Wiley & Sons, p.79-99.

Aznar, M. P., Caballero, M. A., Sancho, J. A., & Francés, E., (2006). *"Plastic Waste Elimination by Co-Gasification with Coal and Biomass in Fluidized Bed with Air in Pilot Plant"*, Fuel Processing Technology, 87(5), p.409-420.

Batchelor, A. W., Loh, N. L., & Chandrasekaran, M., (2011). *"Materials Degradation and Its Control by Surface Engineering"*, Singapore: World Scientific, p.67-174.

Beck, J. S., Vartuli, J. C., Roth, W. J., Leonowicz, M. E., Kresge, C. T., Schmitt, K. D., Schlenker, J. L., (1992). *"A New Family of Mesoporous Molecular Sieves Prepared with Liquid Crystal Templates"*, Journal of the American Chemical Society, 114(27), p.10834-10843.

Brahmkhatri, V., & Patel, A., (2011). *"12-Tungstophosphoric Acid Anchored to SBA-15: An Efficient, Environmentally Benign Reusable Catalysts for Biodiesel Production by Esterification of Free Fatty Acids"*, Applied Catalysis A: General, 403 (1-2), p.161-172.

Brodhacker, K. Lisa., (2006). *"The Polymer Chemistry and Optical Testing of Epoxy Mirrors"*, Doctoral Thesis, University of South Carolina, Columbia, USA.

Buekens, A., & Huang, H., (1998). *"Catalytic Plastics Cracking for Recovery Of Gasoline-Range Hydrocarbons From Municipal Plastic Wastes"*, Resources, Conservation and Recycling, *23*(3), p.163-181.

Chaianansutcharit, S., Katsutath, R., Chaisuwan, A., Bhaskar, T., Nigo, A., Muto, A., & Sakata, Y., (2007). "*Catalytic Degradation of Polyolefins over Hexagonal Mesoporous Silica: Effect of Aluminum Addition"*, Journal of Analytical and Applied Pyrolysis, 80 (2), p.360-368.

Chandler, A. J., (1997). *"Municipal Solid Waste Incinerator Residues"*, Amsterdam: Elsevier.

Che, Q., Yang, M., Wang, X., Yang, Q., Chen, Y., Chen, X., Chen, W., Hu, J., Zeng, K., Yang, H., Chen, H., (2019). *"Preparation of mesoporous ZSM-5 catalysts using green templates and their performance in biomass catalytic pyrolysis"*, Bioresource Technology, 289:121729.

Chen, Y., Zhang, X., Chen, X., Dong, B., & Zheng, X., (2013). *"MCM-41 Supported 12-tungstophosphoric Acid Mesoporous Materials: Preparation, Characterization, and Catalytic Activities for Benzaldehyde Oxidation with H_2O_2"*, Solid State Sciences, 24, p.21-25.

Chi, Y., Xue, J., Zhuo, J., Zhang, D., Liu, M., & Yao, Q., (2018). *"Catalytic co-pyrolysis of cellulose and polypropylene over all-silica mesoporous catalyst MCM-41 and Al-MCM-41"*, Science of the Total Environment, p.1105-1113.

Dullien, F. A. L., (1992). *"Porous Media: Fluid Transport and Pore Structure"*, New York; Toronto: Academic Press, p.6-110.

Durmuş, A., Koç, S. N., Pozan, G. S., & Kaşgöz, A., (2005). *"Thermal-catalytic Degradation Kinetics of Polypropylene over BEA, ZSM-5 and MOR Zeolites"*, Applied Catalysis B: Environmental 61(3-4), p.316-322.

Europa, https://ec.europa.eu/environment/waste/plastic_waste.htm, last accessed date: 07.10.2019

Fulvio, P. F., Pikus, S., & Jaroniec, M., (2005). *"Short-Time Synthesis of SBA-15 Using Various Silica Sources"*, Journal of Colloid and Interface Science, 287 (2), p.717-720.

Fraissard, J. P., (1997). *"Physical Adsorption: Experiment, Theory, and Applications"*, Dordrecht: Kluwer Academic, p.33-65.

Geyer, R., Jambeck, J. R., & Law, K. L. (2017). *"Production, Use, and Fate of All Plastics Ever Made"*, Science Advances, 3(7).

Gibson, L. T., (2014). *"Mesosilica Materials and Organic Pollutant Adsorption: Part A Removal from Air"*, Chemical Society Reviews, 43(15), p.5163.

Goldstein, J., Newbury, D.E., Echlin, P., Joy, D.C., Fiori, C., Lifshin, E., (1981). *"Scanning Electron Microscopy and X-ray Microanalysis: A Text for Biologists, Materials Scientists, and Geologists"*, New York: Springer, p.273-339.

Goswami, B. C., Anandjiwala, R. D., & Hall, D. M., (2004). "*Textile Sizing*", New York: Marcel Dekker, p.3-119.

Goto, M., (2009). *"Chemical Recycling of Plastics Using Sub- and Supercritical Fluids"*, The Journal of Supercritical Fluids, 47(3), p.500-507.

Gupta, P., & Paul, S., *(2014*). *"Solid Acids: Green Alternatives for Acid Catalysis"*, Catalysis Today, 236, p.153-170.

Harrison, R. M., & Hester, R. E., (1994). *"Waste Incineration and the Environment"*, Cambridge: The Royal Society of Chemistry, p.27-52.

Huirache-Acuña, R., Nava, R., Peza-Ledesma, C., Lara-Romero, J., Alonso-Núez, G., Pawelec, B., & Rivera-Muñoz, E., (2013). *"SBA-15 Mesoporous Silica as Catalytic Support for Hydrodesulfurization Catalysts-Review"*, Materials, 6(9), p.4139-4167.

Ishizaki, K., Komarneni, S., & Nanko, M., (1998). *"Porous Materials: Process Technology and Applications"*, Dordrecht: Kluwer Academic, p.7.

Islam, M. R., Khan, M. M., & Chhetri, A. B., (2010). *"The Greening of Petroleum Operations: The Science of Sustainable Energy Production"*, Hoboken, NJ: John Wiley & Sons, p.352.

Jiraroj, D., Chaipurimat, A., Kerdsa, N., Hannongbua, S., & Tungasmita, D. N., (2016). "*Catalytic Cracking of Polypropylene Using Aluminosilicate Catalysts",* Journal of Analytical and Applied Pyrolysis, 120, p.529-539.

John, M. J., & Thomas, S., (2012). *"Natural Polymers: Composites"*, Cambridge: Royal Society of Chemistry, p.1-7.

Kaminsky, W., & Zorriqueta, I. N., (2007). *"Catalytical and Thermal Pyrolysis of Polyolefins"*, Journal of Analytical and Applied Pyrolysis, 79 (1-2), p.368-374.

Karger-Kocsis, J., (1995). *"Polypropylene: Structure, Blends and Composites"*, London: Chapman & Hall, p.1-71.

Kasapoğlu, C., (2013). *"Synthesis and Characterization of TPA Loaded Mesoporous Catalysts and Their Performance in Pyrolysis of Polypropylene",* MSc Thesis, Middle East Technical University, Ankara, Turkey.

Kozhevnikov, I.V., (2007). *"Sustainable Heterogeneous Acid Catalysis by Heteropoly Acids"*, Journal of Molecular Catalysis A: Chemical, 262 (1-2), p.86-92.

Kresge, C. T., Vartuli, J. C., Roth, W. J., & Leonowicz, M. E.., (2004). *"The Discovery of ExxonMobil's M41S Family of Mesoporous Molecular Sieves"*, Mesoporous Crystals and Related Nano-Structured Materials, Proceedings of the Meeting on Mesoporous Crystals and Related Nano-Structured Materials Studies in Surface Science and Catalysis, p.53-72.

Kunwar, B., Cheng, H., Chandrashekaran, S. R., & Sharma, B. K., (2016). *"Plastics to Fuel: A Review"*, Renewable and Sustainable Energy Reviews, 54, p.421-28.

Lee, K., & Shin, D., (2006). *"A Comparative Study of Liquid Product On Non-Catalytic and Catalytic Degradation of Waste Plastics Using Spent FCC Catalyst"*, Korean Journal of Chemical Engineering Korean J, Chem. Eng., 23(2), p.209-215.

Letcher, T. M., and Daniel A. Vallero., (2011). "*Waste: A Handbook for Management",* Burlington, MA: Academic, p.238.

Li, K., Lee, S., Yuan, G., Lei, J., Lin, S., Weerachanchai, P., . . . Wang, J., (2016). *"Investigation into the Catalytic Activity of Microporous and Mesoporous Catalysts in the Pyrolysis of Waste Polyethylene and Polypropylene Mixture",* Energies, 9(6), p.431.

López, A., Marco, I. D., Caballero, B., Laresgoiti, M., Adrados, A., & Aranzabal, A., (2011). *"Catalytic Pyrolysis of Plastic Wastes with Two Different Types of Catalysts: ZSM-5 Zeolite and Red Mud."* Applied Catalysis B: Environmental, 104(3-4), p.211-219.

Maier, C., & Calafut, T., (1998). *"Polypropylene: The Definitive User's Guide and Databook",* New York: Plastic Design Library, p.1-9.

Malpass, D. B., (2010). *"Introduction to Industrial Polyethylene: Properties, Catalysts and Processes"*, Hoboken, NJ: Wiley-Scrivener, p.1-20.

Manfredi, S., Tonini, D., Christensen, T. H., & Scharff, H., (2009) *"Landfilling of Waste: Accounting of Greenhouse Gases and Global Warming Contributions"*, Waste Management & Research, 27(8), p.825-836.

Mantia, F. L., (2002). *"Handbook of Plastics Recycling"*, Shropshire: Rapra Technology, p.11.

Marcilla, A., Gómez-Siurana, A., & Berenguer, D., (2006). *"Study of The Influence of the Characteristics of Different Acid Solids in The Catalytic Pyrolysis of Different Polymers",* Applied Catalysis A: General, 301(2), p.222-231.

Martins-Rubber, http://www.martins-rubber.co.uk/2015/09/nonlinear-finite-element-analysis-of-rubber/, last accessed date: 15.10.2019.

Mazrouaa, A. M., (2012). *"Polypropylene Nanocomposites"*, Rijeka, Croatia: In Tech, p.265-286.

Nisar, J., Khan, M. A., Ali, G., Iqbal, M., Shah, A., Shah, M. R., … Rehman, N. U. (2019). *"Pyrolysis of polypropylene over zeolite mordenite ammonium: kinetics and products distribution"*, Journal of Polymer Engineering, 39(9):785-793.

Obalı, Z., Sezgi, N. A., & Doğu, T., (2012). *"Catalytic Degradation of Polypropylene over Alumina Loaded Mesoporous Catalysts"*, Chemical Engineering Journal, 207-208, p.421-425.

Owen, J., (1984). *"Degradation and Stabilisation of PVC"*, London: Elsevier Applied Science Publishers, p.1-19.

Patel, A., (2013). "*Environmentally Benign Catalysts: For Clean Organic Reactions"*, Dordrecht: Springer, p.12-35.

Patrick, S., (2005). *"Practical Guide to Polyvinyl Chloride"*, Shrewsbury: Rapra Technology Limited, p.4.

Peacock, A. J., (2000). *"Handbook of Polyethylene: Structures, Properties, And Applications"*, New York: Marcel Dekker, p.1-6.

Perego, C., & Millini, R., (2013). *"Porous Materials in Catalysis: Challenges for Mesoporous Materials"*, Chem. Soc. Rev., 42(9), p.3956-3976.

Pielichowski, K., & Njuguna, J., (2005). *"Thermal Degradation of Polymeric Materials"*, Shawbury: Rapra Technology, p.31-32.

Puente, G. D., & Sedran, U., (1998). *"Recycling Polystyrene into Fuels by Means of FCC: Performance of Various Acidic Catalysts."* Applied Catalysis B: Environmental, 19(3-4), p.305-311.

Qi, P., Chang, G., Wang, H., Zhang, X., Guo, Q., (2018). *"Production of aromatic hydrocarbons by catalytic co-pyrolysis of microalgae and polypropylene using HZSM-5"*, Journal of Analytical and Applied Pyrolysis, p.178-185.

Rahmat., (2010). *"A Review: Mesoporous Santa Barbara Amorphous-15, Types, Synthesis and Its Applications towards Biorefinery Production"*, American Journal of Applied Sciences, 7(12), p.1579-1586.

Rouquerol, F., Rouquerol, J., & Sing, K., (1999). Introduction. *"Adsorption by Powders and Porous Solids"*, p.1-26.

Schwarz, J. A., Contescu, C. I., & Putyera, K., (2004). *"Dekker Encyclopedia of Nanoscience and Nanotechnology"*, New York: Marcel Dekker, p.230-233.

Sharma, D., (2005). *"A Handbook of Polymer Chemistry"*, New Delhi: International Scientific Publishing Academy, p.96-97.

Sharuddin, S. D., Abnisa, F., Daud, W. M., & Aroua, M. K., (2016). *"A Review On Pyrolysis of Plastic Wastes"*, Energy Conversion and Management, 115, p.308-326.

Statista, http://www.statista.com/statistics/282732/global-production-of-plastics-since-1950/, last accessed date: 07.10.2019

Statista, http://www.statista.com/statistics/320417/polypropylene-consumption-in-china/, last accessed date: 07.10.2019

Taguchi, A., & Schüth, F., (2005). *"Ordered Mesoporous Materials in Catalysis"*, Microporous and Mesoporous Materials, 77(1), p.1-45.

Thielemann, J. P., Girgsdies, F., Schlögl, R., & Hess, C., (2011). *"Pore Structure and Surface Area of Silica SBA-15: Influence of Washing and Scale-up"*, Beilstein Journal of Nanotechnology 2, p.110-118

Toju, K. S., (1999). *"Plastic Catalytic Degradation Study of the Role of External Catalytic Surface, Catalytic Reusability and Temperature Effects"*, Doctoral Thesis, University College London.

Tuttle, M. E., (2013). *"Structural Analysis of Polymeric Composite Materials"*, Boca Raton, Fla: CRC-Press, p.9-16.

Vasile, C., & Pascu, M., (2005). *"Practical Guide to Polyethylene"*, Shrewsbury: RAPRA Technology, p.34-35.

Velinni, A. A., (2007). *"Landfill Research Trends"*, New York: Nova Science, p.76-77.

Walendziewski, J., (2002). *"Engine Fuel Derived from Waste Plastics by Thermal Treatment"*, Fuel 81(4), p.473-481.

Zhao, D., (1998). *"Triblock Copolymer Synthesis of Mesoporous Silica with Periodic 50 to 300 Angstrom Pores"*, Science, 279 (5350), p.548-552.

APPENDICES

A. CALCULATION OF TPA AMOUNT TO BE ADDED INTO THE SBA-15 SUPPORT

All the calculations in this part were made based on the assumption that SBA-15 was purely composed of SiO_2. In this study, 8 g TEOS was used as silica source for the synthesis. Molecular weight of TEOS is 208.33 g/mol. From Equation A.1, number of moles of TEOS (n_{TEOS}) is calculated as 0.0384 where M_{TEOS} is the mass of TEOS and MW_{TEOS} is the molecular weight of TEOS:

$$(n_{TEOS}) = M_{TEOS} / MW_{TEOS} \quad (A.1)$$

Number of moles of Si (n_{Si}) is equal to the number of moles of TEOS ($SiC_8H_{20}O_4$). Number of moles of tungsten (n_W) for a desired molar ratio of W/Si was calculated using Equation A.2:

$$n_W / n_{Si} = Z \quad (A.2)$$

where n_W is the mole number of W and Z is the desired ratio of W/Si.

When the mole number of tungsten was calculated, knowing that in 1 mole of TPA ($H_3PW_{12}O_{40}$), there is 12 moles of tungsten; number of moles of TPA is 1/12 of n_W. So, the amount of TPA to be used in the synthesis of the catalyst was found using Equation A.3:

$$M_{TPA} = (n_W / 12) \times MW_{TPA} \quad (A.3)$$

where M_{TPA} is the mass of TPA and MW_{TPA} is the molecular weight of TPA, which is 2880 g/mol. Amounts of TPA to be added into the SBA-15 support were given in Table A.1.

Table A.1. Amount of TPA to be loaded into the SBA-15 material

Material	**M_{TPA} (g)**
SBA15-TPA0.05	0.46
SBA15-TPA0.10	0.92
SBA15-TPA0.15	1.38
SBA15-TPA0.20	1.84

B. EDS SPECTRA OF THE SYNTHESIZED MATERIALS

EDS spectra of the synthesized materials are given in Figures B.1-B.4.

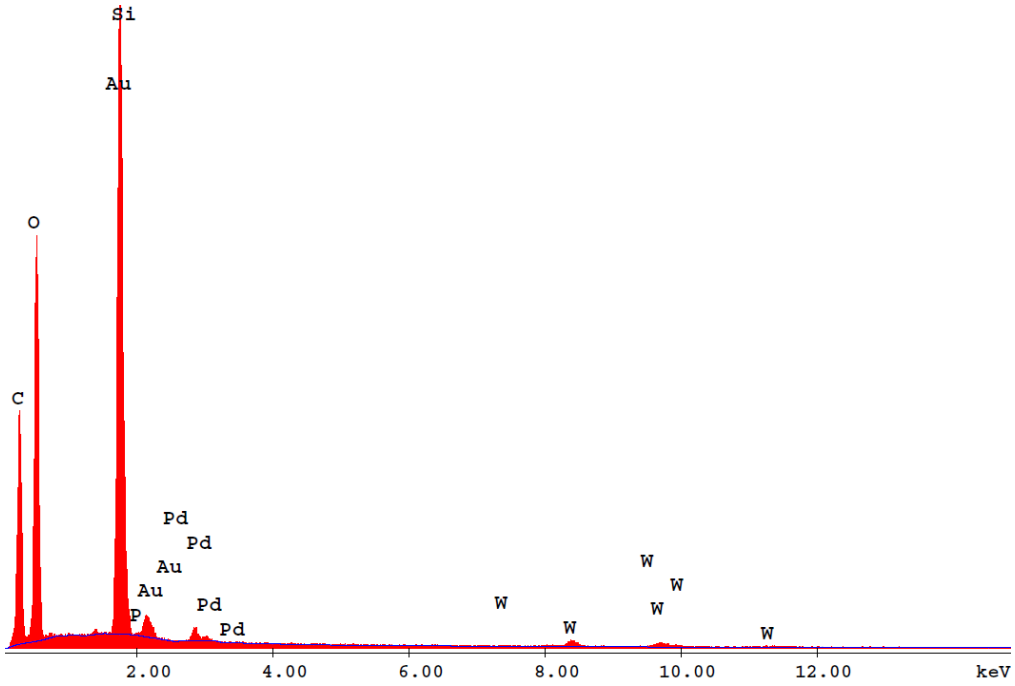

Figure B.1. EDS spectrum of SBA15-TPA0.05

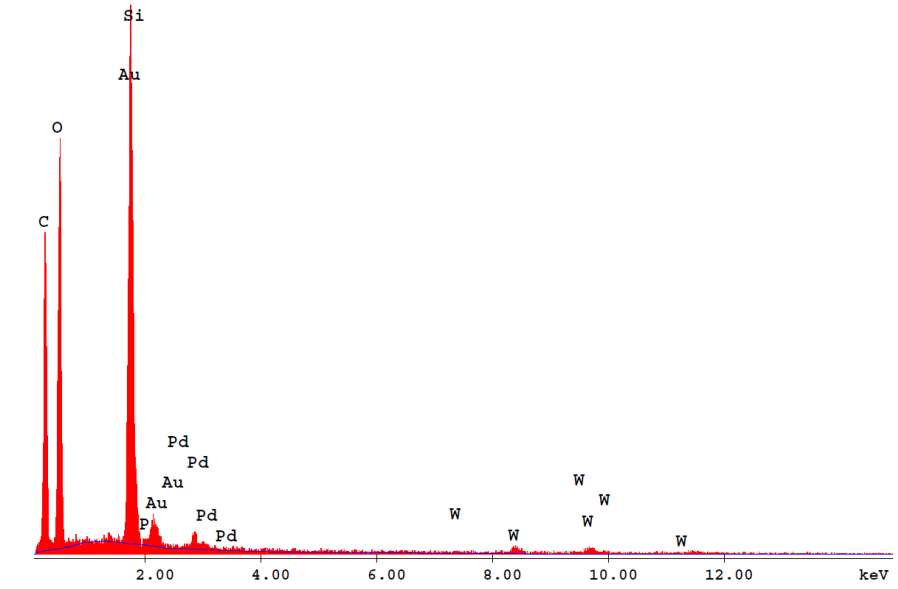

Figure B.2. EDS spectrum of SBA15-TPA0.10

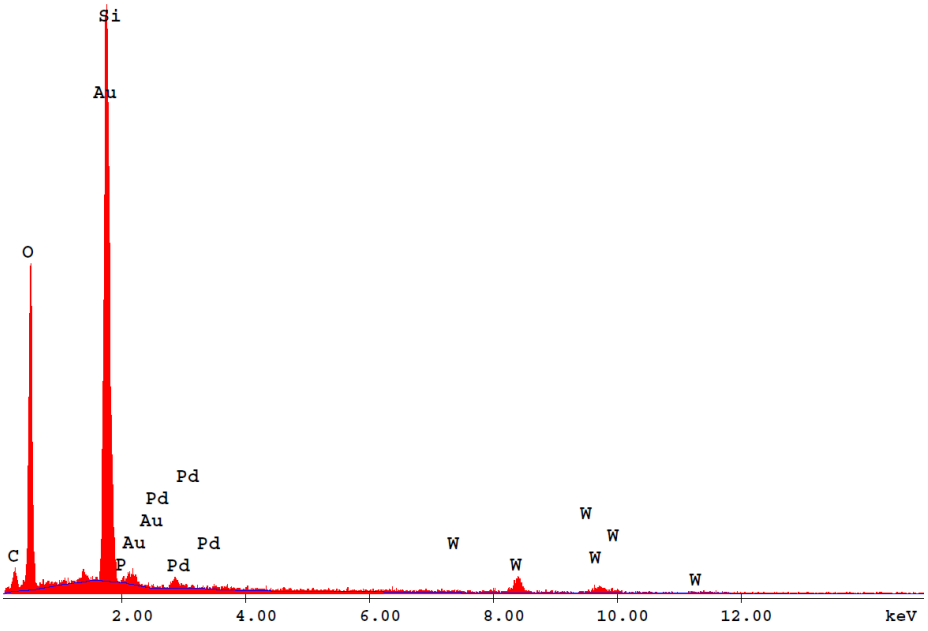

Figure B.3. EDS spectrum of SBA15-TPA0.15

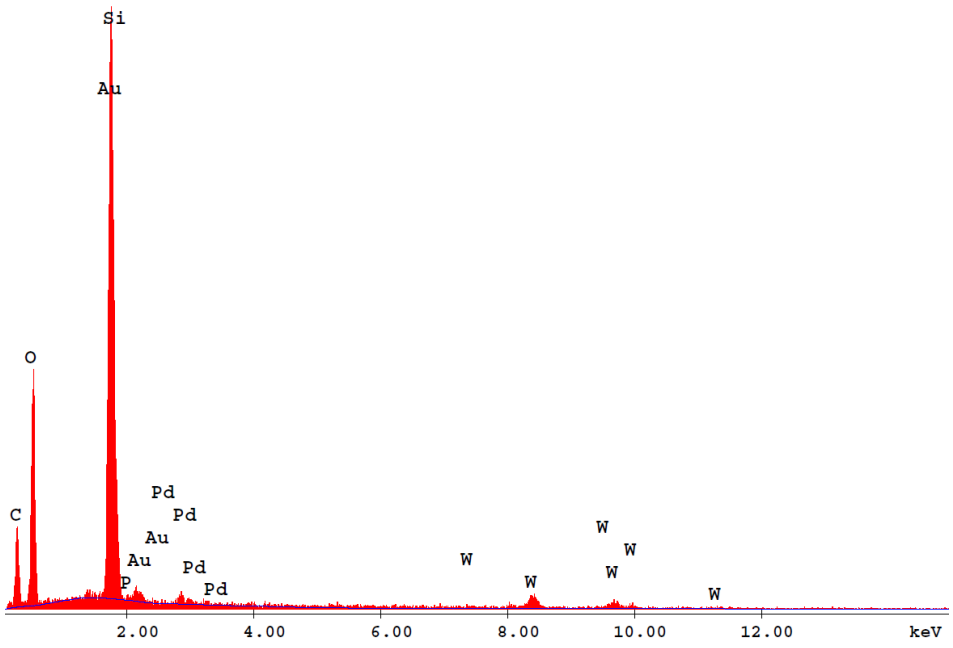

Figure B.4. EDS spectrum of SBA15-TPA0.20

C. CALCULATION OF ACTIVATION ENERGY OF POLYPROPYLENE DEGRADATION REACTION

The reaction which takes place during the cracking of polymer P is given below;

$$pP_{(s)} \longrightarrow bB_{(s)} + cC_{(g)}$$

The rate of disappearance of P is;

$$d\alpha/dt = k_{avg}(1-\alpha)^n \qquad (C.1)$$

where α is the fraction of P decomposed at time t, n is the overall reaction order and k_{avg} is the rate constant. α can be defined as;

$$\alpha = (w_0 - w_t) / (w_0 - w_\infty) \qquad (C.2)$$

where w_0, w_t and w_∞ are the initial weight of the sample, weight at time t and final weight values, respectively. The rate constant can be described in terms of Arrhenius equation:

$$k_{avg} = Aexp^{-E/RT} \qquad (C.3)$$

where A and E are the pre-exponential factor and activation energy of the reaction, respectively.

The temperature value at any time is given as;

$$T = T_0 + qt \qquad (C.4)$$

where q is the heating rate, t is time and T_0 is the initial temperature value.

By inserting the Equations (C.3) and (C.4) into the Equation (C.1) and rearranging, the rate expression for the decomposition becomes as;

$$\frac{\mathrm{d}\alpha}{(1-\alpha)^{\mathrm{n}}} = \frac{\mathrm{A}}{q}\exp\left(\frac{-\mathrm{E}}{\mathrm{RT}}\right)\mathrm{dT} \qquad \text{(C.5)}$$

Making the substitution u=E/RT and using the following relation;

$$\int_u^{\infty} e^{-u}\, u^{-b}\, \mathrm{d}u = u^{1-u} \sum_{n=0}^{\infty} \frac{(-1)^{\mathrm{n}}\ (b)_{\mathrm{n}}}{u^{(\mathrm{n}+1)}}$$

Equation (C.5) is integrated using the following boundary conditions:

$T=T_0$, $\alpha=0$

T=T, $\alpha=\alpha$

Ignoring the higher order terms of the series, following equation is obtained for n≠ 1;

$$\frac{1-(1-\alpha)^{(1-\mathrm{n})}}{(1-\mathrm{n})\mathrm{T}^2} = \frac{\mathrm{AR}}{\mathrm{qE}}\left(1-\frac{2\mathrm{RT}}{\mathrm{E}}\right)\exp\left(\frac{-\mathrm{E}}{\mathrm{RT}}\right) \qquad \text{(C.6)}$$

Equation (C.6) can be simplified assuming 2RT/E≪ 1, and by taking the natural logarithm of the both sides. Obtained equation (C.7) can be used for estimating the kinetic parameters from TGA;

$$\ln\frac{1-(1-\alpha)^{(1-\mathrm{n})}}{(1-\mathrm{n})\mathrm{T}^2} = \ln\frac{\mathrm{AR}}{\mathrm{qE}} - \frac{\mathrm{E}}{\mathrm{RT}} \qquad \text{(C.7)}$$

Integration of Equation (C.5) for the first order reaction (n=1), equation becomes;

$$\ln\frac{-\ln(1-\alpha)}{\mathrm{T}^2} = \ln\frac{\mathrm{AR}}{\mathrm{qE}} - \frac{\mathrm{E}}{\mathrm{RT}} \qquad \text{(C.8)}$$

By using TGA values and plotting the left hand side of equations (C.7) and (C.8) versus 1/T, activation energy and pre-exponential factor can be obtained from the slope and intercept of the straight line, respectively.

The plots for the first and second order pyrolysis reactions are given in Figure C.1. Since the R^2 value of the first order degradation reaction of polypropylene (0.9685) is greater than the value for the second order (0.9197), reaction order is accepted as "1".

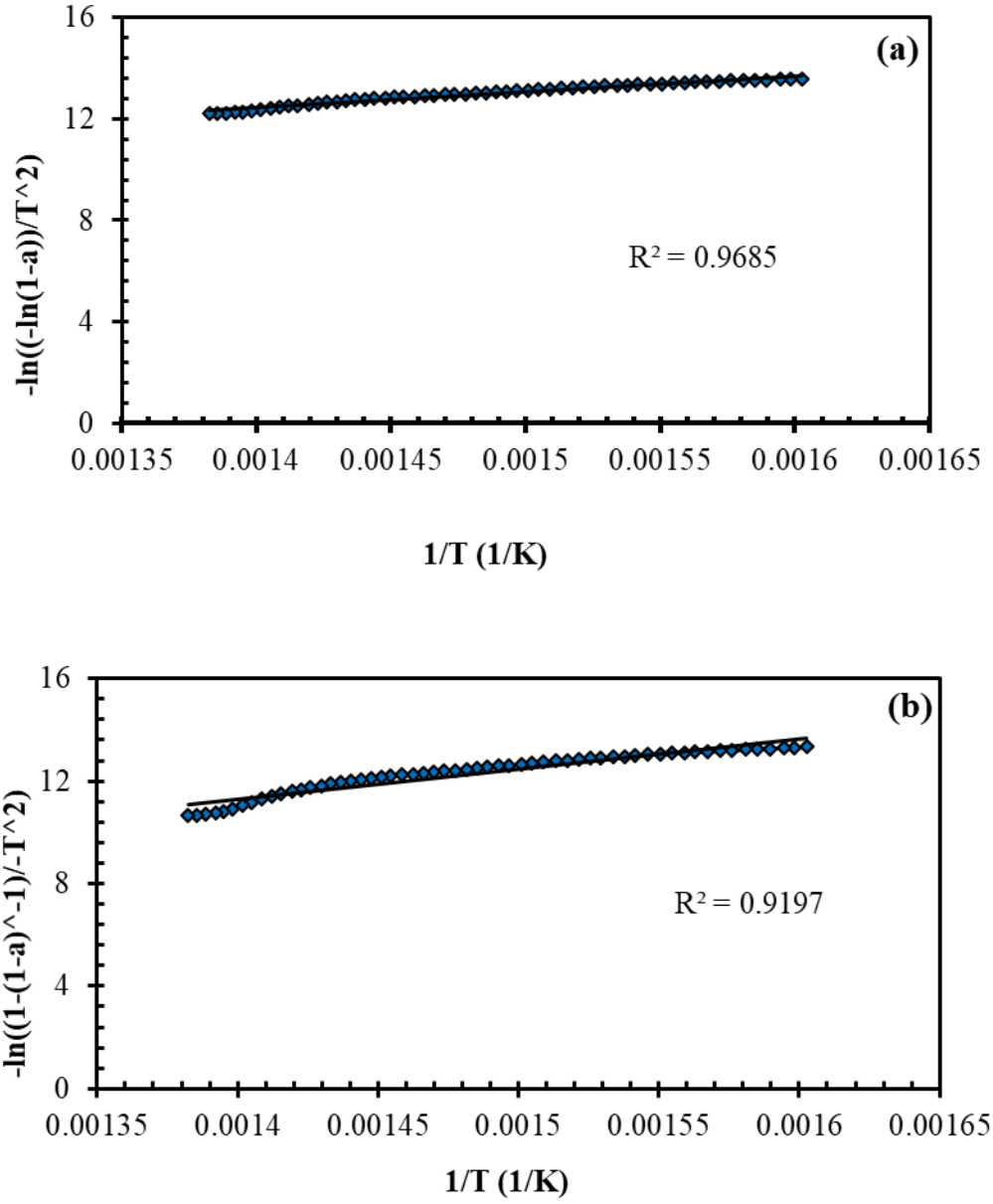

Figure C.1. Determination of PP degradation reaction order (a) for first order, (b) for second order

D. CALCULATION OF GAS CHROMATOGRAPHY CALIBRATION FACTORS FOR GAS PRODUCTS

Calibration experiments were carried out in order to determine the retention times and calibration factors of the gas products obtained from the catalytic and non-catalytic pyrolysis of polypropylene. Calibration of the gas products was carried out using a standard gas mixture. Mole fraction of each component in the calibration gas mixture was 1% and the rest of the mixture was N_2. Obtained calibration factors for gaseous products are given in Table D.1.

Table D.1. Retention times, average areas and calibration factors of gas products

Gas ID	Retention Time (min)	$A_{average}$ (mVolt.sec)	Calibration factor, β
CH_4	0.56	13.2	1
C_2H_2	1.51	29.8	0.44
C_2H_6	1.92	19.2	0.69
C_2H_4	3.21	31.7	0.42
C_3H_6	6.42	24.7	0.54
C_3H_8	7.13	23.7	0.56
n-C_4H_{10}	29.78	22.6	0.59
i-C_4H_{10}	25.01	22.6	0.59

In order to make the calculations, calibration factor of CH_4 (A) was taken as 1. Equation D.2 was obtained from Equation D.1 and it was used to calculate the β factors of gas component i.

$$\frac{\mathbf{n_i}}{\mathbf{n_A}} = \frac{\mathbf{A_i} * \boldsymbol{\beta_i}}{\mathbf{A_A} * \boldsymbol{\beta_A}} \qquad (\boldsymbol{D.1})$$

$$\boldsymbol{\beta_i} = \frac{\mathbf{A_A} * \boldsymbol{\beta_A}}{\mathbf{A_i}} * \frac{\mathbf{n_i}}{\mathbf{n_A}} \qquad (\boldsymbol{D.2})$$

where;

n_i: Number of moles of component i

A_i: The GC peak area of component i

β_i: The calibration factor of component i

E. CALCULATION OF GAS CHROMATOGRAPHY CALIBRATION FACTORS FOR LIQUID PRODUCTS

In order to determine the retention times and calibration factors (β) of the liquid products which were obtained from the pyrolysis of PP, calibration experiments were carried out with GC. Three paraffin mixtures which were given in Table E.1 and ten equal volume mixtures including n-hexane which were given in Table E.2 were used for the calibration.

Table E.1. Standard paraffin mixtures used in liquid calibration (C_9-C_{18})

Mixture 1		**Mixture 2**		**Mixture 3**	
Liquid ID	**wt %**	**Liquid ID**	**wt %**	**Liquid ID**	**wt %**
n-C_9H_{20}	25	n-$C_{11}H_{24}$	25	n-$C_{12}H_{26}$	25
n-$C_{10}H_{22}$	25	n-$C_{12}H_{26}$	25	n-$C_{14}H_{30}$	25
n-$C_{11}H_{24}$	25	n-$C_{13}H_{28}$	25	n-$C_{16}H_{34}$	25
n-$C_{12}H_{26}$	25	n-$C_{14}H_{30}$	25	n-$C_{18}H_{38}$	25

Table E.2. Calibration mixtures prepared using equal volumes

Mixture	**Compounds**	**Volume (%)**
1	n-hexane + n-pentane	50-50
2	n-hexane + isooctane	50-50
3	n-hexane + cyclohexane	50-50
4	n-hexane + benzene	50-50
5	n-hexane + xylene	50-50
6	n-hexane + toluene	50-50
7	n-hexane + n-heptane	50-50
8	n-hexane + n-octane	50-50
9	n-hexane + n-decane	50-50
10	n-hexane + n-dodecane	50-50

While calculating the calibration factors, a β value of n-hexane was taken as 1 to be able to calculate the β values of other products. The equation which was used for the calculation of β values was given in E.1.

$$z_A = x_A \frac{MW_A}{\rho_A} \qquad (E.1)$$

Equation E.2 was used to calculate the total number of moles of the paraffin mixture. In the equation E.2; A, B, C and D represents C9, C10, C11 and C12, respectively. Equation 3 is used to calculate the mole fraction of liquid products. When β value of one product is known, β value of the second product is calculated with equation E.4, calculating the mole fraction using equation E.1.

$$n_{total} = A_A\beta_A + A_B\beta_B + A_C\beta_C + A_D\beta_D \qquad (E.2)$$

$$x_A = \frac{n_A}{n_{total}} = \frac{A_A\beta_A}{A_A\beta_A + A_B\beta_B + A_C\beta_C + A_D\beta_D} \qquad (E.3)$$

$$\frac{x_A}{x_i} = \frac{n_A}{n_i} = \frac{A_A\beta_A}{A_i\beta_i} \qquad (E.4)$$

All calibration factors were calculated using this procedure. Table E.3 shows the retention times and calibration factors of the liquid products.

Table E.3. Retention times and calibration factors of liquid hydrocarbons

Liquid Compound	Formula	Retention Time (min)	Calibration Factor (β)
n-Pentane	n-C_5H_{12}	2.82	1.20
n-Hexane	n-C_6H_{14}	3.30	1.00
Cyclohexane	C_6H_{12}	4.03	0.83
Benzene	C_6H_6	4.10	0.92
n-Heptane	n-C_7H_{16}	4.66	0.59
Iso-octane	i-C_8H_{18}	4.84	0.80
Toluene	C_7H_8	6.80	0.76
n-Octane	n-C_8H_{18}	7.77	0.66
m,p-xylene	$C_6H_4(CH_3)_2$	12.70	0.69
n-Nonane	n-C_9H_{20}	14.75	0.95
n-Decane	n-$C_{10}H_{22}$	19.00	0.61
n-Undecane	n-$C_{11}H_{24}$	23.10	0.60
n-Dodecane	n-$C_{12}H_{26}$	26.60	0.47
n-Tridecane	n-$C_{13}H_{28}$	29.74	0.41
n-Tetradecane	n-$C_{14}H_{30}$	32.64	0.38
n-Hexadecane	n-$C_{16}H_{34}$	40.79	0.34
n-Octadecane	n-$C_{18}H_{38}$	56.42	0.30

F. CALCULATION OF MOLE & WEIGHT FRACTIONS AND SELECTIVITIES OF PRODUCTS

Calculation of mole and weight fractions of compound i were done from Equation F.1 and F.2, respectively.

A: CH_4 B: C_2H_2 C: C_2H_4 D: C_2H_6 E: C_3H_6

F: C_3H_8 G: n-C_4H_{10} H: i-$C4H_{10}$

$$y_i = \frac{n_i}{n_{total}} = \frac{A_i\beta_i}{A_A\beta_A+A_B\beta_B+A_C\beta_C+A_D\beta_D+A_E\beta_E+A_F\beta_F+A_G\beta_G} \quad \text{(F.1)}$$

$$w_i = \frac{m_i}{m_{total}} = \frac{y_iMW_i}{y_AMW_A+y_BMW_B+y_CMW_C+y_DMW_D+y_EMW_E+y_FMW_F+y_GMW_G+y_HMW_H} \quad \text{(F.2)}$$

For selectivity calculations, carbon balance was done (F.3).

$$S_i = \frac{n_i}{n_A+2n_B+2n_C+2n_D+3n_E+3n_F+4n_G+4n_H} \quad \text{(F.3)}$$

A sample calculation for C_3H_6 is given as below:

-Mole fraction of C_3H_6 was calculated using F.1;

$$y_E = \frac{n_E}{n_{total}} = \frac{10.88}{4.17+2.60+10.88+3.86} = 0.51$$

-Weight fraction of C_3H_6 was calculated using F.2;

$$w_E = \frac{m_E}{m_{total}} = \frac{0.51 \text{ x } 42}{(0.19\text{x}30)+(0.12\text{x}28)+(0.51\text{x}42)+(0.18\text{x}58)} = 0.52$$

-Selectivity of C_3H_6 was calculated using F.3;

$$S_E = \frac{10.88}{(4.17X2)+(2.60X2)+(10.88X3)+(3.86X4)} = 0.18$$

Table F.1. Compounds, area values and moles obtained from the non-catalytic thermal degradation reaction of PP at 400 °C

Gas ID	**$A_{average\ i}$ (mVolt.sec)**	**Calibration Factor** β_i	**n_i (mol)**	**Weight (kg)**
CH_4	0	1	0	0
C_2H_2	0	0.44	0	0
C_2H_6	6.05	0.69	4.17	0.13
C_2H_4	6.18	0.42	2.60	0.07
C_3H_6	20.2	0.54	10.9	0.48
C_3H_8	0	0.56	0	0
n-C_4H_{10}	0	0.59	0	0
i-C_4H_{10}	6.55	0.59	3.86	0.22

G. MOLE & WEIGHT FRACTIONS AND SELECTIVITY VALUES OF GAS PRODUCTS

Mole and weight fractions and selectivity of gas products obtained from the non-catalytic and catalytic thermal degradation of polypropylene at 315 °C and 400 °C, 30 min. in the presence of different catalysts are tabulated in Tables G1-G10.

Table G.1. Mole and weight fractions and selectivity of gas products obtained from the non-catalytic degradation of PP at 315 °C

Gas products	$A_{average}$ (mVolt.sec)	Mole fraction, yi	Weight fraction, wi	Selectivity, Si
CH_4	0.00	0.00	0.00	0.00
C_2H_2	0.00	0.00	0.00	0.00
C_2H_6	0.00	0.00	0.00	0.00
C_2H_4	6.20	1.00	1.00	1.00
C_3H_6	0.00	0.00	0.00	0.00
C_3H_8	0.00	0.00	0.00	0.00
n-C_4H_{10}	0.00	0.00	0.00	0.00
i-C_4H_{10}	0.00	0.00	0.00	0.00

Table G.2. Mole and weight fractions and selectivities of gas products obtained from the catalytic degradation of PP at 315 °C (SBA15-TPA 0.05)

Gaseous products	$A_{average}$ (mVolt.sec)	Mole fraction, yi	Weight fraction, wi	Selectivity, Si
CH_4	0.00	0.00	0.00	0.00
C_2H_2	0.00	0.00	0.00	0.00
C_2H_6	0.00	0.00	0.00	0.00
C_2H_4	1.62	0.13	0.07	0.08
C_3H_6	2.23	0.24	0.20	0.21
C_3H_8	0.00	0.00	0.00	0.00
$n\text{-}C_4H_{10}$	1.24	0.15	0.17	0.16
$i\text{-}C_4H_{10}$	4.08	0.48	0.56	0.55

Table G.3. Mole and weight fractions and selectivities of gas products obtained from the catalytic degradation of PP at 315 °C (SBA15-TPA 0.10)

Gaseous products	$A_{average}$ (mVolt.sec)	Mole fraction, yi	Weight fraction, wi	Selectivity, Si
CH_4	0.00	0.00	0.00	0.00
C_2H_2	0.00	0.00	0.00	0.00
C_2H_6	0.00	0.00	0.00	0.00
C_2H_4	3.42	0.14	0.08	0.08
C_3H_6	3.37	0.18	0.15	0.16
C_3H_8	0.00	0.00	0.00	0.00
$n\text{-}C_4H_{10}$	1.62	0.09	0.10	0.10
$i\text{-}C_4H_{10}$	10.2	0.59	0.67	0.66

Table G.4. Mole and weight fractions and selectivities of gas products obtained from the catalytic degradation of PP at 315 °C (SBA15-TPA 0.15)

Gaseous products	$A_{average}$ (mVolt.sec)	Mole fraction, yi	Weight fraction, wi	Selectivity, Si
CH_4	0.00	0.00	0.00	0.00
C_2H_2	0.00	0.00	0.00	0.00
C_2H_6	0.00	0.00	0.00	0.00
C_2H_4	2.66	0.23	0.13	0.14
C_3H_6	1.67	0.18	0.16	0.16
C_3H_8	0.00	0.00	0.00	0.00
n-C_4H_{10}	0.00	0.00	0.00	0.00
i-C_4H_{10}	4.78	0.59	0.71	0.70

Table G.5. Mole and weight fractions and selectivities of gas products obtained from the catalytic degradation of PP at 315 °C (SBA15-TPA 0.20)

Gaseous products	$A_{average}$ (mVolt.sec)	Mole fraction, yi	Weight fraction, wi	Selectivity, Si
CH_4	0.00	0.00	0.00	0.00
C_2H_2	0.00	0.00	0.00	0.00
C_2H_6	0.00	0.00	0.00	0.00
C_2H_4	4.55	0.28	0.17	0.17
C_3H_6	1.71	0.13	0.11	0.12
C_3H_8	0.00	0.00	0.00	0.00
n-C_4H_{10}	1.56	0.13	0.16	0.16
i-C_4H_{10}	5.36	0.46	0.56	0.55

Table G.6. Mole and weight fractions and selectivities of gas products obtained from the non-catalytic degradation of PP at 400 °C

Gaseous products	$A_{average}$ (mVolt.sec)	Mole fraction, yi	Weight fraction, wi	Selectivity, Si
CH_4	0.00	0.00	0.00	0.00
C_2H_2	0.00	0.00	0.00	0.00
C_2H_6	6.05	0.19	0.14	0.14
C_2H_4	6.18	0.12	0.08	0.08
C_3H_6	20.2	0.51	0.52	0.53
C_3H_8	0.00	0.00	0.00	0.00
$n\text{-}C_4H_{10}$	0.00	0.00	0.00	0.00
$i\text{-}C_4H_{10}$	6.55	0.18	0.26	0.25

Table G.7. Mole and weight fractions and selectivities of gas products obtained from the catalytic degradation of PP at 400 °C (SBA15-TPA 0.05)

Gaseous products	$A_{average}$ (mVolt.sec)	Mole fraction, yi	Weight fraction, wi	Selectivity, Si
CH_4	0.00	0.00	0.00	0.00
C_2H_2	0.00	0.00	0.00	0.00
C_2H_6	0.00	0.00	0.00	0.00
C_2H_4	2.68	0.08	0.04	0.04
C_3H_6	6.76	0.25	0.20	0.21
C_3H_8	0.00	0.00	0.00	0.00
$n\text{-}C_4H_{10}$	2.18	0.09	0.10	0.10
$i\text{-}C_4H_{10}$	14.4	0.58	0.66	0.65

Table G.8. Mole and weight fractions and selectivities of gas products obtained from the catalytic degradation of PP at 400 °C (SBA15-TPA 0.10)

Gaseous products	$A_{average}$ (mVolt.sec)	Mole fraction, yi	Weight fraction, wi	Selectivity, Si
CH_4	0.00	0.00	0.00	0.00
C_2H_2	0.00	0.00	0.00	0.00
C_2H_6	0.00	0.00	0.00	0.00
C_2H_4	8.73	0.34	0.21	0.21
C_3H_6	2.26	0.11	0.10	0.11
C_3H_8	0.00	0.00	0.00	0.00
n-C_4H_{10}	1.55	0.09	0.11	0.11
i-C_4H_{10}	8.37	0.46	0.58	0.57

Table G.9. Mole and weight fractions and selectivity of gas products obtained from the catalytic degradation of PP at 400 °C (SBA15-TPA 0.15)

Gaseous products	$A_{average}$ (mVolt.sec)	Mole fraction, yi	Weight fraction, wi	Selectivity, Si
CH_4	0.00	0.00	0.00	0.00
C_2H_2	0.00	0.00	0.00	0.00
C_2H_6	0.00	0.00	0.00	0.00
C_2H_4	9.67	0.41	0.26	0.27
C_3H_6	1.74	0.10	0.09	0.09
C_3H_8	0.00	0.00	0.00	0.00
n-C_4H_{10}	0.00	0.00	0.00	0.00
i-C_4H_{10}	8.12	0.49	0.65	0.64

Table G.10. Mole and weight fractions and selectivity of gas products obtained from the catalytic degradation of PP at 400 °C (SBA15-TPA 0.20)

Gaseous products	$A_{average}$ (mVolt.sec)	Mole fraction, yi	Weight fraction, wi	Selectivity, Si
CH_4	0.00	0.00	0.00	0.00
C_2H_2	0.00	0.00	0.00	0.00
C_2H_6	0.00	0.00	0.00	0.00
C_2H_4	21.9	0.75	0.59	0.60
C_3H_6	0.00	0.00	0.00	0.00
C_3H_8	0.00	0.00	0.00	0.00
$n\text{-}C_4H_{10}$	0.00	0.00	0.00	0.00
$i\text{-}C_4H_{10}$	5.20	0.25	0.41	0.40

H. MOLE & WEIGHT FRACTIONS AND SELECTIVITY VALUES OF LIQUID PRODUCTS

Mole fraction and selectivity of liquid products obtained from the catalytic thermal degradation of polypropylene at 315 °C and 400 °C, 30 min. in the presence of different catalysts are tabulated in Tables H1-H8.

Table H.1. Mole fraction and selectivity of liquid products obtained from the catalytic degradation of PP at 315 °C (SBA15-TPA 0.05)

Liquid products	**$A_{average}$ (mVolt.sec)**	**Mole fraction, yi**	**Selectivity, Si**
n-Pentane	47.07	0.00480	0.00200
n-Hexane	7.70	0.00066	0.00033
Cyclohexane	0.00	0.00000	0.00000
Benzene	0.00	0.00000	0.00000
n-Heptane	3.32	0.00017	0.00010
Iso-octane	1.32	0.00009	0.00006
Toluene	7.74	0.00050	0.00029
n-Octane	0.00	0.00000	0.00000
m,p-xylene	64.53	0.00379	0.00252
n-Nonane	570.32	0.04609	0.03450
n-Decane	2497.53	0.12961	0.10780
n-Undecane	3803.64	0.19416	0.17763
n-Dodecane	6022.63	0.24082	0.24035
n-Tridecane	4501.70	0.15702	0.16978
n-Tetradecane	5998.15	0.19391	0.22579
n-Hexadecane	755.85	0.02186	0.02909
n-Octadecane	255.43	0.00652	0.00976

Table H.2. Mole fraction and selectivity of liquid products obtained from the catalytic degradation of PP at 315 °C (SBA15-TPA 0.10)

Liquid products	**$A_{average}$ (mVolt.sec)**	**Mole fraction, yi**	**Selectivity, Si**
n-Pentane	17.79	0.00084	0.00040
n-Hexane	709.50	0.02781	0.01611
Cyclohexane	687.65	0.02237	0.01296
Benzene	193.00	0.00696	0.00403
n-Heptane	35.70	0.00083	0.00056
Iso-octane	1149.50	0.03605	0.02784
Toluene	1040.40	0.03100	0.02094
n-Octane	1439.72	0.03725	0.02877
m,p-xylene	1949.70	0.05274	0.04073
n-Nonane	3797.40	0.14142	0.12286
n-Decane	7322.35	0.17509	0.16902
n-Undecane	6450.85	0.15172	0.16111
n-Dodecane	7959.05	0.14664	0.16987
n-Tridecane	4197.25	0.06746	0.08466
n-Tetradecane	6083.65	0.09062	0.12247
n-Hexadecane	704.68	0.00939	0.01451
n-Octadecane	154.66	0.00182	0.00316

Table H.3. Mole fraction and selectivity of liquid products obtained from the catalytic degradation of PP at 315 °C (SBA15-TPA 0.15)

Liquid products	**$A_{average}$ (mVolt.sec)**	**Mole fraction, yi**	**Selectivity, Si**
n-Pentane	2.03	0.00007	0.00003
n-Hexane	282.15	0.00793	0.00432
Cyclohexane	429.90	0.01003	0.00546
Benzene	205.65	0.00532	0.00290
n-Heptane	438.90	0.00728	0.00463
Iso-octane	726.55	0.01634	0.01187
Toluene	884.55	0.01890	0.01201
n-Octane	1402.73	0.02603	0.01890
m,p-xylene	2090.05	0.04054	0.02945
n-Nonane	4811.70	0.12851	0.10501
n-Decane	9511.95	0.16312	0.14810
n-Undecane	10613.05	0.17902	0.17879
n-Dodecane	11404.05	0.15068	0.16417
n-Tridecane	6502.35	0.07495	0.08846
n-Tetradecane	12649.90	0.13514	0.17177
n-Hexadecane	2861.55	0.02735	0.03973
n-Octadecane	1043.51	0.00880	0.01438

Table H.4. Mole fraction and selectivity of liquid products obtained from the catalytic degradation of PP at 315 °C (SBA15-TPA 0.20)

Liquid products	**$A_{average}$ (mVolt.sec)**	**Mole fraction, yi**	**Selectivity, Si**
n-Pentane	73.14	0.00811	0.00402
n-Hexane	427.35	0.03950	0.02348
Cyclohexane	271.685	0.02084	0.01239
Benzene	74.5	0.00633	0.00377
n-Heptane	367.8	0.02006	0.01391
Iso-octane	401.485	0.02969	0.02353
Toluene	376.05	0.02641	0.01832
n-Octane	562.69	0.03432	0.02721
m.p-xylene	984.405	0.06278	0.04977
n-Nonane	1513.915	0.13292	0.11855
n-Decane	3287.5	0.18534	0.18366
n-Undecane	2933.85	0.16269	0.17734
n-Dodecane	3085.675	0.13404	0.15939
n-Tridecane	1655.65	0.06274	0.08082
n-Tetradecane	1992.23	0.06997	0.09707
n-Hexadecane	132.62	0.00417	0.00661
n-Octadecane	3.08	0.00009	0.00015

Table H.5. Mole fraction and selectivity of liquid products obtained from the catalytic degradation of PP at 400 °C (SBA15-TPA 0.05)

Liquid products	**$A_{average}$ (mVolt.sec)**	**Mole fraction. yi**	**Selectivity. Si**
n-Pentane	10.09	0.00033	0.00016
n-Hexane	235.45	0.00651	0.00365
Cyclohexane	369.55	0.00849	0.00476
Benzene	195.15	0.00497	0.00278
n-Heptane	648.75	0.01059	0.00692
Iso-octane	1159.90	0.02567	0.01918
Toluene	1568.60	0.03298	0.02157
n-Octane	2325.35	0.04246	0.03173
m.p-xylene	2365.72	0.04516	0.03375
n-Nonane	4600.00	0.12090	0.10164
n-Decane	9055.55	0.15282	0.14275
n-Undecane	11100.60	0.18427	0.18933
n-Dodecane	10838.25	0.14093	0.15797
n-Tridecane	10852.80	0.12310	0.14949
n-Tetradecane	8487.50	0.08923	0.11669
n-Hexadecane	1045.92	0.00984	0.01470
n-Octadecane	209.35	0.00174	0.00292

Table H.6. Mole fraction and selectivity of liquid products obtained from the catalytic degradation of PP at 400 °C (SBA15-TPA 0.10)

Liquid products	**$A_{average}$ (mVolt.sec)**	**Mole fraction. yi**	**Selectivity. Si**
n-Pentane	2.17	0.00014	0.00007
n-Hexane	520.10	0.02870	0.01637
Cyclohexane	120.61	0.00552	0.00315
Benzene	390.55	0.01983	0.01131
n-Heptane	157.50	0.00513	0.00341
Iso-octane	1146.67	0.05062	0.03849
Toluene	988.81	0.04147	0.02759
n-Octane	1029.50	0.03750	0.02851
m.p-xylene	1394.68	0.05311	0.04038
n-Nonane	2819.83	0.14783	0.12644
n-Decane	4310.70	0.14511	0.13791
n-Undecane	3545.60	0.11740	0.12273
n-Dodecane	4429.72	0.11490	0.13103
n-Tridecane	4404.45	0.09966	0.12312
n-Tetradecane	3903.47	0.08186	0.10891
n-Hexadecane	1968.22	0.03693	0.05615
n-Octadecane	862.96	0.01429	0.02444

Table H.7. Mole fraction and selectivity of liquid products obtained from the catalytic degradation of PP at 400 °C (SBA15-TPA 0.15)

Liquid products	**$A_{average}$ (mVolt.sec)**	**Mole fraction. yi**	**Selectivity. Si**
n-Pentane	0.00	0.00000	0.00000
n-Hexane	67.60	0.00444	0.00242
Cyclohexane	151.25	0.00824	0.00450
Benzene	179.95	0.01087	0.00593
n-Heptane	53.40	0.00207	0.00132
Iso-octane	441.10	0.02317	0.01685
Toluene	399.62	0.01994	0.01269
n-Octane	451.51	0.01956	0.01423
m.p-xylene	764.83	0.03465	0.02520
n-Nonane	1771.50	0.11049	0.09042
n-Decane	4479.50	0.17940	0.16312
n-Undecane	4977.85	0.19609	0.19613
n-Dodecane	5129.50	0.15828	0.17271
n-Tridecane	2885.50	0.07767	0.09181
n-Tetradecane	5243.15	0.13081	0.16652
n-Hexadecane	900.40	0.02010	0.02924
n-Octadecane	213.95	0.00421	0.00690

Table H.8. Mole fraction and selectivity of liquid products obtained from the catalytic degradation of PP at 400 °C (SBA15-TPA 0.20)

Liquid products	**$A_{average}$ (mVolt.sec)**	**Mole fraction. yi**	**Selectivity. Si**
n-Pentane	1.84	0.00014	0.00006
n-Hexane	154.40	0.00987	0.00538
Cyclohexane	71.97	0.00382	0.00208
Benzene	169.25	0.00996	0.00542
n-Heptane	63.15	0.00238	0.00151
Iso-octane	596.83	0.03053	0.02217
Toluene	421.53	0.02048	0.01301
n-Octane	621.67	0.02623	0.01905
m.p-xylene	877.11	0.03869	0.02810
n-Nonane	1929.25	0.11718	0.09572
n-Decane	4618.45	0.18012	0.16348
n-Undecane	4314.70	0.16552	0.16525
n-Dodecane	4800.66	0.14426	0.15712
n-Tridecane	2884.65	0.07562	0.08922
n-Tetradecane	5464.04	0.13275	0.16868
n-Hexadecane	1418.59	0.03084	0.04478
n-Octadecane	605.79	0.01162	0.01898